Composite Functional Materials
2025, 1(2): 20250205 https://doi.org/10.63823/20250205

REVIEW ARTICLE

3D printing technology for photocatalysis: review and prospect

Haoyuan Yin[a], Biyang Zhang[a], Xiaomei Dai[a], Jinman Yang[a,*], Jizhou Jiang[b,c,*], Hui Xu[a,d,*]

a. School of the Environment and Safety Engineering, Jiangsu University, Zhenjiang, Jiangsu 212013, PR China
b. School of Materials Science and Engineering, State Key Laboratory of Green and Efficient Development of Phosphorus Resources, Engineering Research Center of Phosphorus Resources Development and Utilization of Ministry of Education, Key Laboratory of Green Chemical Engineering Process of Ministry of Education, Hubei Key Laboratory of Plasma Chemistry and Advanced Materials, Novel Catalytic Materials of Hubei Engineering Research Center, Wuhan Institute of Technology, Wuhan 430205, China
c. National Innovation Institute of Additive Manufacturing, Xi'an 710300, China
d. Jiangsu Collaborative Innovation Center of Technology and Material of Water Treatment, Suzhou University of Science and Technology, Suzhou 215009, China

ABSTRACT: Environmental pollution and energy shortage pose major challenges to sustainable development. Photocatalytic technology using solar energy for pollutant degradation and resource conversion is a promising solution. However, conventional photocatalysts and reactors have limitations such as narrow light absorption, fast charge recombination, difficulty in recovery and continuous operation. The characteristics of surface reactions in photocatalytic technology also put forward higher requirements for light field design. 3D printing (Additive manufacturing) provides an innovative strategy to solve these problems. It enables the controllable design of photocatalyst microstructures in terms of pore size, morphology and surface characteristics through high-precision and customizable manufacturing methods, thus significantly improving the specific surface area, enhancing the light capture ability and carrier separation efficiency. At the same time, 3D printing technology can also manufacture photocatalytic reactors with complex flow channel structures, multi-scale mass transfer interfaces and integrated functional units, which can effectively optimize the distribution and transmission of reactants and light, realize the collaborative enhancement of reaction-mass transfer-illumination, and support the system integration of multifunctional modules. This review systematically summarizes the technical progress, core challenges and application potential of this cross-field, and provides reference for the subsequent research on 3D printing innovation of photocatalytic materials and devices.

KEYWORDS: Additive Manufacturing, 3D printing, Photocatalysis, Photocatalyst, Reactor

Received: November 5, 2025; Revised: December 25, 2025; **Accepted:** December 25, 2025; **Available online:** December 30, 2025
***Corresponding author:** jmyang@ujs.edu.cn (J. Yang) ; 027wit@163.com (J. Jiang); xh@ujs.edu.cn (H. Xu)

1 Introduction

Environmental pollution and energy shortage are becoming more and more serious, posing great challenges to global sustainable development [1-3]. The continuous accumulation of organic pollutants in water and the widespread presence of volatile organic compounds (VOCs), nitrogen oxides (NO_x) and carbon dioxide (CO_2) in the atmosphere seriously threaten ecological security and public health [4-7]. Traditional physical, chemical, and biological treatment technologies are often energy-intensive, inefficient, and prone to secondary pollution, struggling to degrade stable pollutants [8-12]. Thus, efficient, clean, and sustainable conversion technologies are urgently needed. In this context, photocatalysis, as a green and energy-saving advanced oxidation process, has shown great potential and broad application prospects [13-16]. It directly harnesses solar energy to drive pollutant degradation and resource-oriented conversion under mild conditions, avoiding secondary pollution [17-23], and has been widely studied in wastewater treatment, air purification, hydrogen production, CO_2 reduction, and high-value organic synthesis [24-29].

Photocatalyst is the core of photocatalytic process, and its performance directly determines the photocatalytic efficiency [30]. At present, the commonly used photocatalysts mainly include TiO_2, bismuth compounds, metal sulfide and other semiconductor materials [31-36]. TiO_2 is widely studied and applied because of its high chemical stability, low cost, non-toxic and other advantages [37]. However, traditional photocatalysts generally have a narrow light response range, mostly limited to the ultraviolet region, and low utilization of solar energy [38]. The recombination rate of photogenerated electron hole pairs is high, which leads to the problem of low quantum efficiency, and it is difficult to achieve efficient conversion in CO_2 reduction and other reactions [39, 40]. Traditional reactors such as tank and tube reactors further hinder industrialization due to uneven catalyst dispersion, poor mass transfer, and difficulty in continuous production [41, 42]. Furthermore, among the forms of photocatalysts, powder photocatalysts account for the majority, but they have certain shortcomings: (1) Difficult to recycle. The particles of powder catalysts are tiny and easily dispersed, making it difficult to completely separate them through conventional methods during reuse, resulting in significant loss and increasing operating costs, as well as potentially affecting the purity of the products. (2) Prone to agglomeration. Due to their high surface energy, they are prone to agglomeration, leading to a decrease in specific surface area and coverage of active sites, significantly reducing the photocatalytic activity. (3) Poor applicability in continuous flow. In continuous reaction systems for pollutant degradation and hydrogen production, suspended solids are easily carried away by the fluid and may cause pipeline blockage. This problem makes it difficult to maintain long-term stable operation of the system.

Additive manufacturing, also known as 3D printing, has developed rapidly in recent years [43]. The basic principle of this technology is to achieve rapid fabrication from scratch by computer generated geometric information or by obtaining reverse geometric information through 3D scanning of the object [44]. It was first proposed in the 1980s, inspired by the slicing forming method. After decades of development, it has formed mainstream technologies such as direct inkjet writing (DIW) fused deposition modeling (FDM), stereolithography (SLA), and selective laser sintering (SLS), which can process various materials including plastics, metals, ceramics, and biological materials [45]. As an emerging technology based on the principle of layer-by-layer stacking, 3D printing has significant advantages over traditional manufacturing [46-49]. First, it can achieve a high degree of customization and precise molding of complex structures. At the same time, its material utilization rate is very high, far beyond the traditional subtractive manufacturing [50]. Secondly, it does not rely on molds. This allows it to quickly switch between small-batch production and multi-variety production, thereby reducing initial costs [51]. Finally, its digital drive model supports the integrated manufacturing of complex structures such as hollow meshes and internal flow channels. At the same time, the multi-head synergy technology can realize the accurate composite of a variety of materials [52]. These features make it possible to integrate functional devices.

3D printing technology based on photocatalysis provides a new solution for the design of traditional photocatalysts and the fabrication of photocatalytic reactors. With the precise prototyping capability of 3D printing, photocatalytic materials and devices with specific microstructures and macroscopic shapes can be customized. This not only optimizes the capture, transmission and utilization efficiency of light, but also regulates the transfer process of reactants and products. At the same time, by introducing functional materials, the performance of photocatalysts can be further improved and multifunctional integration can be achieved [53]. Specifically, 3D printing can be used to fabricate photocatalysts with graded porous structure to increase their specific surface area and promote

adequate contact between reactants and catalysts [54]. The constructed microchannel structure can also optimize the flow state of gas or liquid, thereby realizing a continuous and controllable photocatalytic reaction process [55]. In addition, with the multi-material molding ability of 3D printing, the photocatalyst can be combined with auxiliary materials such as conductive materials and high thermal conductivity materials to construct new photocatalytic systems suitable for different scenarios, which will further promote the development and practical application of this technology [56-58]. With the rapid development and wide application of 3D printing technology, the attention in the field of photocatalyst research has increased significantly. The number of relevant publications has shown a steady increase over the years, reflecting that this cross-cutting research direction is gaining increasing academic attention (Fig. 1).

3D printing technology based on photocatalysis has achieved significant research progress, yet it remains at an early developmental stage [59]. The integration of 3D printing and photocatalysis is not merely a simple technological overlay, but a targeted breakthrough addressing the core pain points of traditional photocatalytic technology. It can not only solve the problems of difficult recovery and easy agglomeration faced by traditional powder photocatalysts through

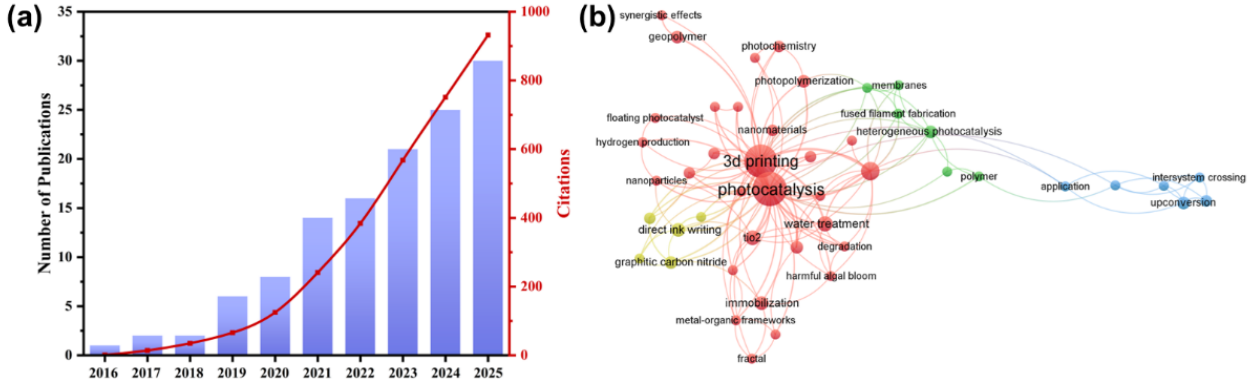

Fig. 1 (a) The number of papers published and the number of citations in the Web of Science database during the period from 2016 to 2025, with "3D printing" and "photocatalysis" as the keywords. (b) Keyword cluster analysis in this field.

macro-micro structural formation, but also address the deficiencies of fixed reactor structures and insufficient coordination among various parts through customized design. Therefore, systematically reviewing the technological progress, core challenges, and application potential in this interdisciplinary field holds crucial theoretical and practical significance for promoting the transition of photocatalytic technology from the laboratory to industrial applications [60]. As shown in Fig. 2, this review will comprehensively summarize and deeply explore various applications of 3D printing technology in the field of photocatalysis. Firstly, this review introduces the basic principles of photocatalytic technology and 3D printing technology, and briefly introduces their historical development and influencing factors. Subsequently, several representative 3D printing technologies are introduced in detail, including the research and application of fused deposition modeling, direct ink writing, laser etching and stereolithography in the direct shaping of photocatalysts and the construction of photocatalyst support. Then, the latest progress and application of 3D printing technology in the fabrication of photocatalytic reactors and the construction of photocatalytic systems are analyzed.

2 Fundamentals of photocatalytic technology and 3D printing technology

2.1 Overview of photocatalytic technology

Photocatalytic technology, as a highly promising cutting-edge science, was first discovered by Akira Fujishima when he found that TiO_2 electrodes could decompose water to produce hydrogen and oxygen under ultraviolet light [69-71]. This phenomenon is known as the Hondo-Fujishima effect. This discovery marked the beginning of the development of photocatalytic technology in the scientific community. The publication of relevant research results in a

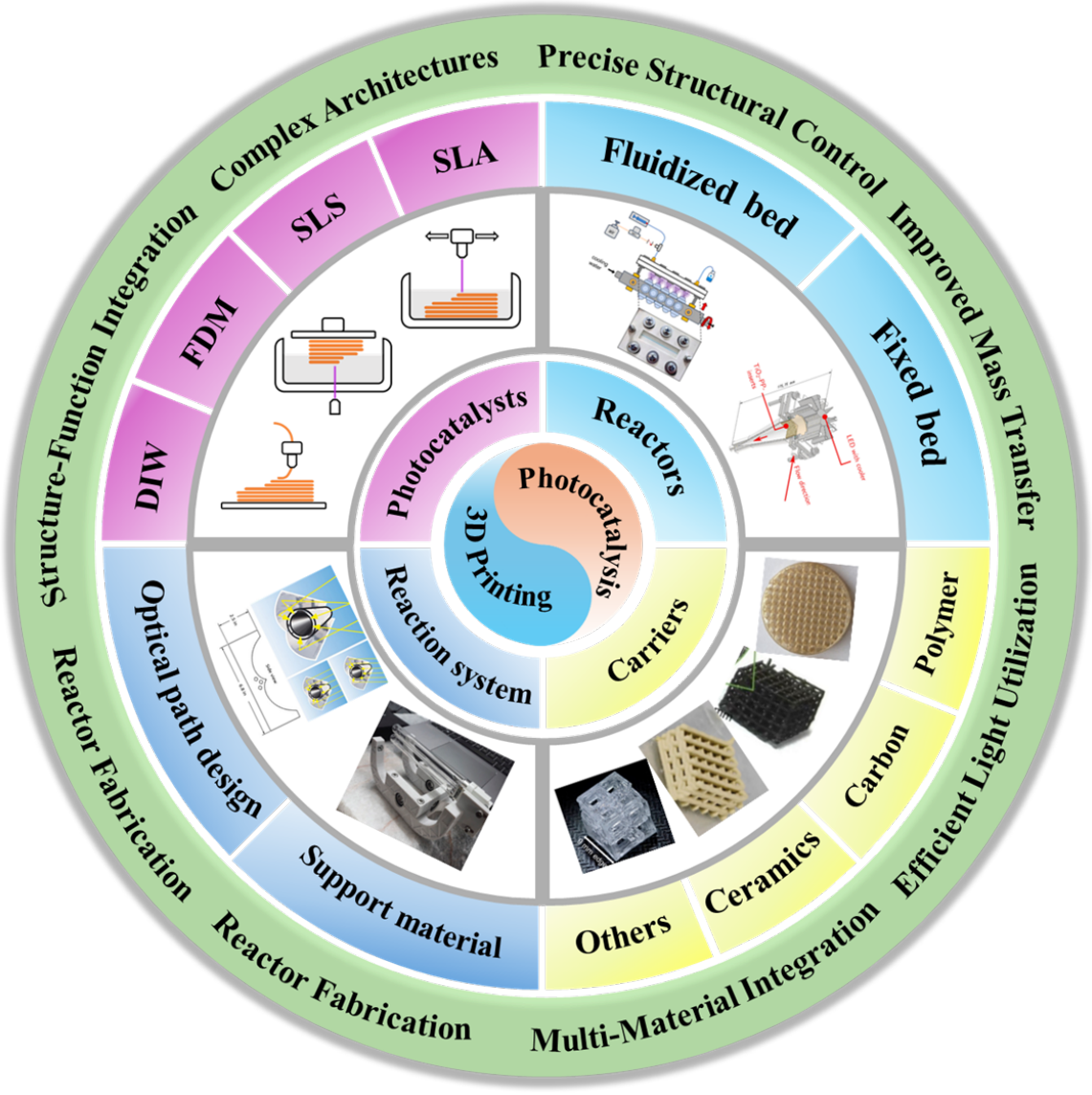

Fig. 2 Various applications of 3D printing (Additive Manufacturing, AM) in the field of photocatalysis (PC). Some inset figures are reproduced from ref. [61] (Copyright 2024, Frontiers); ref. [62] (Copyright 2025, Elsevier); ref. [63] (Copyright 2024, Elsevier); ref. [64] (Copyright 2020, Elsevier); ref. [65] (Copyright 2025, Wiley-VCH); ref. [66] (Copyright 2025, Elsevier); ref. [67] (Copyright 2025, Springer); ref. [68] (Copyright 2023, RSC Publishing); respectively.

magazine in 1972 officially announced the birth of photocatalytic technology. After that, researchers conducted a series of fundamental studies on photocatalytic technology [72-75]. Researchers have focused on the photocatalytic mechanism of TiO_2 and discovered that it cannot only decompose water but also degrade organic pollutants and has a bactericidal function. On this basis, researchers began to explore other semiconductor materials, such as ZnO and WO_3 etc. However, these materials have wide band gaps and can only absorb ultraviolet light, with a very low utilization rate of solar energy [76]. This problem greatly limits the practical application of photocatalytic technology. To break through this core obstacle at the principal level, since the 21st century, researchers have focused on the modification and optimization of photocatalytic materials, optimizing the principal process through targeted measures: The photogenerated carrier separation efficiency is enhanced by element doping [77], the photocatalytic performance is strengthened by heterostructure construction [78], and combined with cocatalyst loading, morphology

regulation and other methods [79, 80]. It not only broadens the light response range of the material, but also enhances the utilization rate of light energy and the efficiency of carrier separation, fundamentally promoting technological breakthroughs and achieving leapfrog development.

2.1.1 Photocatalytic mechanism

The core principle that supports this series of developments can be broken down into three interlinked steps, as shown in Fig. 3. The first step is light absorption. When the energy of the irradiated light is equal to or higher than the band gap (Eg) of the photocatalyst, the electrons in the valence band are excited and jump to the conduction band with higher energy, at the same time, holes are generated in the valence band and photo-induced electron-hole pairs are formed. The second step is charge transfer [81-83]. Direct recombination of electrons and holes results in energy loss. Therefore, it is essential to promote the directional migration of electrons and holes while inhibiting their recombination through approaches like material modification. The third step is surface reaction. Electrons and holes that migrate to the surface of the catalyst, respectively, undergo reduction and oxidation reactions with the species adsorbed on the surface, ultimately enabling key conversion processes−including pollutant degradation, CO_2 reduction, and hydrogen production through photolysis of H_2O [84, 85]. Throughout the entire process, the separation efficiency of electron-hole pairs, the adsorption capacity of surface-active species, and the lifetime of photogenerated carriers are the three core factors determining the efficiency of photocatalytic reactions [86-90]. At present, although photocatalytic technology has shown great application potential in the fields of environmental governance and energy conversion, its practical implementation still faces urgent problems to be solved, including low quantum efficiency and insufficient catalyst stability [91-93]. Based on the above analysis of the development history and principle of photocatalytic reaction, researchers have done a lot of work to optimize the efficiency of photocatalysis, mainly including the design of materials and the search for new catalyst materials. Among the diverse material modification strategies for optimizing photocatalytic performance, heterojunction construction has become a research focus due to its remarkable ability to regulate the core factors mentioned above. By rationally assembling two or more semiconductors with complementary band

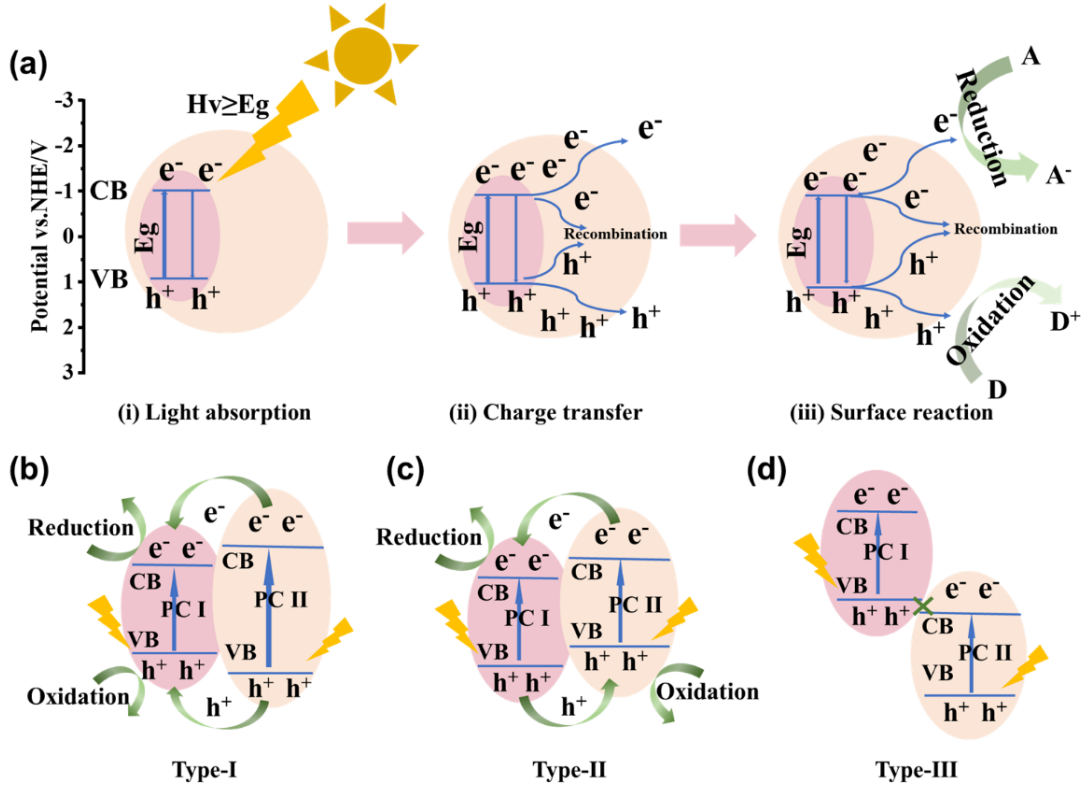

Fig. 3 (a) Core mechanism of photocatalytic reaction, which can be divided into three steps: (i) light absorption, (ii) charge transfer, and (iii) surface reaction. Carrier transfer of (b) type-I, (c) type-II, and (d) type-III heterojunctions.

structures, heterojunctions can construct interfacial charge transfer paths or internal electric fields, which effectively promote the directional migration of photoinduced electrons and holes, drastically inhibiting their recombination and thus extending the lifetime of photogenerated carriers. Moreover, the synergistic effect between heterogeneous components can also enhance the surface adsorption capacity for target reactants and adjust the optical absorption properties of the catalyst, further improving the utilization efficiency of incident light. In recent years, various types of heterojunctions (such as Type-II heterojunctions, Z-scheme heterojunctions, and S-scheme heterojunctions) have been widely explored and applied, achieving significant improvements in photocatalytic activity for pollutant degradation, CO_2 reduction, and water splitting. However, challenges such as interfacial compatibility issues, high charge transfer resistance at the heterointerfaces, and poor long-term stability still restrict the practical application of heterojunction-based photocatalysts. Therefore, developing efficient and innovative new catalysts to achieve low-cost and high-efficiency conversion in photocatalysis is of vital importance. A variety of new types of catalysts, including metal oxides, metal sulfides, and bismuth halogen oxide materials, have been developed and applied in the field of photocatalysis [94-98].

2.1.2 Photocatalysts

As the basis of artificial photosynthesis, the development of photocatalytic materials with appropriate and excellent catalytic performance is particularly crucial. A series of photocatalytic materials with photoresponsivity properties, including semiconductor materials, noble metal coordination compounds and organic molecular materials, have been proven to be ideal for driving photocatalytic reactions. Among these categories, semiconductor materials find extensive application in the photocatalysis field, attributed to their advantages of excellent light absorption capacity, favorable stability, abundant resource reserves, and low material costs [99-102]. Based on their composition, semiconductor materials can currently be classified into several types of photocatalysts, including metal oxides, metal sulfides, metal oxynitrides/halide oxides and non-metals (Fig. 4). As the earliest discovered and studied photocatalytic material within metal oxides, TiO_2 demonstrates traits of good chemical stability, non-toxicity, and low cost, thereby securing wide application in the photocatalysis field. However, traditional TiO_2 materials still have limitations in terms of their wide band gap and high recombination rate of photogenerated carriers. Therefore, a series of modification methods have been adopted for the design of materials based on the traditional TiO_2 phase. Liang et al. reviewed the research on black TiO_2, which has been widely used in environmental and energy fields due to its excellent light absorption capacity [103]. Yang et al. systematically investigated the progress and paradigm shifts in the development of mesoporous TiO_2 photocatalysts [104]. Mesoporous TiO_2-based structures significantly enhance the activity of photocatalysts due to their tunable pore topology, increased surface-to-volume ratio, and improved mass transfer performance. In addition to the well-known TiO_2 material, several other metal oxides, including ZnO [105], WO_3 [106] and In_2O_3 [107], have also been widely reported to be applied in the field of photocatalysis. Nevertheless, limited by the inherent band structure of metal oxide semiconductor materials, these materials have poor absorption in the visible light range. Different from metal oxides, metal sulfide semiconductors usually have a smaller band gap, making them widely used in visible light-driven photocatalytic reactions. According to existing reports, metal sulfides, such as CdS [108] and ZnS [109], exhibit favorable photocatalytic effects. The application of these materials, however, has been constrained to a certain extent, hindered by issues including the inherent toxicity and low stability of metal sulfides themselves. In view of the problem that metal oxides have poor light absorption capacity due to their large band gap, researchers have proposed the design and research of metal oxynitrides [110] and metal halide oxides [111]. Among them, metal oxynitrides formed by doping nitrogen into metal oxides significantly expand the light absorption range to the visible light region [112]. Taking bismuth oxyhalide, a type of metal halide oxide, as an example, its light absorption shows a red-shift from the ultraviolet to the visible light region as the contained halogen element changes from chlorine to iodine [113]. In comparison with metal compound materials, non-metallic materials have found extensive application in the photocatalysis field, leveraging advantages of abundant resources, favorable stability, and low cost[114-117]. Some common non-metallic materials, including graphene [118], carbon nitride [119] and black phosphorus [120], have been confirmed to possess good photocatalytic activity. Wang et al. proposed loading nitrogen-doped graphene quantum dots (NGQDs) onto the surface of $Mn_xCd_{1-x}S$ solid solution nanowires [121]. The optimized $Mn_{0.2}Cd_{0.8}S$/NGQDs ($M_{0.2}NG_5$) composite achieved a high production rate of 6885 μmol g^{-1} h^{-1}. Jang et al. developed a method to produce one-dimensional (1D) P-doped carbon nitride nanotubes via supramolecular

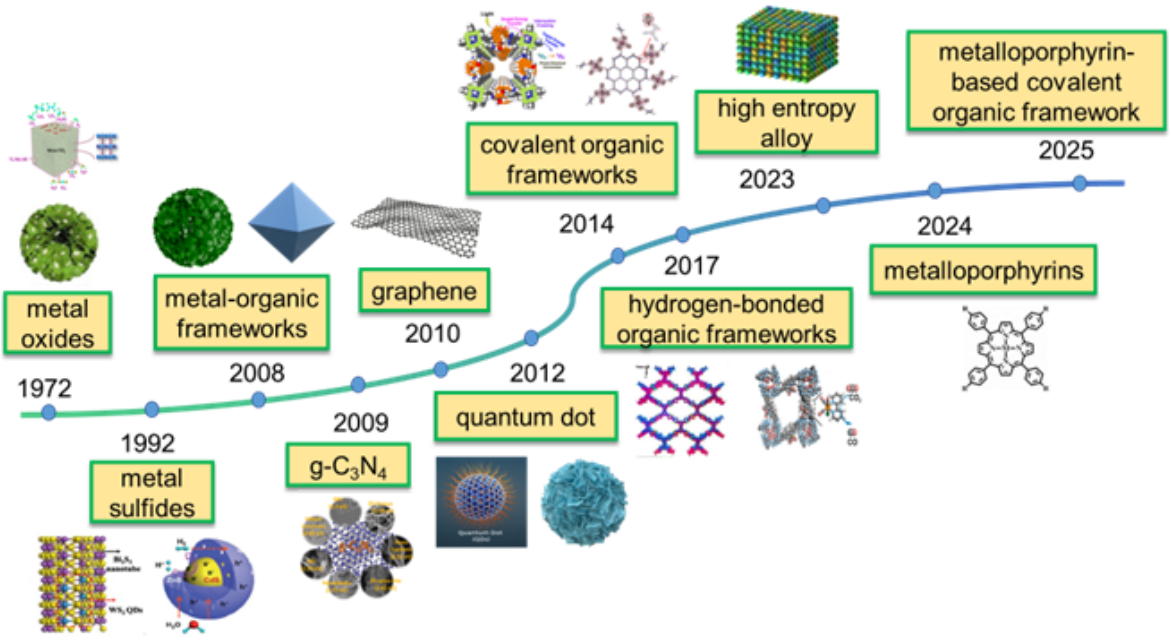

Fig. 4 Development of photocatalytic materials. Some inset figures are reproduced from ref.[106] (Copyright 2025, Elsevier); ref.[104] (Copyright 2025, Wiley-VCH); ref.[128] (Copyright 2019, Wiley-VCH); ref.[129] (Copyright 2019, Elsevier); ref.[130] (Copyright 2021, Springer); ref.[131] (Copyright 2023, Elsevier); ref.[132] (Copyright 2025, Elsevier); ref.[133] (Copyright 2024, ACS Publications); ref.[125] (Copyright 2021, Wiley-VCH); ref.[134] (Copyright 2020, ACS Publications); ref.[135] (Copyright 2021, Wiley-VCH); respectively.

self-assembly, which exhibited good photocatalytic HER activity [122]. Shen et al. synthesized a Ni_2P-BP photocatalyst by selectively growing Ni_2P on the edges of BP nanosheets, and this catalyst achieved 100% selectivity for the photocatalytic reduction of N_2 to NH_3 [123]. In contrast to traditional photocatalysts, reticular framework materials, particularly metal-organic frameworks (MOFs) and covalent organic frameworks (COFs), have emerged as highly promising photocatalytic materials. This status is attributed to their characteristics of ultra-high surface area, customizable pore environment, and modular functionality [124]. A large number of reports have shown that MOFs, COFs and their composite materials are excellent photocatalytic materials. Chen et al. proposed and constructed a series of covalently linked multi-component Ti-MOF/COF hybrid materials, with the optimal composite achieving a photocatalytic H_2 evolution rate of 12.8 mmol g^{-1} h^{-1} under simulated sunlight irradiation [125]. Wang et al. successfully synthesized three MOFs based on tetrakis(4-carboxyphenyl) porphyrin (TCPP) via a solvothermal method, and the Zr-Ni PMOF showed a coupling reaction conversion rate of 89% for benzylamine under visible light, with a selectivity of 95% for the target product [126]. Deng et al. designed and constructed PDI/COFs hybrid materials with different ratios via a solvothermal method, denoted as PDI/TAPB-PDA (where TAPB=1, 3, 5-tris(4-aminophenyl) benzene and PDA = terephthaldehyde) [127]. Among these materials, the optimal composite PDI/TAPB-PDA-5 shows the highest photocatalytic performance for Cr(VI) reduction. To tackle issues including low solar energy utilization efficiency, high recombination rate, and limited activity, considerable research efforts have been devoted to the preparation and selection of catalysts. However, the structural impact of the catalyst substrate itself has been neglected, and traditional methods for the preparation of catalyst matrices remain restricted by factors such as the complexity of catalyst loading, as well as the stability and corrosion rate of the support.

2.1.3 Photocatalytic reactors

A photocatalytic reactor is a device that utilizes semiconductor-based photocatalysts to drive a series of redox reactions under visible light or simulated solar illumination, with the aim of achieving goals like environmental pollutant degradation and energy conversion [136]. Its core function lies in its comprehensive enhancement of photocatalytic reaction performance by improving light energy utilization efficiency, optimizing the mass transfer process, and refining the contact between the catalyst and reactants [137]. In recent years, a variety of novel photocatalytic reactor designs have emerged, including photocatalytic

membrane reactors that integrate catalytic functionality with separation membranes, microchannel reactors that leverage microscale effects to enhance mass transfer and light absorption, and bionic structured reactors constructed based on 3D printing technology [138-141]. Among these, the latter simulates the efficient light-harvesting and mass transfer pathways in natural photosynthesis, demonstrating significant advantages. Particularly in the field of photocatalyst design, 3D printing technology has achieved breakthrough progress. It enables the controllable construction of hierarchical porous structures, achieves precise regulation of heterojunction interfaces, and realizes optimization of active site distribution, all of which effectively enhance the performance and stability of catalytically active components [142]. The efficient implementation of photocatalytic reactions is not only regulated by core factors including catalysts, reactants and reactors, but also highly dependent on the adaptability between catalysts and reaction environments, the optimization of energy input conditions, and the efficiency of mass transfer processes [143]. These multiple factors collectively constitute the key variables affecting reaction performance. Therefore, the configuration design and system integration of the reactor itself play a crucial role in improving overall catalytic efficiency, and also represent a key direction for the future development of this field.

From the fixed loading of catalysts to the precise control of reaction flow fields, from the improvement of light utilization efficiency to the integrated operation of multiple reaction unit, the limitations of traditional manufacturing methods in achieving structural and functional matching have become increasingly prominent [144]. For example, mechanical processing is difficult to produce micro-sized or nano-sized irregular flow channels, and injection molding cannot achieve material gradient distribution. These defects make it difficult to effectively transform the optimization of a single catalyst's performance into an overall efficiency increase of the reaction system, becoming a key bottleneck restricting the industrialization of photocatalytic technology.

Therefore, further expanding the design freedom and manufacturing accuracy of 3D printing technology to the level of photocatalytic reactors and the overall system, and solving the coupling problems of multiple elements through structural innovation, has become a key link in breaking through the bottlenecks of traditional photocatalytic technology applications and promoting its transition from laboratory research to industrial application.

2.1.4 *In-situ* characterization for revealing mechanisms

As a complement to the prospective methodology introduced in the previous section, this section focuses on in-situ characterization techniques that are already mature in traditional photocatalysis but have not yet been widely adopted in the cross-disciplinary field of 3D printed photocatalysis. Given that the current research emphasis is on verifying the feasibility of 3D printing and demonstrating performance at the macroscale, mechanistic studies are still preliminary. However, as the field matures, in-situ characterization will become an essential tool for decoding microscale mechanisms. The following is a brief overview of validated in-situ techniques, laying the foundation for future research in this interdisciplinary field.

In-situ characterization technology can monitor various changes in the process of photocatalytic reaction in real time, which provides key information for understanding the performance and reaction mechanism of photocatalysts [145]. By combining different in-situ technologies, we can more comprehensively reveal the various steps in the photocatalytic process, and provide a theoretical basis for the design of more efficient and stable photocatalysts [146]. In-situ characterization technology has not been widely used in the characterization of photocatalysts combined with 3D printing technology. At this stage, the primary goal of many studies is to verify the feasibility of 3D printing as a manufacturing method in the field of photocatalysis. Therefore, the research focus tends to show the superiority of macro performance, temporarily reducing the urgency of deep mining of micro mechanism. However, it can be predicted that with the further research, more in-situ characterization techniques will be applied to the study of the reaction mechanism of 3D printing photocatalysts. At the same time, a series of in-situ characterization techniques have been widely used in the field of photocatalysis. Therefore, it is necessary to briefly introduce these validated in-situ characterization techniques.

A single photocatalytic reaction usually occurs between microseconds and milliseconds. In situ characterization technology allows real-time monitoring of the structure, electronic properties of the catalyst and the dynamic changes of reaction intermediates under real reaction conditions, so as to directly reveal the reaction mechanism. At present, Fourier transform infrared spectroscopy (FTIR), Raman spectroscopy (Raman), electron paramagnetic resonance (EPR) and atomic absorption spectroscopy (XAS) are mainly used to identify and quantify the

activation/conversion and mass transfer of reactants [147]. In-situ FTIR is an important tool to study the adsorption, activation and transformation of reactants in photocatalytic reactions. Three operating modes, namely, diffuse reflectance infrared Fourier transform spectroscopy (DRIFTS), transmission mode and attenuated total reflection (ATR) mode, are usually used to process materials with different properties. Fu et al. studied the photocatalytic oxidation of methanol by TiO_2 using in-situ DRIFTS, and determined that the photocatalytic activity of TiO_2-(101) surface was higher than that of TiO_2-(001) and TiO_2-(100) surfaces through spectral changes [148]. TiO_2-(101) surface could activate CH_3OH and CH_3O-, while TiO_2-(001) and TiO_2-(100) surfaces mainly activated CH_3O-. Ana et al. monitored the photocatalytic oxidation of cyclohexane in real time by in-situ ATR-FTIR [149]. The absorption band appears only after oxygen isotope exchange treatment, which indicates that dissolved oxygen is not directly involved in the photocatalytic oxidation of cyclohexane. With the passage of time, the absorption band of cyclohexanone carbonyl ($C=^{18}O$) on the surface of TiO_2 catalyst gradually increased, indicating that the formation of cyclohexanone is a continuous process. In-situ Raman technology can identify chemical substances by inelastic light scattering, which can provide information about the structure and surface properties of photocatalysts. Cai and his colleagues prepared 4-NTP monolayer photocatalysts on Au(111) surface by drop coating method and impregnation method to study the photocatalytic coupling reaction [150]. Through the changes of the spectrum, it was found that most of the surface areas of the drop coating samples had efficient photocatalytic coupling reaction, while most of the surface areas of the impregnation samples had no reaction, and only a few isolated areas had reaction. This shows that the arrangement of molecules has a significant effect on the efficiency of photocatalytic coupling reaction. In-situ EPR technology can detect the free radicals and unpaired electrons produced in the photocatalytic process, so as to provide dynamic information about the generation, migration and reaction of free radicals, and help reveal the mechanism of electron transfer in the photocatalytic reaction. Zhang et al. Synthesized a Cu monatomic catalyst (CuSA-TiO_2) for photocatalytic hydrogen production [151]. The CuSA-TiO_2 catalyst achieves a photocatalytic hydrogen evolution rate of 356 μmol g^{-1} h^{-1} under UV-visible light, with a quantum yield of 8.2% at 420 nm. In situ EPR results showed that Cu^{2+} was reduced to Cu^{+} during the photocatalytic reaction, and the subsequent oxidation process exposed to air showed that Cu species had a reversible redox cycle in the reaction, which might be one of the key factors for the high photocatalytic activity of CuSA-TiO_2. In-situ XAS technology can monitor the changes of the electronic structure and chemical state of the catalyst in the photocatalytic reaction in real time. It can provide information about the oxidation state, coordination environment and electron density of metal ions in the catalyst, which is helpful to understand the activity and stability of the catalyst. Liu et al. observed the changes of Cu during the experiment by in-situ XANES and found that the high activity of Cu/Ti(H_2) catalyst was attributed to the abundant Cu^{+} species on its surface, and these Cu^{+} species were prone to oxidation during the reaction, thus leading to the deactivation of the catalyst [152]. By combining different in-situ characterization techniques, we can more comprehensively reveal the various steps in the photocatalytic process, and provide a theoretical basis for the design of more efficient and stable photocatalysts.

2.1.5 DFT calculation for revealing mechanisms

This section introduces density functional theory (DFT) calculations, a core theoretical tool in the field of photocatalysis, and focuses on exploring its potential value and existing challenges in the cross-field of 3D printing and photocatalysis. Although DFT excels in exploring mechanisms at the atomic scale, combining it with the macroscale structural advantages of 3D printing requires multiscale modeling to bridge the gap between atomic simulations and macroscale effects. This topic will be discussed alongside the basic principles and applications of DFT in the following sections.

Thanks to the rapid development of computer technology, theoretical calculation can help researchers in many aspects such as experimental design, result analysis and mechanism exploration at each stage of the experiment [153, 154]. First principles calculations are widely used in the field of photocatalysis, mainly due to the development and improvement of density functional theory (DFT) [155-157]. The core idea of DFT is to describe the physical properties of a system using the electron density of the system's ground state instead of complex many-body wave functions, which significantly simplifies the calculation [158]. To solve it practically, DFT employs some key approximations, among which the exchange-correlation functional is the core [159]. Common approximation methods include the Local Density Approximation (LDA) and the Generalized Gradient Approximation (GGA), with the latter being more commonly used. To calculate the semiconductor band gap more accurately, a hybrid functional is also used [160]. A typical DFT calculation

is a self-consistent iterative process: first, an initial electron density is guessed, then the Kohn-Sham equation is solved to obtain a new electron density, the new and old densities are compared, and the process is repeated until convergence, thereby obtaining the ground state energy and electronic structure of the system. In the field of photocatalysis, DFT calculations can be applied to band structure and state density analysis, reaction path and free energy calculation, heterojunction and interface design, mechanism analysis of cocatalysts, and high-throughput screening of new materials. Wu et al. successfully synthesized a cobalt-based triphenylene framework catalyst with a staggered stacking structure in pure aqueous phase, achieving a synthesis yield as high as 90% [161]. Density functional theory calculations indicated that the CO yield was mainly influenced by ΔG*H, electronegativity (χ), optical band gap, and the increment of reaction rate, rather than the traditionally believed ΔG (*COOH). This new understanding reveals that the photocatalytic CO_2 reduction is a complex process involving the synergy of multiple factors in both kinetics and thermodynamics, providing a new perspective for the design of novel catalysts. The unique advantage of 3D-printed photocatalysts lies in their designable macroscopic three-dimensional structure. DFT is proficient in simulating catalytic reactions at the atomic scale within a few nanometers. However, to effectively correlate the effects of atomic-scale simulations on the light absorption and mass transfer efficiency of complex three-dimensional structures at the macroscopic millimeter or even centimeter scale is a significant challenge currently faced by computational science.

The disconnection between DFT simulations and macroscale 3D structural effects underscores the pivotal role of multiscale modeling in this interdisciplinary field, yet it faces two major challenges. Firstly, there is the computational complexity of integrating DFT calculations with macroscale fluid dynamics and optical simulations. Secondly, there is a lack of standardized models to correlate 3D printing-induced microstructures with atomic-level catalytic activity. Despite these obstacles, there are significant opportunities. Multiscale modeling can guide the rational design of 3D printed photocatalysts, optimize printing parameters to match active sites identified by DFT, or predict how macroscale porous structures enhance light capture and reactant diffusion. As this interdisciplinary field matures, multiscale modeling will become a crucial bridge to maximize the synergistic effect between 3D printing structural control and atomic-scale activity in photocatalysis.

2.2 Overview of 3D printing technology

3D printing technology, also known as additive manufacturing technology, is a manufacturing technique that builds three-dimensional objects by layering materials based on digital model files [162-164]. Its core feature is layer-by-layer fabrication and successive addition, which contrasts sharply with the material removal approach of traditional subtractive manufacturing methods [165-167]. In 1984, Charles Hull invented SLA technology and obtained a patent, which marked the official birth of 3D printing technology. In 1988, Scott Crump proposed FDM technology, promoting the development of low-cost equipment. From the 1990s to the early 21st century, technologies such as SLS and Selective Laser Melting (SLM) emerged one after another, further expanding the range of applicable materials. After 2010, with the popularization of open-source technology and the expiration of patents, the cost of 3D printing has significantly decreased, and its application fields have expanded from industrial prototypes to aerospace, medical care, architecture and other fields [59, 168-171]. According to the ISO/ASTM 52900:2021 standard, 3D printing technologies can be classified into seven categories, as shown in Fig. 5 [172]. Vat Polymerization initiates curing reactions by irradiating liquid photopolymers with light sources, with core representative technologies including SLA, Digital Light Processing (DLP), and Continuous Digital Light Processing (CDLP). Material Extrusion relies on heated nozzles to extrude and deposit molten thermoplastic plastics, typically represented by FDM or Fused Filament Fabrication (FFF). Powder Bed Fusion achieves melting and solidification of powder particles using high-energy sources, covering SLS, SLM, Multi Jet Fusion (MJF), and Electron Beam Melting (EBM). Material jetting deposits shapeable materials in the form of droplets and finishes curing. The representative technologies include material jetting (MJ), nanoparticle jetting (NPJ), and on-demand drop (DOD). Binder Jetting realizes the bonding of particulate materials by depositing liquid binders, represented by Binder Jetting (BJ) technology. Direct Energy Deposition synchronously completes the processes of metal melting, deposition, and fusion, with representative technologies including Laser Engineered Net Shaping (LENS) and Electron Beam Additive Manufacturing (EBAM). Sheet Lamination achieves manufacturing through cutting and forming of material sheets and layer-by-layer lamination, with Laminated Object Manufacturing (LOM) technology as the core. The specific details are shown in Table. 1.

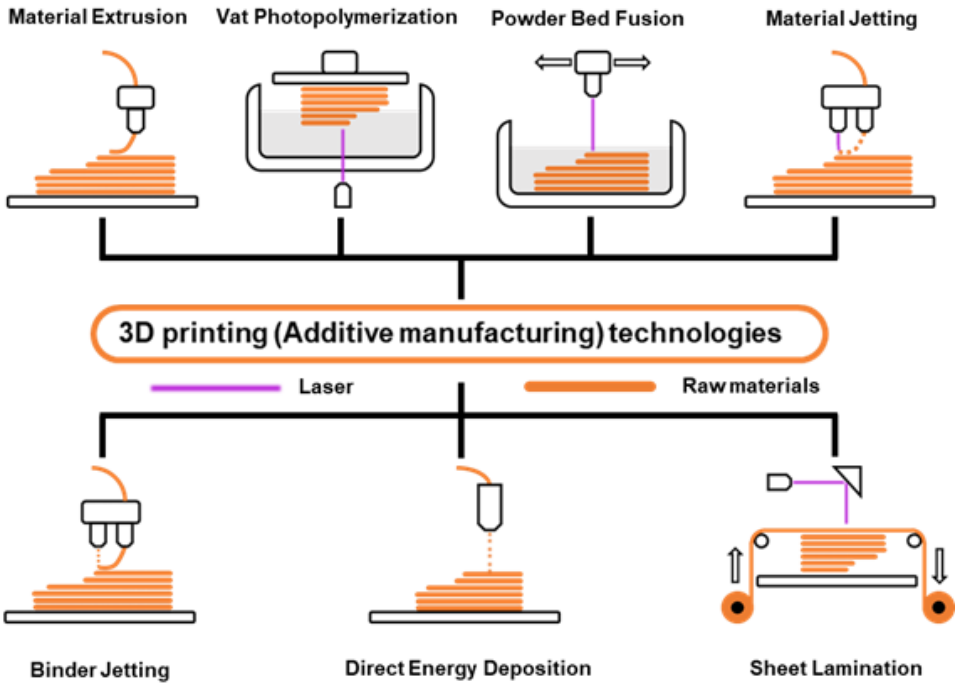

Fig. 5 Different kinds of 3D printing technologies.

Table. 1 Classification, Principles and Applications of 3D Printing Technology

Technology Category	Principle	Common Materials	Characteristics and Applications	Relevance to Photocatalysis	Ref.
Vat Photopolymerization	Using ultraviolet or visible light to selectively irradiate liquid photosensitive resins, causing them to undergo photopolymerization reactions and solidify into shapes	Photosensitive resins	High forming precision (±0.02-0.1 mm), good surface finish, relatively brittle material mechanical properties, suitable for fine models, mold prototypes, micro-nano structure manufacturing	High, relevance	[59]
Material Extrusion	Materials are extruded from nozzles or orifices through mechanical driving, and deposited layer by layer for solidification to form shapes	Thermoplastic polymer filament, ceramic slurries, bio-inks, etc.	Low equipment cost, simple operation, medium precision (±0.1-0.5 mm), suitable for small and medium-sized parts, education, household use, customized parts, bio-scaffold preparation	Most widely used	[50]
Powder Bed Fusion	Lasers or electron beams are used to selectively melt or sinter the surface materials of powder beds, stacking layer by layer to form solids	Metal powders, polymer powders	No support structure required, high part density, high equipment cost, suitable for complex metal components, high-strength plastic parts	Medium-high relevance	[45]
Material Jetting	Similar to the principle of 2D inkjet printing, tiny material droplets are accurately jetted through nozzles and solidified by cooling or photopolymerization	Photosensitive resins, waxy materials, metal inks	High precision (±0.05 mm), multi-material composite printing available, slow speed, high cost, suitable for multi-material prototypes, precision casting wax pattern preparation	Medium relevance	[172]
Binder Jetting	Binders are selectively jetted onto powder beds to bond powder particles into shapes, requiring subsequent sintering or impregnation for reinforcement	Metal powders, ceramic powders, sand, polymer powders	Fast forming speed, high material utilization, post-processing required, suitable for sand casting molds, metal/ceramic part pre-forming, architectural models	Medium relevance	[44]
Directed Energy Deposition	Focused high-energy beams are used to melt synchronously delivered materials for point-by-point deposition and forming	Metal filaments/powders, ceramic powders	High material density, large component manufacturing available, part repair available, expensive equipment, suitable for aerospace, shipping and other high-end industrial fields	Low relevance	[51]
Sheet Lamination	Thin materials are cut by lasers and bonded layer by layer to form three-dimensional structures	Glue-coated paper, composite thin sheets, metal foils	Fast forming speed, low cost, low precision, low material utilization, gradually decreasing applications, suitable for rapid prototypes, low-cost model making	Low relevance	[53]

Compared with traditional manufacturing methods, 3D printing technology shows significant technical advantages [173-175]. Firstly, it has extremely high design freedom, which can break through the limitations of traditional processing on molds and tool paths, and directly manufacture parts with complex inner cavities, hollow structures, and topology-optimized shapes, providing unlimited possibilities for structural innovation. Secondly, the production cycle is significantly shortened. The conversion cycle from digital models to physical parts can be reduced to several hours to days, which is especially suitable for rapid prototype verification in the product research and development stage. For small-batch production, there is no need to open molds, which significantly reduces time and economic costs. Thirdly, the material utilization rate is significantly improved. The material utilization rate of traditional subtraction manufacturing is low, while the material utilization rate of 3D printing technology can be significantly improved. For high-priced materials such as titanium alloys and precious metals, the economic benefits are particularly prominent. Fourthly, it has outstanding personalized customization capabilities. Personalized design and production of products can be realized only by modifying digital models without adjusting the production line, which has irreplaceable advantages in the fields of medical implants and personalized consumer goods. Fifthly, it has excellent integrated manufacturing capabilities, which can integrally form structures that need to be assembled with multiple components in traditional manufacturing, reducing assembly links, lowering error accumulation, and improving the reliability of overall performance [176-178].

Different 3D printing technologies show unique advantages in application scenarios due to differences in principles and material properties. DIW technology in material extrusion, which forms shapes by extruding high-viscosity slurries, can flexibly adjust material composition and structure, and is especially suitable for preparing photocatalytic carriers with multi-level pore structures [179]. FDM uses low-cost polymer filaments as raw materials, and the equipment is highly popular, suitable for preparing photocatalytic reactor shells or basic structural parts [180]. The SLA technology in vat photopolymerization, relying on high-precision forming capabilities, can prepare photocatalytic devices with micro-nano scale channels, improving photocatalytic reaction efficiency [181]. The SLS technology in powder bed fusion can directly sinter ceramic or composite powders to prepare high-strength and high-stability photocatalytic materials, meeting the needs of complex working conditions [182]. These technologies, with their respective characteristics, have become mainstream means for constructing new catalytic materials and devices in the field of photocatalysis, providing a new technical path for the structural optimization and performance improvement of photocatalytic reaction systems [183].

3 3D printing technology applied to photocatalysis

The design of photocatalysts and their carriers is the core factor determining the efficiency and stability of photocatalytic reactions [184]. The density of active sites, electron transfer pathways, and light absorption range of photocatalysts, as well as the specific surface area, pore structure, and surface affinity of the carriers, are coupled with each other and jointly constitute the key factors affecting the performance of photocatalysis [185]. Traditional preparation methods have significant limitations in constructing complex micro-nano structures, achieving precise multi-component composites, and regulating interface characteristics. The sol-gel method is difficult to control the uniform dispersion of catalyst particles, the impregnation method often leads to insufficient loading of active components and uneven distribution, and the pore volume and pore size distribution of the carrier are difficult to be finely adjusted in the conventional sintering process. These deficiencies directly restrict the separation efficiency of photogenerated carriers and the mass transfer rate of reactants.

Therefore, 3D printing technology, with its flexibility in layer-by-layer manufacturing, compatibility in multi-material co-printing, and designability of cross-scale structures, provides a new approach for the innovative design of photocatalysts and carriers. 3D printing technology can break through the geometric constraints and material limitations of traditional manufacturing processes. By directing the regulation of the structure, it can achieve atomic-level doping of active components, multi-level layered pore structure design of photocatalyst, and multi-level complex carrier framework construction, enabling controllable design for the optimization of material performance.

3.1 Design of photocatalysts

3.1.1 FDM technology for photocatalyst fabrication

Fused Deposition Modeling 3D printing technology has become the most popular 3D printing method due

to its simple forming method and low cost. It consists of five parts: nozzle, wire feeding system, drive system, heater and working platform [186]. The equipment melts filamentous consumables into liquid from the nozzle through an extrusion head equipped with a heater. The extrusion head moves along the contour of each cross-section of the printed object, and the extruded semi-fluid material cools and solidifies into a fine thin layer to cover the printed object [187]. After the molding is completed, the worktable descends by one height, and the extrusion head repeats the upper steps, depositing layer by layer and stacking layer by layer to form a solid model [188]. For the commonly used desktop FDM 3D printers, the layer height of the model in the Z-axis direction should reach at least 100 μm, and the accuracy in the X-axis and Y-axis directions can be controlled within 500 μm [189]. However, the models printed by FDM 3D have clear layering patterns. For objects with high requirements for surface flatness, post-processing methods such as polishing are needed [190]. The materials of FDM 3D printing technology are polymer filaments with thermoplastic properties, including polylactic acid (PLA), acrylonitrile butadiene styrene (ABS), polycarbonate (PC), etc. [191-193]. However, the glass transition temperature and exposed surface area of these thermoplastic polymers are relatively low, making them unsuitable for direct use in catalytic reactions. Meanwhile, they exhibit poor stability and are easily affected by heat and light, thereby altering their physical and chemical properties [194].

There are two methods for preparing FDM 3D printing catalysts. One is to incorporate the catalytic active components into the organic polymer framework and fully mix them to form a composite material for the manufacturing of integral catalyst 3D printing. This blending process is generally completed during the preparation of printing consumables. Firstly, the polymer materials are melted or dissolved in a solvent and uniformly blended with catalytic materials to form filaments, which are then made into integral catalytic materials through FDM 3D printing. This method is prone to cause the active site to be wrapped by the polymer material, making it difficult to come into contact with the reaction substrate and reducing the activity [199]. Majooni et al. used FDM 3D printing technology to construct PLA porous scaffolds with various structures and optimized the filling structure [65]. Among them, the surface area of the helical structure was 3259.2 mm^2, and the loading of nanocomposites was the highest. Acetone etching was used to enhance the surface roughness of the scaffolds, and combined with polydopamine as a biological adhesive, the loading capacity of the Cu-TiO_2/rGO nanocomposite coating was increased by 378% and the leaching amount was reduced by 200%. The composite scaffold could remove 89% methylene blue (MB) under visible light for 60 min, 93% for 120 min, and 91.4% for 30 cycles (Fig. 6a). Ortega-Columbrans et al. fabricated PLA/TiO_2 composite filament by FDM 3D printing technology, and printed 3D scaffolds with linear and helical filling structures, while fabricating 2D composite membrane by the flow-through method [195]. Under UV light, the degradation rate of methyl orange was 98% for 2D films, 80% for spiral filled scaffolds, and 60% for linear scaffolds. The 50% degradation time of methyl orange of the spiral scaffold was 6.1 h, which was better than that of the linear scaffold (8.9 h), and the composite wires had good thermal stability (Fig. 6b, c).

Another rule is to combine the catalytic material on the surface of the catalyst by means of grafting and bonding, etc. to carry out catalytic action. However, this method is prone to causing the shedding of active sites. The preparation process of FDM 3D printing catalysts has strong universality and is compatible with various common desktop 3D printers on the market, making it easy to apply and promote [200]. Khezri *et al.* used FDM 3D printing to fabricate a hollow tubular intelligent dust robot using graphene/PLA as raw material [196]. The Fe_3O_4 nanoparticles were immobilized on the surface for magnetically controlled recovery, and then coated with a chitosan/carbon nitride (g-C_3N_4) hydrogel layer to desorb picric acid under visible light due to the synergistic adsorption property of chitosan and the photocatalytic activity of g-C_3N_4. The degradation efficiency was up to 38% within 10 min, and the activity was still maintained after 3 cycles of recycling, which provided a new scheme for mobile photocatalytic degradation of pollutants (Fig. 6d). Munoz et al. used FDM 3D printing to construct G/PLA nanocomposite scaffolds, which were activated by DMF to synthesize amorphous Ag_3PO_4 (a-Ag_3PO_4) and faceted Ag_3PO_4 (f-Ag_3PO_4) nanostructures in situ [197]. Using this scaffold for visible light photocatalysis, the degradation rate of rhodamine B (RhB) by f-Ag_3PO_4@G/PLA was significantly higher than that by a-Ag_3PO_4@G/PLA, and the photocurrent of water and oxygen development was 18 times higher than that of the latter, and the charge transfer resistance was lower (Fig. 6e). Mimerand et al. designed single-layer and multi-layer superimposed fractal scaffolds by FDM 3D printing of PLA fractal structures (fracmids and fracones) [198]. They used plasma grafting technology to fix the ZnO@PAA core-shell nanoparticles on the surface of

the scaffold. The prepared composite materials degrade 63% RhB under simulated sunlight for 5.5 h, and can be reused after ultrasonic cleaning. It is proved that the fractal structure printed by FDM can effectively improve the contact efficiency between the catalyst and the pollutants (Fig. 6f). In another study, they used the same method to print PLA fractal scaffolds, and fixed ZnO, TiO_2 and Fe-MOF nano catalyst by plasma grafting, respectively [201]. The degradation rate of RhB in the ZnO@PAA2.5 loaded four-layer fractal scaffold was 94.3%, and the removal rate of ciprofloxacin in the Fe-MOF loaded scaffold was 42%. The photoactivity of the ZnO@PAA core-shell catalyst was increased by 20%, and the efficiency of the scaffold was only decreased by 10.6% after three cycles of cycling, reflecting the application value of FDM printing in the fixation and efficient degradation of multitype photocatalysts.

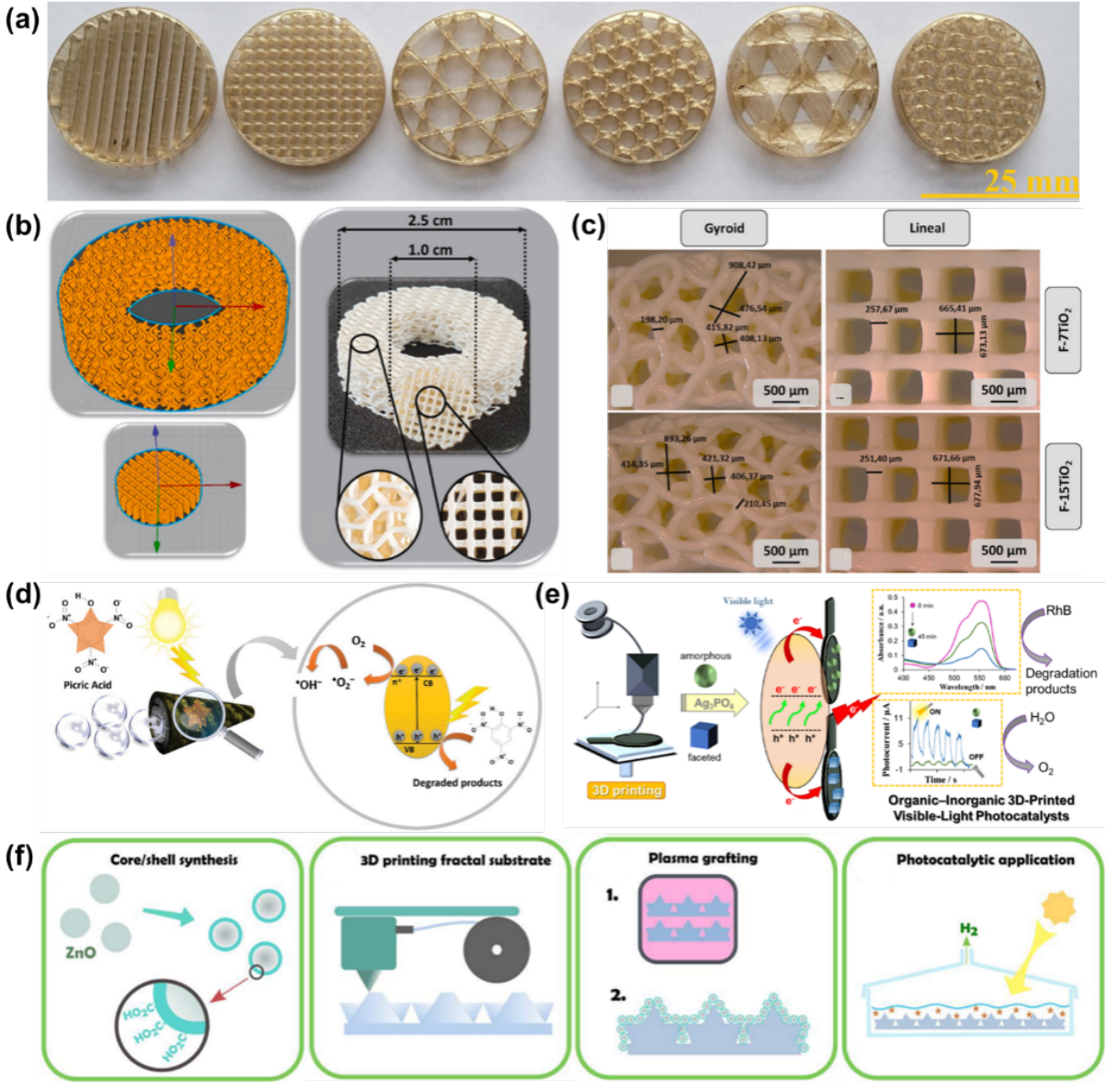

Fig. 6 (a) Six different 3D printed scaffold designs.[65] (Copyright 2025, Wiley-VCH) (b) Virtual Models with Gyroscopic and Linear Filling and Their Physical Diagrams. (c) Details of the scaffold structures with different doping amounts (TiO_2 7 vol% and 15 vol%) and different structures (gyro, linear).[195] (Copyright 2023, Elsevier) (d) Illustration of the photocatalytic degradation mechanism on the 3D-printed robots.[196] (Copyright 2020, Wiley-VCH) (e) Schematic illustration for the faceted crystal nano architectonics of organic−inorganic 3D-printed visible-light photocatalysts and their environmental applications.[197] (Copyright 2022, ACS Publications) (f) Different stages of the manufacturing and usage process of photocatalysts.[198] (Copyright 2019, ACS Publications)

In summary, FDM technology, with its low cost and widespread equipment availability, has become the most easily scalable method for preparing 3D-printed photocatalysts. However, the poor heat resistance of polymer substrates and the tendency for active components to be encapsulated limit its application in high-temperature reactions or scenarios demanding high activity. Additionally, insufficient printing accuracy can easily affect the uniformity of the microstructure, necessitating post-processing optimization such as acetone etching.

3.1.2 DIW technology for photocatalyst fabrication

Ink direct writing is another 3D printing technology based on extrusion [202]. DIW 3D printing technology uses ink pastes with high solid content to print parts with high aspect ratios or without bridging structures and supports. During the process, the ink is placed in a rubber cylinder. As the printing nozzle moves, the air pressure or mechanical device uses the shear thinning ability of the slurry to extrude it out, completing the layer-on-layer stacking and maintaining the shape. After the solvent evaporates, it densifies or self-cross-links and solidifies to form a three-dimensional object. It can directly extrude masterbatch materials without the need for melting and solidification processes [203]. In the early stage of the development of ink direct writing 3D printing forming, the related technical concept was first proposed by the team of J. Cesarano at Sandia National Laboratories in the United States [204]. It was widely used in the forming process of ceramic materials, using ceramic suspension slurry as raw material to prepare uniform, fine and controllable three-dimensional ceramic structures [205]. The DIW 3D printing technology is typically used in the preparation process of catalysts by compounding catalytic components with materials such as polymers, metal oxides or gels, adding appropriate solvents to prepare 3D printing inks for three-dimensional manufacturing, and then the object undergoes post-processing to obtain the catalyst [206]. 3D printing ink needs to have its components and quantities adjusted to ensure good fluidity for smooth extrusion. At the same time, it also needs sufficient plasticity to maintain its shape after extrusion molding [207]. The rheological properties of 3D printing ink can be expressed by the Herschel-Bulkley formula, as shown in formula (1).

$$\tau = \tau_\gamma + K\gamma^n \quad (1)$$

where, n represents the shear thinning index, γ represents the shear rate, K represents the viscosity index, τ_γ represents the yield stress, and τ represents the shear stress. The 3D printing ink slurry needs to flow and deform. Due to the existence of τ_γ, the shear stress τ must be greater than the yield stress τ_γ of the material itself. Meanwhile, when $0< n< 1$, the apparent viscosity τ_γ of the slurry decreases with the increase of the shear rate, and the shear thinning behavior occurs. In addition to shear thinning and deformation, the printing conditions of 3D printing ink slurry also need to meet the requirement of having sufficient viscoelasticity to maintain its own structure. The viscoelasticity of the slurry is expressed by the following formula (2).

$$y = k\left(\frac{\varphi}{\varphi_{gel}} - 1\right)^x \quad (2)$$

In the formula, φ_{gel} represents the volume fraction of solid content at the gel point, φ represents the volume fraction of the solid phase, and y represents the elastic modulus. Therefore, the solid content of the slurry can be increased and the solid content at the gel point can be reduced to improve the elastic modulus of the 3D printing slurry.

DIW technology is one of the most reported methods for manufacturing 3D printed monolithic catalysts at present [214]. Its greatest advantage is that there are fewer restrictions on the types of materials. The water-based colloid paste system, degradable organic paste system and polyelectrolyte paste system in ink dispensing technology can be matched with the DIW 3D printing process, enriching the selection range of raw materials [215-217]. Yu et al. prepared a grid-like photocatalytic material A-bio-Cu-BTC. Pollen was used as a biological template to assemble Cu-BTC nanoparticles [208]. SA, CMC and catalyst were mixed to make printing ink, which was cross-linked and freeze-dried by $CaCl_2$ after printing. The material is used for organic dye degradation. During recycling, the surface porosity exposes more active sites, the Cu(I)/Cu(II) ratio increases from 0.80 to 1.67 to enhance the catalytic activity, and the tensile strength reaches 0.45 MPa. The specific surface area of Cu-BTC only decreased by 8.9% after soaking in 60℃ deionized waters for 24 h, and the hydrolytic stability and mechanical properties were significantly better than those of pure Cu-BTC (Fig. 7a). Lu et al. prepared 3D-FeO/C electrodes by DIW 3D printing, and mixed Fe_3O_4 nanoparticles, carbon black, PAN and HPMC to make printing ink [209]. After printing, the macroscopic ordered pore structure was formed by pyrolysis at 600℃. This electrode can efficiently degrade ornidazole and actual pharmaceutical wastewater (TOC removal of 51.13% in 420 min), reduce metal leaching (Fe leaching < 0.2 mg L^{-1}) by the active site of FeO encapsulated in carbon layer, and enhance mass transfer by macroscopic pore structure. The

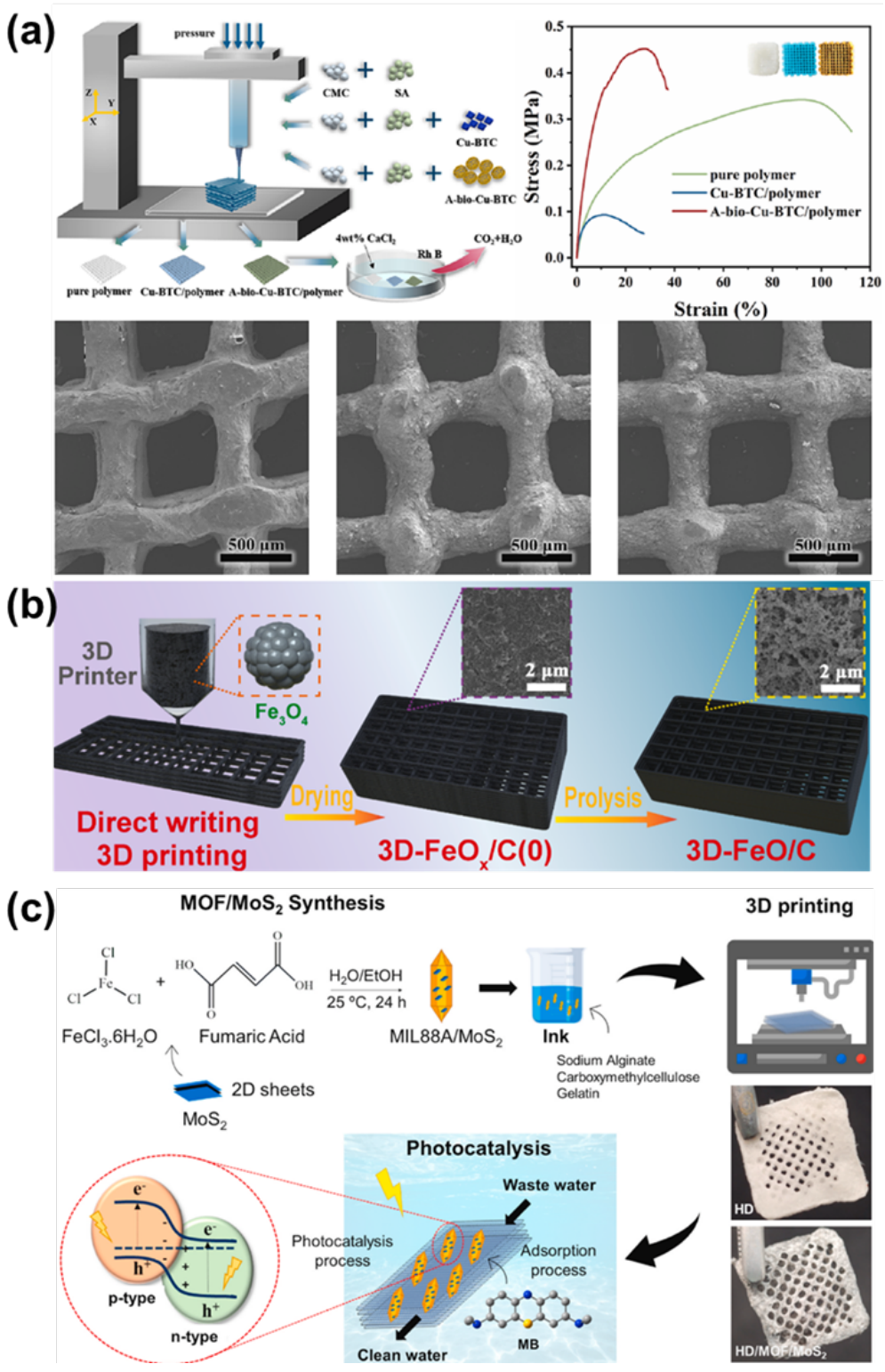

Fig. 7 (a) Preparation route of different catalysts, the stress-strain curves of the 3d printed grids, and the SEM images of pure polymer, Cu-BTC/ polymer, and A-bio-Cu-BTC/polymer.[208] (Copyright 2024, Elsevier) (b) The fabrication process of 3D-FeO/C.[209] (Copyright 2024, Elsevier) (c) Schematic illustration of the manufacture of aerogels incorporated with MOF MIL88A/MoS_2 used in photocatalysis experiments for degradation of dyes present in water.[210] (Copyright 2024, Elsevier)

degradation efficiency was above 92% after 5 cycles (Fig. 7b). Alves et al. used DIW 3D printing to prepare MOF/MoS_2 composite aerogel [210]. Alginate, CMC and gelatin were used as substrates, and MOF/MoS_2 was added to make printing ink. After printing, the ink was cross-linked by $BaCl_2$ and lyophilized. The aerogel was used for MB adsorption and photocatalytic degradation. The adsorption efficiency of 7.5 wt.% MOF/MoS_2 loaded aerogel was 95.86%, and the photocatalytic degradation efficiency was 89%. The efficiency remained high after 5 cycles of recycling (Fig. 7c). Shao et al. used DIW 3D printing to prepare clay/biochar based monolithic material (CBM), adding $ZnCl_2$ to the printing ink to activate the sludge, and preparing Fe/CBM-S_x-Zn catalyst by impregnating $Fe(NO_3)_3$ after printing [211]. The catalyst was used to activate peroxymonosulfate (PMS) to degrade levofloxacin. The degradation efficiency of Fe/CBM-$S_{10\%}$-Zn loaded by 10% sludge reached 80% within 20 min, the Fe leaching amount was less than 0.2 mL^{-1}, and the structure was stable during recycling. Efficient degradation is achieved through free radical (SO_4^{-}·, ·OH) and non-free radical ($^1O_2$) pathways (Fig. 8a). Martins et al. prepared the In_2O_3 monoliths material by DIW 3D printing, mixing the In_2O_3 powder with Pluronic F-127 to make the printing ink, which was sintered at 500℃ after printing to preserve the active structure [212]. The material was used for adsorption and degradation of perfluorooctanoic acid (PFOA) in a circulating flow system. The removal rate reached 53% within 3 h, and the removal rate increased to 75% after pyrolysis and regeneration at 500℃. The adsorption capacity reached 0.16 mg g^{-1} (Fig. 8b). Barisic et al. used DIW 3D printing to prepare a TiO_2 mono-material by mixing the TiO_2 powder with a binder to make ink and using a rapid sintering process to retain photoactivity [213]. The monolithic material was used for the photocatalytic degradation of the organic micropollutant primidone. The quantum yield reached 1.1×10^{-5} and the power consumption was only 13 kWh/m^3 in a circulating flow reactor, which was significantly better than that reported in the literature (Fig. 8c).

Overall, DIW technology's primary strength lies in its extensive material versatility, enabling it to process diverse precursors while precisely engineering hierarchical porous architectures. However, controlling the rheological behavior of inks remains challenging, and following photocatalyst formation, intricate post-treatment steps including thermal annealing or lyophilization are necessary before practical application, which constrains its efficiency for rapid prototyping workflows.

3.1.3 SLS/SLM technology for photocatalyst fabrication

SLM and SLS 3D printing technologies are both forming technologies based on powder bed processing [218]. SLM technology utilizes a high-energy-density laser beam to generate high temperatures to melt the substrate and form a molten layer. As the object descends one layer, the powder bed is leveled by rollers to continue the cladding of the next layer, without the need for adhesives or low-melting-point materials for bonding. SLM printing technology has been extended to the forming processes of many advanced alloy materials and is widely used in aerospace, shipping, high-precision metal processing and other fields. The printing effect of SLM is affected by the metal powder, particle size, scanning speed and time. Compared with SLM, the difference of the SLS process lies in that SLS uses low-melting-point polymer materials as the binder to bond the main material, and the rest of the process is the same as that of SLM. The materials used in SLM printing have a wide range of sources, and the products have excellent mechanical properties and high precision. The consumables of this process are materials that absorb laser energy and have reduced viscosity, including various polymers, ceramics and metal materials. The printed objects of this technology are immersed in powder, which is conducive to reducing the consumption of support materials and simplifying the operation of subsequent processing [219].

SLM 3D printing technology is mostly used in the manufacturing of monolithic metal catalysts. Metals and their alloy materials are commonly used filling materials in industrial catalytic reactions. Meanwhile, metal 3D printed components have good electrical conductivity and are often used to prepare catalysts for electrochemical reactions. Before printing, the printing chamber of this technology needs to be filled with argon gas or the printing should be carried out in a vacuum environment to prevent the catalytic material from being oxidized and provide good prerequisite conditions for the generation of catalytic components. At present, SLS/SLM technology applied in the field of photocatalysis is relatively limited, and is mostly used as catalyst carrier. Direct printing of metal catalysts has some applications in the field of water treatment, which may provide a reference for the application of such technology in the preparation of photocatalysts. Zhang et al. used SLM 3D printing to fabricate a 316 L stainless steel microlattice structure to mimic the Douglas fir dual-mode pore design overlapping metamaterials, and made a catalyst by electrochemical deposition of Co loaded on the surface [220]. The catalyst can be activated by PMS for degradation of

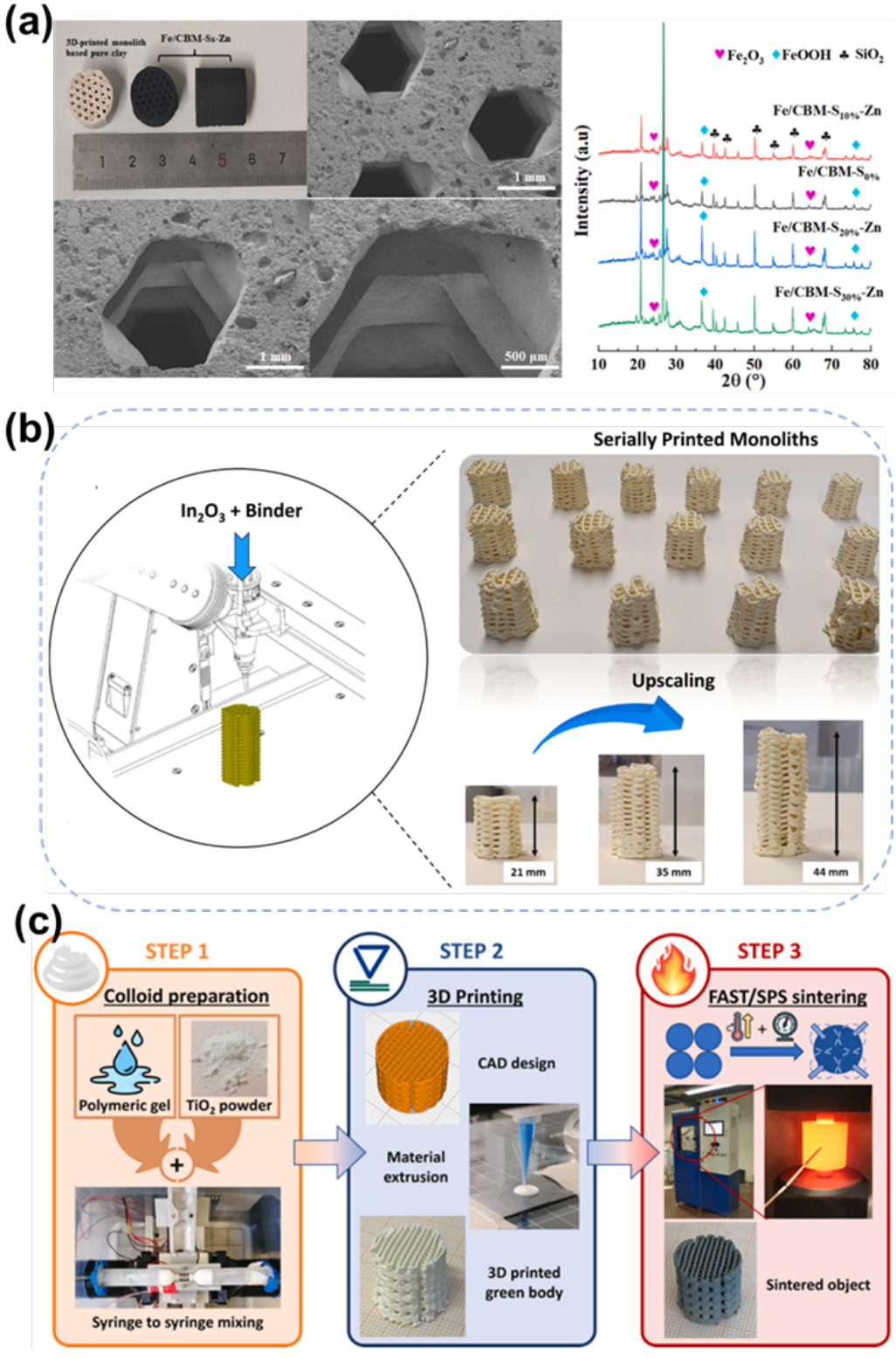

Fig. 8 (a) Photograph and SEM images of Fe/CBM-$S_{10\%}$-Zn, XRD patterns of the as-prepared samples.[211] (Copyright 2023, Elsevier) (b) Schematic of the 3D printer extrusion, successively produced the overall structure of In_2O_3 and its upscaling.[212] (Copyright 2024, Elsevier) (c) Schematic of the manufacturing process of the 3D printed titania monoliths.[213] (Copyright 2024, Elsevier)

sulfamethoxazole. The tensile strength of the structure with 70% overlap rate is 3 times that of the traditional microlattice, the specific surface area per unit volume is increased by 3 times, and the normalized reaction kinetic constant is 4 times that of the traditional structure. It can also run continuously for more than 96 h. It also has high efficiency to remove many kinds of pollutants in actual water (Fig. 9a-c). Liu et al. used SLM 3D printing technology to prepare MoS_2-stainless steel composite catalyst (3DP MoS_2-SS), and mixed MoS_2 and stainless-steel powder and molded by 3D printing [222]. The k_{FLO}/S_{BET} value was 1.60 g/(m^2/min), which was 4.3 times higher than that of MoS_2-SS powder catalyst. Mo^{4+} can promote the Fe^{2+}/Fe^{3+} cycle and accelerate the formation of active species. It can also degrade a variety of organic compounds such as 2-chlorophenol and acetaminophen. The degradation efficiency remains above 80% after 4 cycles of recycling, and the leaching amount of metal ions is lower than the drinking water standard. Nurshaun Sreedhar et al. used SLS 3D printing technology to produce polyamide spacers [221]. They designed a structure based on triple cycle minimum surface (TPMS), coated with polydopamine-polyethyleneimine (PDA/PEI). Then β-FeOOH nanorods were mineralized to make photocatalytic spacers. The spacer could degrade MB and 4-nitrophenol under sunlight and H_2O_2, and the degradation rate reached 98% in 4 h at 25 ppm. The alginate flux recovery rate reached 92%. The β-FeOOH nanorods had stable attachment, and the photocatalytic performance did not decrease significantly after repeated use (Fig. 9d).

In summary, SLS and SLM technologies enable the direct additive manufacturing of high-strength metal or ceramic-matrix photocatalysts with exceptional thermal stability and chemical corrosion resistance. However, these techniques involve elevated initial equipment investment, prolonged process cycles, and inherent material oxidation propensity of metallic powders, necessitating stringent inert atmosphere control such as argon or vacuum environments. These constraints substantially hinder scalability for industrial production. Currently, their application scope is primarily confined to carrier fabrication; research on the direct printing of active photocatalytic components remains underexplored, exhibiting low technological maturity due to challenges in microstructure precision and functional component integration.

3.1.4 Stereo-lithography technology for photocatalyst fabrication

Stereo-lithography 3D printing is an additive manufacturing process that uses ultraviolet (UV) laser beams to selectively cure liquid photosensitive polymer resins layer by layer to manufacture objects [223]. The light source generally selects ultraviolet light in the 355 nm and 405 nm bands for curing. Due to the differences in light sources and forming methods, the commonly used methods are divided into SLA, DLP and liquid crystal display forming (LCD) [224]. SLA uses laser dots as the light source to complete layer-by-layer curing through scanning [225]. DLP and LCD, on the other hand, use digital micro-mirror devices (DMD) and LED light sources as the light source to form an ultraviolet light surface and project it onto the photosensitive resin tank [226]. As the curing platform moves, the object is manufactured. The forming speed and efficiency of stereolithography 3D printing are both higher than those of other 3D printing forming technologies. Its precision depends on the resolution of the light spot, not on the diameter of the nozzle or the size of the raw material [227]. Compared with other 3D printing technologies, through the optimization of processes and parameters, the thickness of each layer (resolution in the Z-axis direction) of stereolithography 3D printing can be reduced to less than 10 μm, effectively eliminating the layering phenomenon caused by layer-by-layer stacking, greatly improving the surface effect of printed products, and simultaneously manufacturing highly precise three-dimensional objects with extremely high resolution [228]. With the continuous update of technology, micro-nano 3D printing technology capable of material forming and control at the micro and nano scales has emerged [229-231]. It has been developed based on the evolution of stereolithography 3D printing technology. The material used in stereolithography is photosensitive resin, which is required to have good stability, fast curing rate, low shrinkage rate and appropriate curing depth. It is composed of photo initiators, prepolymer monomers, oligomers and fillers. The curing process of photosensitive resin is as follows: Ultraviolet light is injected into the interior of the photosensitive resin. Under the action of the photo initiator, the prepolymer and the active monomer undergo cross-linking polymerization to form a cured layer. The role of the oligomer is to adjust the physical properties such as viscosity and mechanical properties of the photosensitive resin. The filling process mainly plays a role in increasing the curing rate, adjusting the curing depth and regulating the color, etc. At present, the commonly used photosensitive resins are mainly free radical photosensitive resins composed of acrylic monomers and cationic photosensitive resins composed of vinyl ether monomers. The development and research of photosensitive resins are promoting the continuous development of stereolithography and 3D

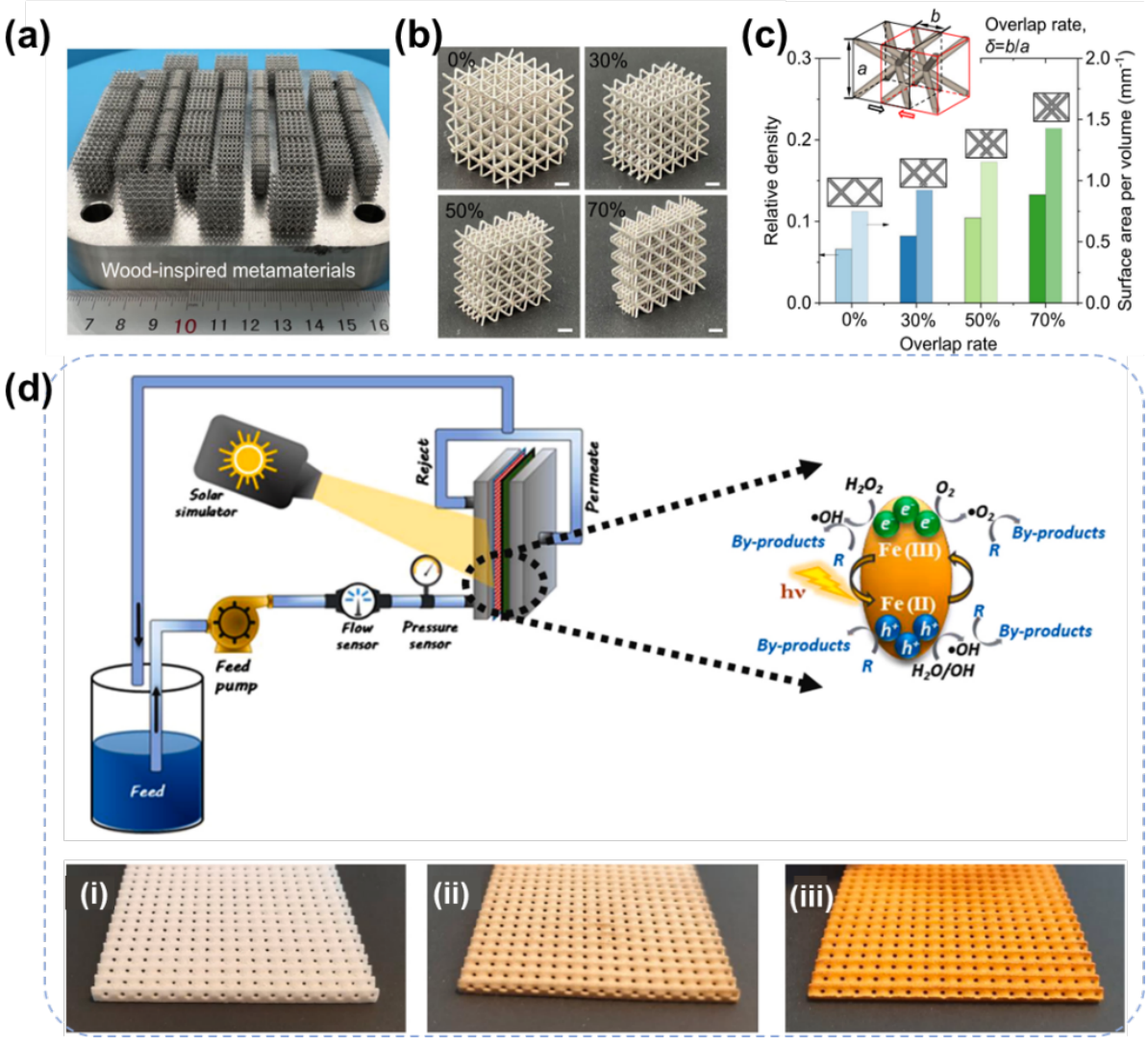

Fig. 9 (a) Optical image of original 3D-printed traditional microlattices and wood-inspired metamaterials, (b) The 3D-printed metamaterials with 0.4 mm diameter and 0, 30, 50, and 70% overlap rates, (c) The relative density and surface area per volume of traditional microlattices and wood-inspired metamaterials. The insert schematic shows the definition of overlap rate.[220] (Copyright 2024, Springer) (d) Schematic of the photocatalytic setup consisting of filtration system and solar simulator as light source and photocatalytic activity in β-FeOOH nanorods and digital photos of (i) uncoated spacer, (ii) PDA/PEI coated spacer and (iii) β-FeOOH nanorods coated spacer.[221] (Copyright 2021, Elsevier)

printing technology. Based on stereolithography 3D printing technology, high-precision, small-sized and high-strength additive manufacturing of ceramics and glass has also emerged, and the range of materials is constantly expanding.

During the preparation of monolithic catalysts, the dense and smooth photosensitive resin is prone to clogging and masking the active substances. Therefore, calcination is usually adopted to remove or transform the photosensitive resin material, thereby exposing the active centers [235]. Finch et al. employed SLA and DLP light-induced 3D printing technology, using PETA resin containing ruthenium (II) complexes as the raw material, to print micro/macro-sized photocatalytic structures [231]. The uniform distribution of ruthenium was verified by time-of-flight secondary ion mass spectrometry. This structure exhibited photocatalytic activity in the activation of aryl bromides for C-H arylation reactions, where the microscopic structure achieved 75% photocatalytic performance using only 1% of the volume of the macroscopic structure (Fig. 10a). Warren et al. used DLP 3D printing

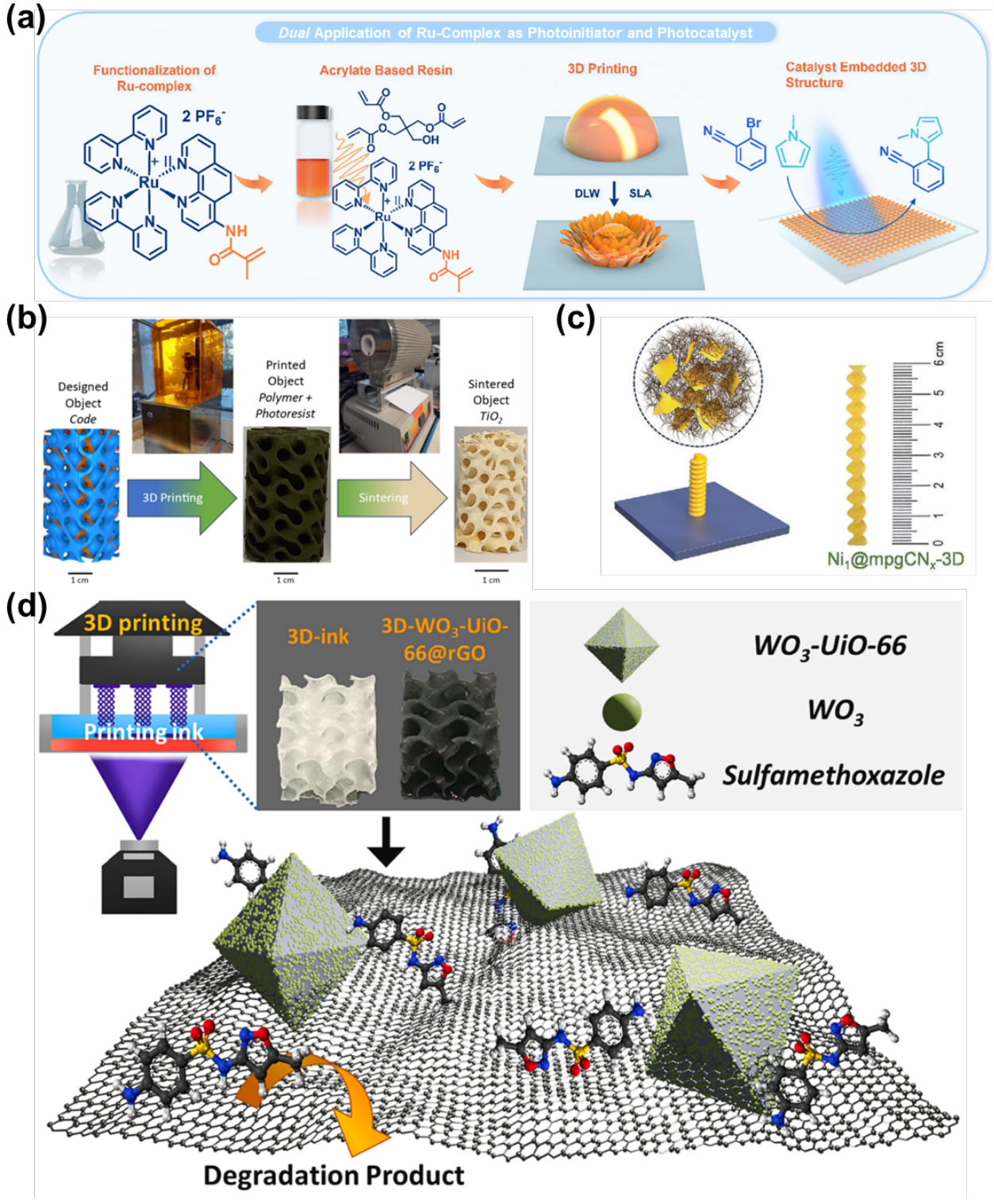

Fig. 10 (a) Schematic diagram of the synthesis of 3D-printed solid catalysts using ruthenium(II) complexes as both comonomers and initiators.[231] (Copyright 2025, Wiley-VCH) (b) Fabrication process steps to obtain mixed phase titania foams via 3D printing.[232] (Copyright 2024, RCS Publishing) (c) VAT photopolymerization for the 3D printing of single-atom catalysts.[233] (Copyright 2024, Wiley-VCH) (d) Scheme of the SMX-degrading photocatalyst system utilizing 3D-printed-WO_3-UiO-66@rGO.[234] (Copyright 2024, Elsevier)

technology to print catalyst structures using titanium acrylate resin as the raw material, and sintered them at 750°C to obtain TiO_2 foam containing rutile and anatase phases [232]. This foam has a porous gyroid structure with a porosity of > 90%. When used in a cyclic flow reactor to degrade carbamazepine, the quantum yield reached 7.6×10^{-3}, with an energy consumption of 67.6 kWh/m^3. The photocatalytic performance was superior to TiO_2 nanoparticle suspensions, and the mechanical stability was good (Fig. 10b). Luo et al. used DLP photopolymerization 3D printing to print a helical structure free-standing photocatalytic reactor by mixing the Ni_1@mpgCN_x single-atom catalyst with resin [233]. When the reactor was used for the continuous stream photocatalytic oxidation of benzyl alcohol to produce benzaldehyde, the activity was higher than that of traditional packed bed reactor, and the quantity was selectively maintained after recycling. No metal ions were dissolved, and the structure was stable in a variety of organic solvents (Fig. 10c). Huong et al. fabricated gyroid structured photocatalysts using DLP 3D printing WO_3-UiO-66@rGO nanocomposites [234]. The degradation rate constant of sulfamethoxazole was 0.02955 min^{-1} in 60 min, which was 6.2 times that of pure WO_3. After repeated use for 10 times, the photocatalytic activity could be completely recovered, and the mechanical strength of the material met the requirements of the flow reaction (Fig. 10d). Gracia-Pinilla et al. 3D printed TiO_2-Al_2O_3 resin by DLP and sintered to obtain hollow microstructures (3DHMs), which were loaded with α-Fe_2O_3 and used for solar photo-Fenton-like reaction [236]. The degradation efficiency of MB in the formulation of $TiOFe_{0.5}$ was 95% within 180 min, and the degradation of acetaminophen was still effective at neutral pH. After three successive cycles, the activity remained stable and no significant iron dissolution was observed.

In summary, SLA technology stands out for its exceptional micro-nanoscale resolution capabilities, enabling breakthroughs such as the fabrication of topologically complex microchannel reactors and hierarchical photocatalyst architectures with ultrafine features. These innovations have demonstrated transformative potential in optimizing light-matter interactions and broadening design possibilities for high-efficiency photocatalytic systems. While challenges persist including thermal degradation effects during resin removal that may induce controlled shrinkage and the need for post-processing compensation, alongside issues of limited interfacial adhesion between resin matrices and active components often necessitating surface functionalization strategies, the field is actively innovating. Researchers are developing novel material formulations and hybrid manufacturing approaches to systematically address these limitations. Such progress positions SLA as a frontier technology poised to redefine benchmarks in advanced photocatalytic device engineering, balancing precision manufacturing with functional performance optimization.

3.1.5 Other 3D printing technologies for photocatalyst fabrication

In addition to the above commonly used mainstream technologies, a variety of emerging 3D printing technologies have shown unique potential in photocatalyst design, and their core advantages are closely related to the needs of photocatalysis [237-239]. In recent years, thanks to the rapid development and wide application of 3D printing technology, some of the latest 3D printing technologies have also been demonstrated in the field of photocatalysis. This subsection will introduce a few works. Laser-induced in situ electrospray printing (E-Jet) is a 3D printing technology that combines the principle of high-energy laser induction and electrospray printing. By controlling the thermal field and flow field distribution of the jet by laser, E-jet can achieve the accurate molding of micro and nano-level porous structures, which can effectively improve the specific surface area of the structure and the exposure rate of photocatalytic sites. Li et al. used this technique to prepare hierarchical porous ZnO structures with a minimum pore size of 130 nm and a maximum pore size of 4 μm by using ZnO ink as raw material and adjusting jet shrinkage and curing with the aid of 2 W laser [240]. When the structure is used for UV photoelectric sensor, the photo response performance is significantly better than that of the sample without laser assistance. Moreover, the porous characteristics improve the separation efficiency of photogenerated carriers, which provides a new idea for the preparation of micro/nano photocatalytic devices (Fig. 11a, b). 3D concrete printing (3DCP) surface coating technology takes advantage of the non-mold forming characteristics of 3D printed concrete, and directly spray photocatalytic coating on the surface of fresh cement-based matrix to avoid the surface smoothness limitation of traditional mold forming and enhance the bonding force between catalyst and matrix. Zahabizadeh et al. sprayed nano-TiO_2 aqueous solution on the surface of 3D printing cement-based materials [241]. At the coating rate of 80 mg/cm^2, the degradation rate of RhB reached 61% after 20h of illumination. When the optical power intensity was increased from 1 mW/cm^2 to 8 mW/cm^2, the degradation efficiency was increased by 86%. SEM

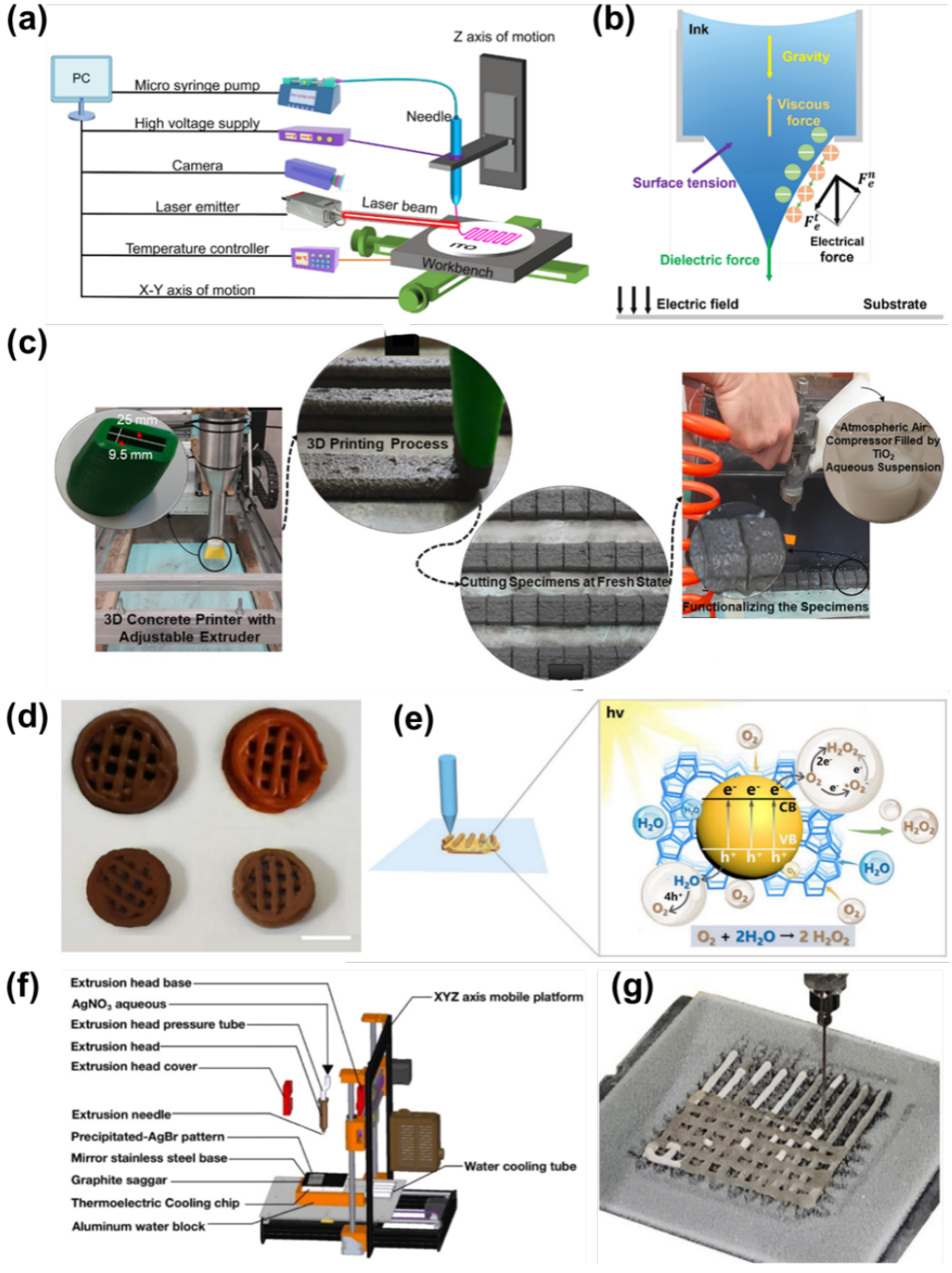

Fig. 11 (a) Experimental equipment. (b) Force distribution diagram of Taylor cone in E-Jet process.[240] (Copyright 2024, Elsevier) (c) Preparation and functionalization of the cementitious specimens.[241] (Copyright 2023, Elsevier) (d) Digital images of3D-printed TP-DBS-COF (upper left), 3D-printed TP-DBS-COF/ZSM-5-15% (upper right), the final product of TP-DBS-COF (lower left), and the final product of TP-DBS-COF/ZSM-5-15% (lower right) (scale bar: 5 mm). (e) The proposed mechanism of photocatalytic H_2O_2 production based on COF/zeolite composites.[242] (Copyright 2025, Wiley-VCH) (f) Schematic diagram and (g) the precipitation structure of the first layer of AgBr and the second Photos in layer printing; photos of four-layer HPHO Ag@AgBr photocatalyst structure.[243] (Copyright 2023, Elsevier)

and EDS analysis confirmed that TiO_2 was uniformly distributed on the surface of the 3D printed matrix without obvious agglomeration (Fig. 11c). Photopolymerization-assisted in situ growth 3D printing technology can prepare organic-inorganic composite printing ink by optimizing the binder and prepolymerization conditions. Photopolymerization is used to realize the formation of macroscopic ordered structure, followed by solvent heat treatment to promote the in-situ crystallization of active components, which can solve the phase separation problem when COF is combined with zeolite. Feng et al. used this technology to prepare TP-DBS-COF/ZSM-5 composite photocatalyst, in which zeolite enhances the hydrophilic and O_2 affinity of the material, and H_2O_2 production is increased by 52% compared with pure TP-DBS-COF [242]. After 4 cycles, the crystallinity and catalytic activity of the composite did not decrease significantly, which was suitable for sustainable photocatalytic hydrogen production (Fig. 11d, e). Kuo et al. used in situ precipitation (ISP) 3D printing to produce a four-layer regular porous Ag@AgBr structure [243]. In this technology, silver nitrate solution is directly printed on the surface of cured sodium bromide, and the regular porous AgBr structure is formed by in situ precipitation at the liquid-solid interface. After sintering and UV photoreduction, Ag@AgBr photocatalyst is prepared without subsequent complex assembly. The degradation rate of Orange II azo dye remained 84.8% after 5 cycles of degradation. Under UV-VIS light irradiation, Escherichia coli can be completely killed within 120 min, and the bactericidal reaction conforms to the hyperbolic kinetics, which is suitable for the synergistic treatment of water pollution (Fig. 11f, g).

3.2 Design of photocatalyst carriers

In addition to direct printing of photocatalytically active materials, the preparation of structured substrates or supports by 3D printing, followed by in-situ growth, coating loading and other subsequent processes combined with photocatalytically active components, is another technical direction of great practical value. Based on the structural design freedom of 3D printing, the substrate with specific morphology, mechanical stability, and mass transfer characteristics is constructed, and the photocatalytically active material is directionally combined on the surface or inside the pores of the substrate by interface regulation to form a composite system of substrate and photocatalytic material [244-246]. On the one hand, 3D printed substrates can optimize the scattering and absorption efficiency of light and the mass transfer path of reactants by adjusting the parameters like porosity, specific surface area, and flow channel geometry. At the same time, the problems of rigid traditional support structure and easy agglomeration and shedding of catalysts can be solved. On the other hand, the choice of substrate materials is diverse, and model materials such as polymers, ceramics, metals, and composites have been widely studied in the field of 3D printing technology [247]. For the needs of liquid-phase degradation, gas-phase reduction, and photoelectric co-catalysis in the field of photocatalysis, the physicochemical properties of different substrates can be used to match the different photocatalytic reaction requirements, and determine the suitability of the subsequent in-situ growth/loading process [248]. The common combination methods include in situ growth of semiconductor nanoarrays by hydrothermal method, coating loading by sol-gel method, and electrochemical deposition of metal-based catalysts [249]. The specific process needs to match the surface properties of the substrate materials and the synthesis requirements of active components [250].

3.2.1 Polymer carrier

With the advantages of strong compatibility, low cost and light weight of 3D printing process, polymer substrate is suitable for liquid photocatalytic reaction at room temperature. Its porous structure can be accurately designed by adjusting the printing parameters like layer thickness and filling rate, providing sufficient loading sites for photocatalytic materials and ensuring the fluidity of reaction media. FDM and SLA are commonly used. Penas-Garzon's team prepared PLA substrate with vertical wing by FDM 3D printing [251]. Graphite phase carbon nitride (CN) powder of urea or dicyandiamide pyrolysis was fixed by polymer adhesion. The CNB-U/PLA material was rich in nitrogen vacancies. The degradation rate of 5mg L^{-1} venlafaxine (VFX) was 90% within 30 min, and the modular design kept its high degradation activity in the mixed pollutant system (Fig. 12a). Melendz-Gonzalez et al. synthesized immobilized Cu_xO semiconductors (3D-Cu_xO, 3D2-Cu_xO) on 3D printed substrates using PLA as substrate by graphite coating, copper electrodeposition and anodization processes [252]. The materials contain CuO/Cu_2O mixed crystal phases. The band gap width of 1.6-1.8 eV can respond to visible light, among which 3D2-Cu_xO has higher carrier concentration and better separation efficiency, and the degradation rate of 10 mg L^{-1} sulfamethoxazole (SMX) can reach 60% after 360 min of visible light irradiation, and the synthesis does not require subsequent heat treatment, taking into account the efficiency and sustainability

(Fig. 12b). Son et al. used FDM technology to prepare ABS-ZnO composite substrate [253]. After plasma treatment and hydrothermal growth, ZnO nanoflowers (NFs) structure was formed on the surface of the substrate, and the degradation rate of 5 mg L^{-1} MB reached 100% within 120 min under UV light. The 3D structure effectively enhances the catalyst loading and stability. Kang's team constructed the Ni-MOF/BiOI/$AgVO_3$ heterojunction by cold plasma fixation and c-ISCAP method using LCD 3D printing fractal pyramid substrate [254]. The double Z-type charge transfer path greatly improved the carrier separation efficiency. The degradation rate of 5 ppm RhB under visible light for 6 h was 100%.

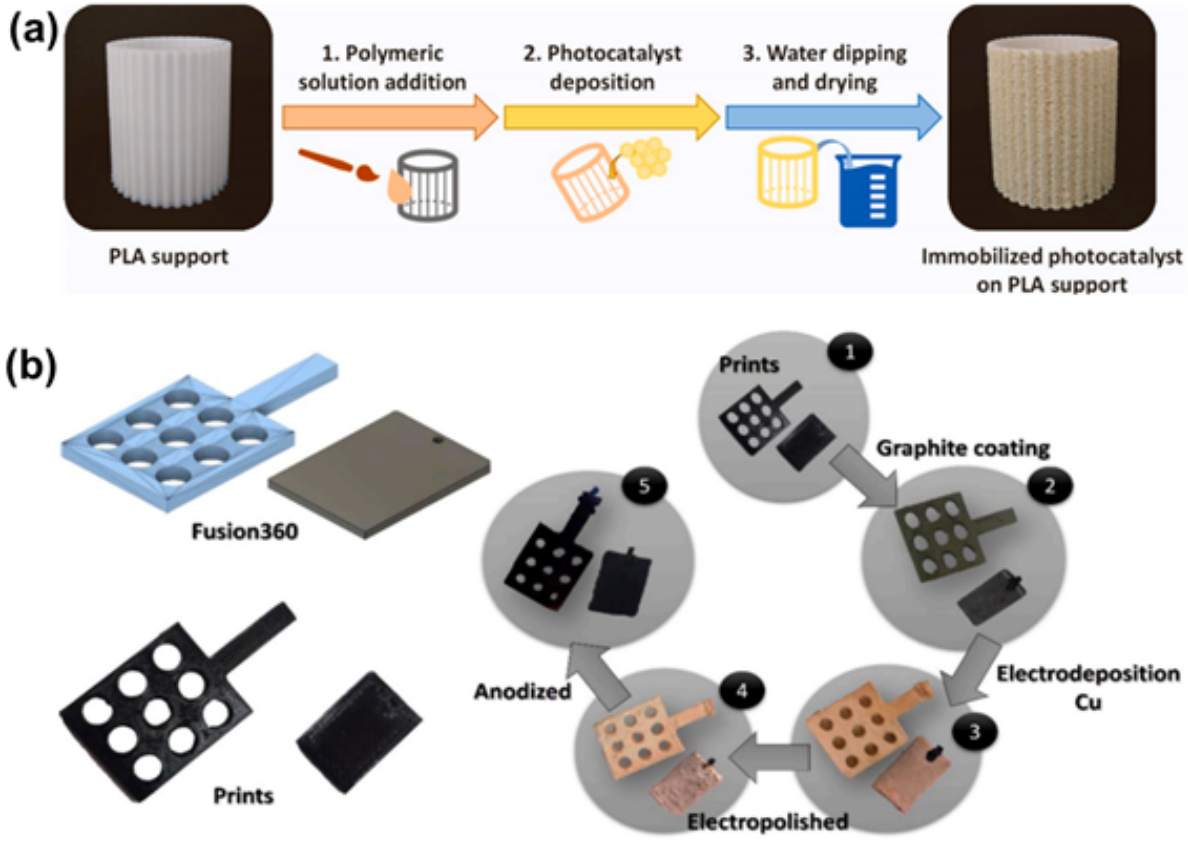

Fig. 12 (a) Schematic of the sequential steps involved in immobilizing CN materials onto the cylindrical PLA support using a polymeric solution.[251] (Copyright 2023, Elsevier) (b) Structural design of catalytic materials, physical samples and synthesis diagrams.[252] (Copyright 2024, Elsevier)

In the field of photocatalytic hydrogen production, Li et al. used DLP 3D printing to prepare substrates with different structures and coated $ZnIn_2S_4$-Pt-Co catalyst to form thermosetting coatings [255]. The inverted pyramid structure had a long light reflection path, and the hydrogen production rate per unit mass of catalyst reached 1555 μmol h^{-1} g^{-1}. It is 4.2 times that of pure powder, and does not need to sacrifice agents, providing a new strategy for large-scale hydrogen production. The team of Perera used DLP and PIPS technology to fabricate UIO-66-MOF polymer composite [256]. The surface of UiO-66 was enriched by HEA monomer, which completely degraded ethylparoxon in 60 min at pH 9-10. The elasticity and stability of the composite material make it suitable for wearable chemical protective equipment.

3.2.2 Carbon carrier

Carbon-based materials themselves are excellent photocatalysts and photocatalyst-supported substrate materials, such as graphene [257], carbon nanotubes [258, 259], activated carbon [260] and carbon quantum dots [261, 262], which have the advantages of high specific surface area, excellent conductivity, and high chemical stability [263]. It can not only provide a loading substrate for photocatalytic materials, but also serve as an electron transport channel to promote the separation of photogenerated charge carriers, which is suitable for energy conversion scenarios like photocatalytic

hydrogen production and CO_2 reduction [264, 265]. Guo et al. used lignin as carbon source and used DIW technology, supplemented by 23 wt.% Pluronic F-127 to adjust the rheological properties of ink [266]. By using the reverse temperature sensitivity of F-127, the printing blockage caused by lignin's strong rigidity and easy aggregation was solved. Self-supporting lignin scaffolds were successfully prepared. Subsequently, PCS were stabilized at 120℃ to eliminate residual water and volatile impurities, and carbonized under nitrogen atmosphere at 800℃ to obtain carbon scaffolds (PCS). The carbon support retained the interconnected porous structure constructed by DIW printing with a porosity of 55%, and its high specific surface area provided sufficient anchoring sites for TiO_2 nanorods and Pd nanoparticles. At the same time, the graphite-like structure formed by lignin carbonization gives the carrier excellent electrical conductivity, which can be used as an electron transport channel to accelerate the photogenerated electron transfer. Together with the Schottky junction formed by Pd and TiO_2 to inhibit the recombination of charge carriers, the Pd/TiO_2/PCS catalyst is finally constructed in the photocatalytic reduction of 4-nitrophenol (4-NP). The turnover frequency (TOF) reached 8.73 min^{-1} and the Pd dissolution amount was less than 0.01 mg L^{-1} after 9 cycles, reflecting the dual enhancement of the stability and catalytic efficiency of the active components by carbon support (Fig. 13a). Kandasamy et al. prepared graphene/MnO_2/Fe_3O_4 hybrid particles by wet impregnation method, mixed with light-curing resin, printed by SLA 3D to obtain graphene-like structure, and carbonized by argon gas at 800℃ to obtain 3D floating carbon support [267]. After carbonization, the conductivity of the carrier increased from 10 S m^{-1} to 15 m^{-1}, graphene ensured high conductivity, Fe_3O_4 gave magnetism and floatability, and provided a loading substrate for MnO_2 while accelerating charge transfer. The degradation rate of 10 ppm MB under sunlight for 120 min reached 95.93%. The activity decreased by only 2% in 10 cycles. Verma et al. used DLP technology and transparent resin to construct micro-lattice structures [67]. After clear curing, the PyC scaffold was obtained by carbonization under argon atmosphere at 900℃. Although the scaffolds shrank by 51% during carbonization, they still maintained intact structure and high mechanical stability. The porous structure of the surface can be used for hydrothermal growth of ZnO nanowires, and the multiple light scattering characteristics improve the light absorption efficiency. The high conductivity of PyC accelerates the electron transfer, and the degradation rate of 10 mg L^{-1} RhB can reach 97.73% after 180 min of UV irradiation. The degradation rate reached 84.04% in 280 min under natural light, and the activity remained 86.22±2.15% after 7 days of cycling (Fig. 13b).

3.2.3 Ceramics carrier

Ceramic support has the characteristics of high temperature resistance, chemical stability, and high mechanical strength, which are suitable for high temperature sintering and harsh reaction environment [268]. 3D printing technology can break through the limitations of traditional ceramic molding, construct complex channels and special topological structures, and optimize photocatalytic performance by adjusting the composition and microstructure. A variety of ceramic carriers such as mullite, Al_2O_3, SiOC, ZnO and various modified ceramics. Mei's team used photosensitive resin containing Al_2O_3 and SiO_2 powder as raw materials, and used SLA technology to prepare square, round, and diamond array hole sheet scaffolds [269]. After 1400℃ step-by-step sintering, pure ceramic support was obtained under air atmosphere, and carbon-ceramic support was obtained under nitrogen atmosphere. The resin pyrolysis under nitrogen atmosphere produced 12.86±2.32 wt.% pyrolysis carbon, which inhibited the mass transfer of ceramic powder, increased the specific surface area of the support from 0.067 m^2 g^{-1} of pure ceramic to 0.509 m^2 g^{-1}, and refined the pore size to about 2 μm. The photodegradation efficiency of RhB loaded with MoS_2 was 45.95%, which was 1.97 times that of pure MoS_2, and the efficiency was 82.35% after 5 cycles. UV-Vis DRS confirmed that pyrolysis carbon can enhance light absorption in the full visible light band, which provides ideas for the design of high specific surface area carriers (Fig. 14a). Huang's team used DLP 3D printing technology to print four minimal surface structure scaffolds like gyroid and diamond with commercial Al_2O_3/SiO_2 ceramic slurry [270]. Adding 5 wt.% ammonium bicarbonate as pore-making agent, the mullite carrier was prepared by sintering at 1500℃. $Cu(OH)_2$ nanoneedles were grown by electrochemical oxidation method, and MoS_2 was supported by sol-gel method to construct a three-pore composite catalyst. Among them, the Diamond structure had the best mechanical properties, with a specific surface area of 89.34 m^2 g^{-1} and a RhB degradation rate of 84.68%, which was 2.26 times that of pure MoS_2. The efficiency remained above 85% after 10 cycles. ESR confirmed that $\bullet O_2^-$ was the main active species, and the Z-type heterojunction promoted carrier separation to realize the synergistic optimization of mechanical properties and photocatalytic activity (Fig. 14b). Based on the self-developed DLP 3D printing technology, Hu's team

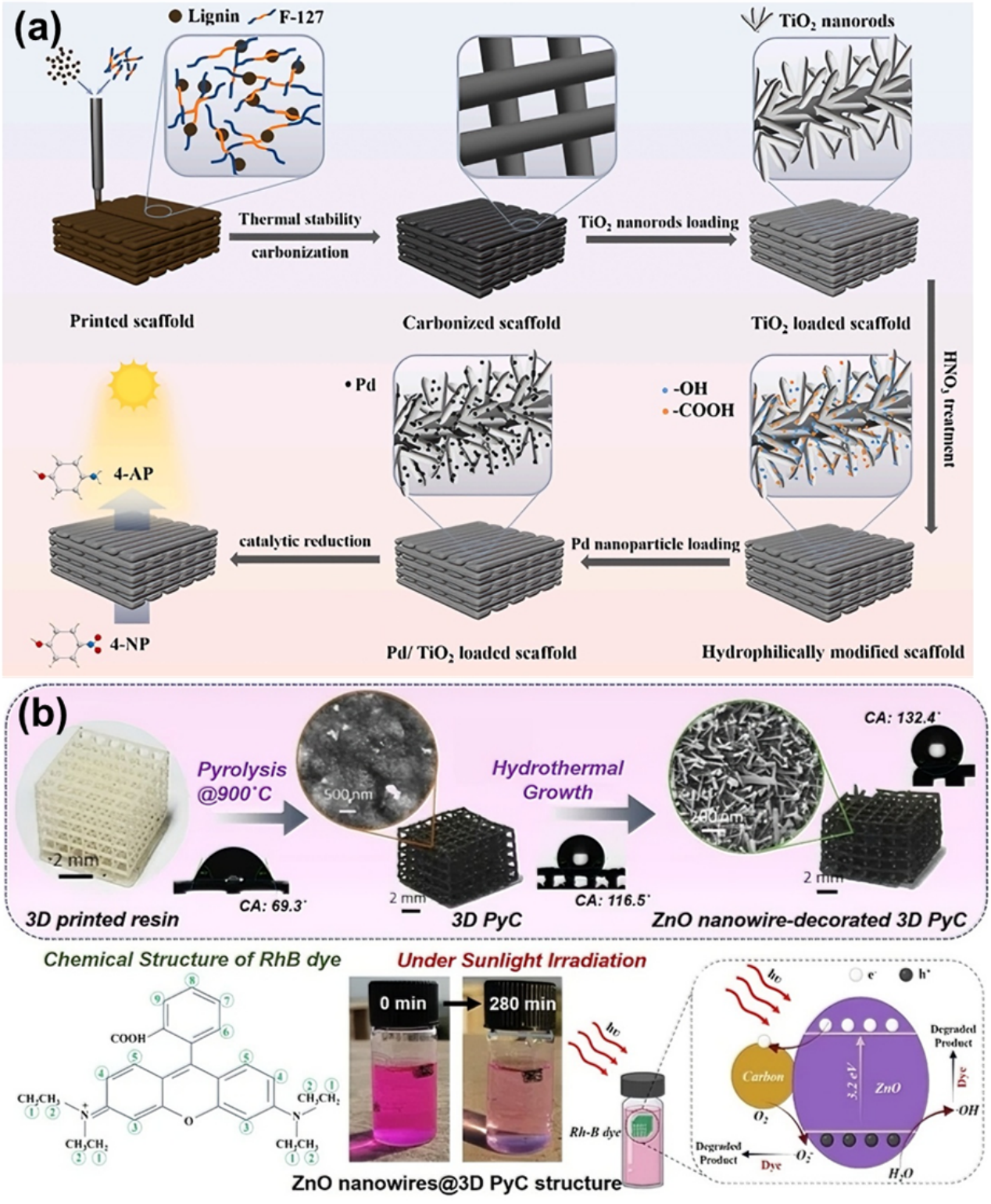

Fig. 13 (a) Schematic illustrating the 3D printing process of high-content lignin to construct hierarchical Pd/TiO_2/PCS photocatalysts for the efficient reduction of 4-NP.[266] (Copyright 2025, Elsevier) (b) Schematic diagram of the synthesis of 3D PyC decorated with ZnO nanowires and the mechanism of RhB removal.[67] (Copyright 2025, Springer)

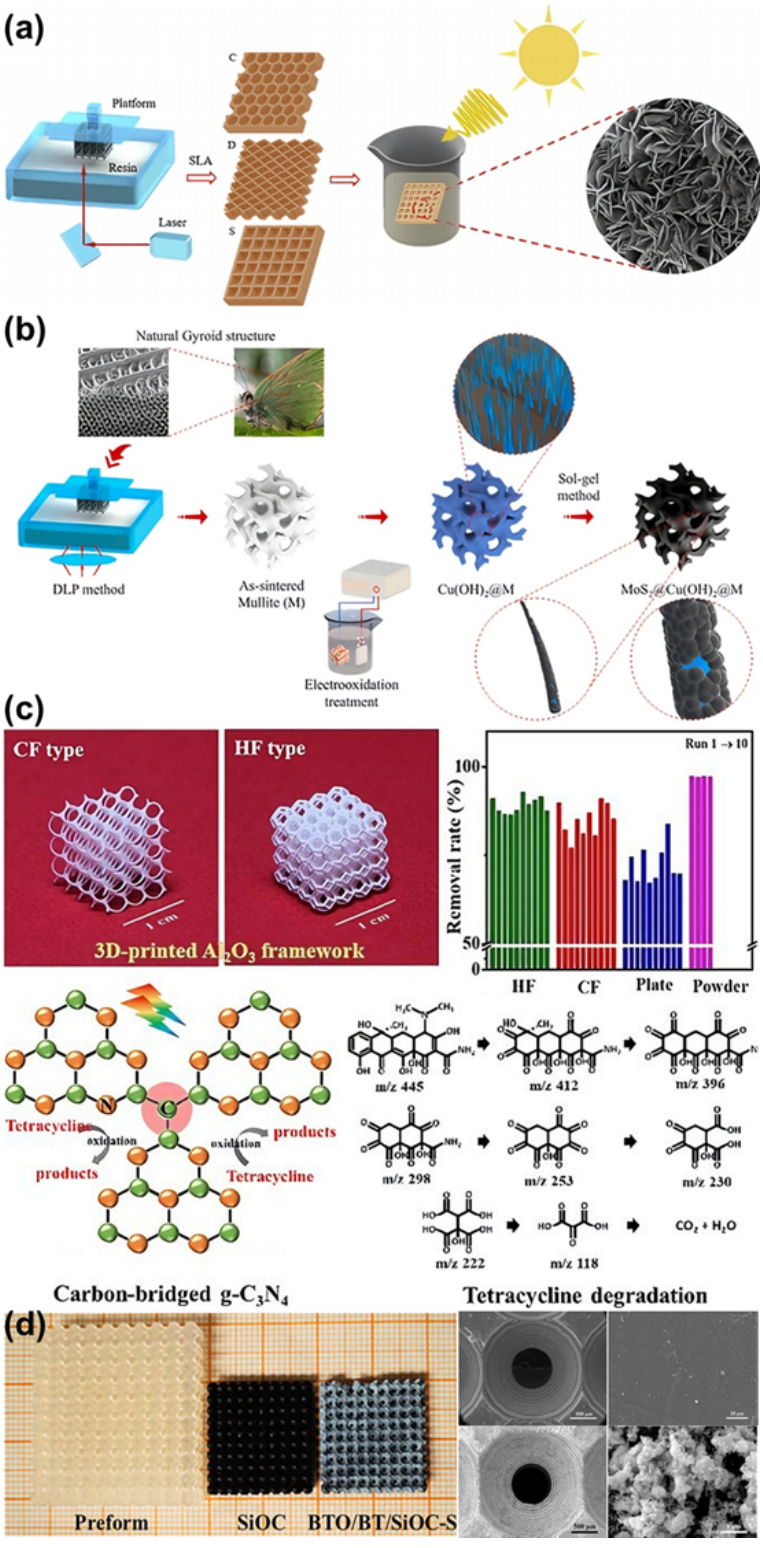

Fig. 14 (a) 3D printing fabricated geometric array samples and their application as support materials for photocatalysts.[269] (Copyright 2019, Elsevier) (b) Scheme diagram of the minimal surface support preparation procedure with MoS_2.[270] (Copyright 2023, Elsevier) (c) Photos, properties and reaction mechanisms of different configurations of 3D-printed alumina frameworks.[271] (Copyright 2024, Elsevier) (d) Photographs of preform, SiOC, and BTO/BT/SiOC-S and SEM of SiOC, and BTO/BT/SiOC-S.[272] (Copyright 2024, Elsevier)

printed CF and HF scaffolds with Al_2O_3 powder and photosensitive resin, and obtained Al_2O_3 carrier by sintering at 1500℃ [271]. Carbon-bridge g-C_3N_4 was prepared by high temperature roasting, coated with polyvinyl alcohol, and then roasting and fixed on the support at 300℃. The band gap width and carrier recombination rate of g-C_3N_4 were reduced by carbon bridge modification. After negative CNMD, the degradation rate of tetracycline reached 91%, the efficiency of 10 cycles remained above 85%, and the TOC removal rate exceeded 82%. LC-MS confirmed that tetracycline was oxidized, deaminated and mineralized to CO_2 and H_2O, which provided a reference for the development of recyclable non-metallic photocatalyst support (Fig. 14c). Liu's team used vat photopolymerization 3D printing technology to print porous preforms with methyl-silsesquioxane resin, and prepared cuboidal and spherical porous SiOC carriers by argon sintering at 900℃ [272]. The $Bi_{12}TiO_{20}/Bi_4Ti_3O_{12}$ S-type heterojunction was formed by coprecipitation ($Bi(NO_3)_3•5H_2O$ and tetrabutyl titanate) and annealing at 600℃ for 1 h. The heterojunction promotes carrier separation and retains strong REDOX capacity with the help of a built-in electric field. The spherical pore can prolong the light reflection path and increase the retention time of the reactant, and the NO removal efficiency is 16.4%, which is 1.39 times that of the cubic pore. After four cycles, the activity is stable, which provides a scheme for the monolithic catalyst for air pollutant treatment (Fig. 14d). In order to solve the problems of high carrier recombination rate and weak light absorption in photocatalytic CO_2 conversion, Pan's team prepared gyroid structure preform by DLP 3D printing with ZnO precursor slurry as raw material [273]. After heat treatment at 500℃ to remove the organic phase and sintering at 1300℃, P-doped ZnO (P-ZO) support was prepared. Bi_2S_3 nanoarrays were loaded onto the surface of the nanocomposites by hydrothermal method to construct S-shaped heterojunction metamaterials. The P-ZO has a significant photothermal effect, which can be heated to 89.2℃ when coupled with Bi_2S_3. The S-type heterojunction inhibits carrier recombination, and the transient photocurrent density is 1.5 times higher than that of pure P-ZO. Under simulated sunlight, the production of CO and CH_4 reached 8.87 and 1.49 μmol h^{-1}, respectively, which were 3.45 and 4.65 times of that of pure P-ZO, and the activity of the material was stable for 5 cycles, which provided a new structure design idea for CO_2 conversion by photothermal catalysis.

3.2.4 Others

Substrates with specific functions such as metal, glass, and composite substrates are limited by difficulties in manufacturing and application fields. Although the application scenarios are less extensive than the first three scenarios, they are irreplaceable in the subdivision field with their unique performance. Metal substrates focus on high strength and conductivity, glass substrates focus on high light transmittance, and composite substrates achieve complementary properties through the cooperation of multiple materials, providing more diverse solutions for photocatalytic loading. In order to improve the photocatalytic performance of TiO_2 and optimize the efficiency of the reactor for environmental remediation, Grandcolas et al. used direct metal laser sintering (DMLS) 3D printing of Ti6Al4V alloy to prepare planar and pyramidal (PYR), honeycombed (HON), and octahedral (OCT) 3D structures [274]. TiO_2 nanotubes were grown by anodization at 60V using a solution of ethylene glycol containing 0.35 wt.% NH_4F and 2 vol% H_2O as the electrolyte. The performance test showed that the photocatalytic efficiency of the 3D structure was significantly improved under the rotation condition. The PYR structure achieved complete degradation of MB within 200 min under UV-LED illumination and rotation mode, while the HON structure only increased the efficiency by 20% due to poor light penetration. This study provides technical ideas for the design of high-efficiency photocatalytic reactors for environmental remediation (Fig. 15a). Addressing the need for recyclable surface-enhanced Raman scattering (SERS) substrates for point-of-care testing (POC) analytical platforms, Malik et al. fabricated metal brushes using laser powder bed melting (L-PBF) 3D printing of Inconel 625 alloy [275]. The IN_EuSTAg substrate was obtained by three-step functionalization. The SERS enhancement factor of RhB on the substrate reached 2.02×10^4, and the RhB degradation rate was 92.3% within 180 min under 370 nm UV light. The RHB could be recycled for 3 times, providing a recyclable SERS solution for the POC analysis platform (Fig. 15b).

Aiming at the problem of low solar energy capture efficiency caused by the change of illumination Angle in PEC water decomposition, Hegde et al. used DLP 3D printing of light-curing silica sol-gels, and prepared transparent 3D silica lattices after aging, degreasing and sintering [68]. Then, ITO and Mo-$BiVO_4$ were deposited sequentially by dip coating method to construct 3DP/ITO/Mo-$BiVO_4$ electrode. The volume current density of the electrode was 1.39 mA/cm^3 under 1.23 V and AM 1.5 G illumination, which was 2.4 times that of the flat glass substrate. The performance fluctuation was only 6% when the illumination Angle

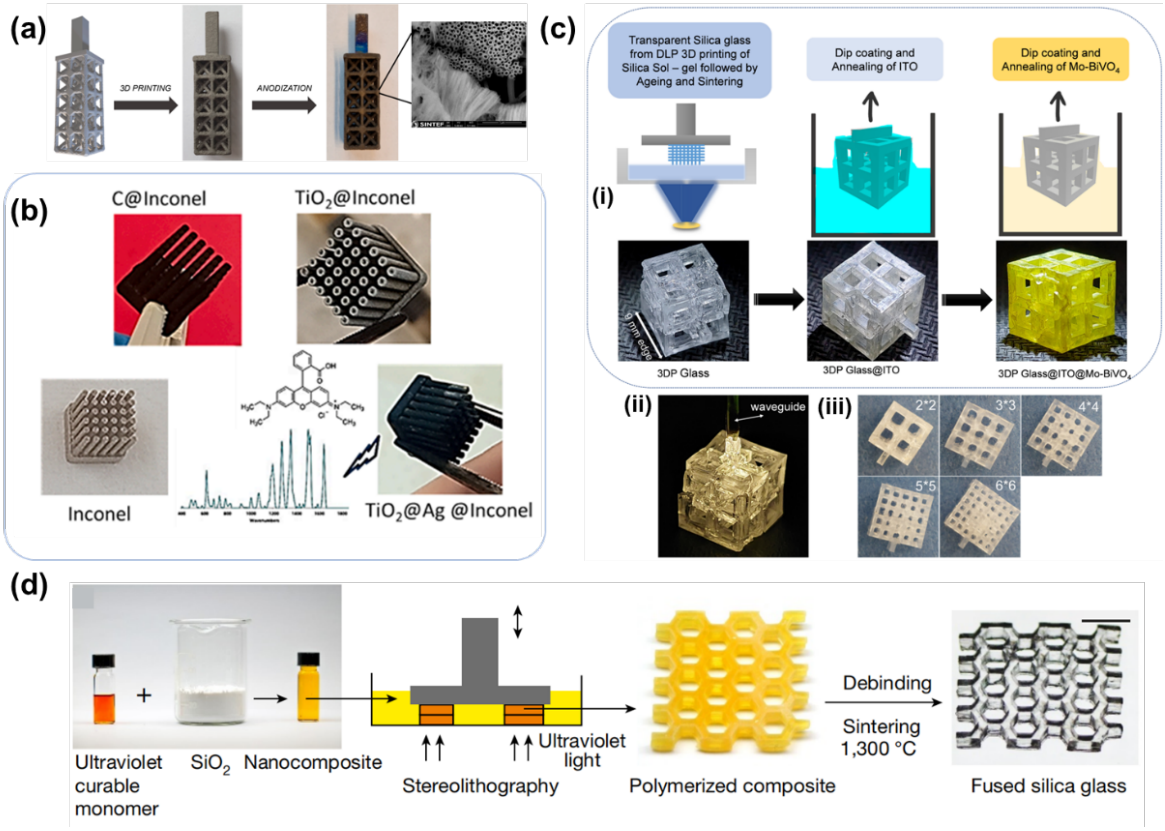

Fig. 15 (a) Manufacturing process diagram and SEM image of the sample surface after anodizing treatment.[274] (Copyright 2025, Elsevier) (b) Colloidal carbon soot templated TiO_2/Ag surface functionalized 3D printed metal brushes as new generation Surface Enhanced Raman Scattering substrates.[275] (Copyright 2024, Elsevier) (c) (i) The manufacturing process of a translucent three-dimensional lattice structure for photoelectrochemical water oxidation, (ii) The light propagation through the lattice structure in the absence of light, (iii) 3D printed lattice structures with different porosities.[68] (Copyright 2023, RSC Publishing) (d) 3D printing of fused quartz glass using the stereolithography system (scale: 7 mm).[276] (Copyright 2017, Springer)

changed. The stability test showed no current attenuation and the Faraday efficiency of oxygen precipitation was 91.24%. An angle-independent and efficient solar energy capture scheme is provided for PEC electrodes (Fig. 15c). Wang et al. focused on the problem of light attenuation and reactor amplification during photocatalysis [277]. A transparent silica cylinder was printed by stereo-lithography technology and used as a catalyst carrier for MB degradation in a packed bed micro-photocatalytic reactor (MPR). The transparent SiO_2 cylinders (S-1, S-2, S-3) were obtained by printing, degreasing and vacuum sintering at 1280°C, and loaded with P25-TiO_2 for MB degradation in a packed bed micro-photocatalytic reactor (MPR). The results showed that the degradation rate of MB of S-1 was 91.4%, while that of Al_2O_3 was less than 60%, and that of SiO_2 was more than 90% (200-800 nm). The reduction of specific surface area and mass transfer limiting efficiency of S-2 and S-3 were significantly reduced. This study provides key data support for the design optimization and scale up of photocatalytic reactors. In addition, in order to overcome the limitation of traditional glass forming technology for the preparation of complex structures, Kotz et al. used SLA to 3D print SiO_2 nanoparticles and photosensitive monomer paste, light curing green parts [276]. A transparent fused silica glass with a surface roughness of 2 nm and no pores was prepared by heat degreasing and vacuum sintering at 1300°C. The light transmittance of the glass is consistent with that of commercial fused quartz, and it can withstand 800°C flames. Colored glass can be made by immersing metal salt with brown parts. Micro-stereo lithography can also realize 80 μm resolution structure, effectively expanding the application scene of glass in the field of optics and microelectromechanical systems (MEMS) (Fig. 15d).

4 3D printing technology applied to photocatalytic reactors and reaction systems

Photocatalytic reaction is a green and efficient technology for pollution control and energy conversion. The improvement of its reaction efficiency largely depends on the performance of photocatalytic reactor and related reaction system. An ideal photocatalytic reactor should have high light utilization efficiency, good mass transfer effect, uniform catalyst loading and contact mode, and structural stability matching with the reaction system. At the same time, it should also meet the practical requirements such as simple operation and easy expansion. Conventional photocatalytic reactors are usually simple in structure and rely on mechanical processing or traditional molding processes [278]. Limited by manufacturing methods, it is often difficult to realize the synergistic optimization of optical path distribution, fluid path, and catalyst spatial arrangement. Such reactors often suffer from serious light scattering, insufficient contact between reactants and catalysts, and high local mass transfer resistance, which results in low photocatalytic efficiency. In addition, it is often necessary to assemble multiple components to integrate complex functions, which not only introduces systematic errors, but also limits the miniaturization and customization of reactors [279].

The emergence of 3D printing technology provides a new approach for the design and manufacture of photocatalytic reactors. Based on its unique principle of layer-by-layer manufacturing and successive assembly, 3D printing can precisely construct complex three-dimensional structures that are difficult to achieve through traditional processes, such as irregular flow channels, micro-nano-level light guiding structures, and gradient porous catalyst carriers [280]. This enables targeted solutions to the inherent defects of traditional reactors in light utilization, mass transfer efficiency, and structural integration. Through digital design and integrated manufacturing, 3D printing can not only achieve precise matching of reactor structure and photocatalytic reaction mechanism but also simplify the setup process of the reaction system, promoting the development of photocatalytic technology towards efficiency, miniaturization, and customization [281]. The following text will elaborate on the specific contributions of 3D printing technology in the innovation of photocatalytic reactor design and the optimization of reaction system setup, revealing how it provides key support for the practical process of photocatalytic technology.

4.1 Design of photocatalytic reactors

4.1.1 Fluidized bed reactor

Based on the form of the catalysts, photocatalytic reactors can be classified into fluidized bed reactors and fixed bed reactors. The fluidized bed photocatalytic reactor is a type of photocatalytic reaction device characterized by a “slurry-like” dispersion system. Its core operation mode is that the catalyst particles and the reactant mixture containing the target pollutants are suspended together in a liquid phase or an air-liquid mixed reaction medium, and a pseudo-fluidized state is formed through the disturbance of the fluid [282]. In terms of the supply method of light radiation, either an external transparent window on the reactor wall can introduce an external light source, or an immersed lamp tube can be directly placed inside the reaction system to provide energy. The regulation of the reaction performance is influenced by multiple factors in a coordinated manner. The concentration of catalyst particles needs to be maintained within a reasonable range. Too low a concentration will lead to insufficient active sites, while too high a concentration will cause enhanced light absorption and scattering due to light obstruction between particles. The matching degree of the wavelength of light radiation, the intensity distribution, and the irradiation path directly determine the efficiency of photon utilization. The flow rate and turbulence degree of the reaction medium, as well as other flow state parameters, significantly affect the mass transfer efficiency and interface contact frequency between the catalyst and the reactants.

The ordinary fluidized bed photocatalytic reactor has significant technical advantages, which can maximize the inherent activity of the catalytic material, expose the active sites on the catalyst surface to the light radiation and the reactant atmosphere to the greatest extent. In addition, it has a simple overall structure and convenient operation, making it suitable for various scenarios of pollutant degradation and energy conversion. However, its inherent drawbacks are also quite prominent. The light scattering effect of suspended particles will lead to local light intensity attenuation, reducing the light utilization efficiency. After the reaction, the separation and recovery of the catalyst require an additional solid-liquid separation process, which not only increases the operation cost but also may cause catalyst loss and secondary pollution due to incomplete separation. Wei et al. used SLS metal 3D printing technology to fabricate three autocatalytic flow-bed reactors of Fe-SCR, Co-SCR,

and Ni-SCR, and designed channels with hemispherical convex inside the reactor to expand the specific surface area [283]. Fe-SCR and Co-SCR can efficiently produce liquid fuels in high pressure Fischer-Trop synthesis and CO_2 hydrogenation. Co-SCR has a C_{5+} selectivity of 65%, and Ni-SCR can achieve 65% CH_4 and 71% CO_2 conversion in high temperature CH_4/CO_2 reforming reaction. The ratio of H_2/CO is close to 1, which can withstand the harsh conditions of high temperature and high pressure, and realize the integration of catalyst and reactor functions in ordinary fluidized bed reactor (Fig. 16a). Zhou et al. prepared two lab-scale 3D-printed plastic sinusoidal flow-through photocatalytic reactors, with Reactor A having no baffles and Reactor B being equipped with baffles [284]. Both reactors were lined with a P25 TiO_2/PLA coating, and after 168 h of UVA pre-conditioning, they could repeatedly photocatalyzed the degradation of circulating aqueous solutions of MB and phenol (PhOH) without obvious activity loss. Owing to the enhanced lateral mixing of laminar flow by baffles, the degradation rate of MB in Reactor B exhibited much lower dependence on flow rate compared to Reactor A. For Reactor A, the photonic efficiencies for MB and PhOH degradation were 0.025% and 0.052%, respectively, and its photocatalytic space-time yields (PSTY) were 0.98×10^{-4} and 1.49×10^{-4} m^3 of reaction solution per (m^3 reactor volume·day·kW), respectively. This work confirms that 3D printing enables the rapid and low-cost fabrication of flow-through photocatalytic reactors with stable performance (Fig. 16b). Ramos et al. fabricated an ABS material plate-packed bed flow-through photocatalytic reactor by fused deposition molding (FFF) 3D printing, filled with 1.0 mm ZnO-coated glass or steel beads for the degradation of para-acetamide [285]. The apparent reaction rate of the steel bead carrier was about 75% higher than that of the glass bead carrier at the first use, but it was easily inactivated. The apparent first-order rate constant of glass beads can reach $1.9\text{-}9.5\times10^{-4}$ s^{-1}, which is 10 times faster than that of conventional suspension bed, which is typical of ordinary packed flow bed reactor (Fig. 16c, d). Phang et al. used DLP 3D printing technology to fabricate a rese-based flow-bed photocatalytic reactor [286]. The main body was made of highly heat-resistant resin, the cover was made of transparent resin, and the bottom of the reactor was coated with g-C_3N_4 homo-junction thermosetting coating. Under 50 W LED irradiation, the degradation efficiency of RhB reached 95.62% within 24 h, the kinetic rate constant was 2.1×10^{-3} min^{-1}, the activity remained 98.5% after 5 cycles, and the TOC removal rate was 78.56%. This study provided an example for the sustainable application of ordinary circulating fluidizing-bed reactor.

To overcome these limitations, researchers have proposed microchannel-type fluidized bed photocatalytic reactors. These reactors fix the catalysts on the inner walls of microchannels or on specific substrate materials, allowing the reaction to take place in a transparent and particle-free clean medium. This design not only significantly simplifies the catalyst recovery process, reduces subsequent processing costs, but also significantly improves the penetration depth and utilization efficiency of light radiation by eliminating particle scattering. Moreover, the miniaturization and micro-miniaturization of the reactor provide great portability and safety, and through structural design, it can achieve more precise control of the reaction process, which is precisely the direction that 3D printing technology excels in. However, compared with the “slurry-like” system, the immobilization of the catalyst will result in a relatively reduced total amount of exposed active sites, sacrificing some reaction activity to a certain extent. Roibu et al. printed a PLA material microchannel flow-bed photocatalytic reactor by FDM technology, with a channel cross section of 1×1 mm [63]. The reduced TiO_2 was made into a film, which was fixed on a glass substrate and integrated into the reactor. With imidacloprid as the target pollutant, the degradation efficiency of P25 coating was 28.4% in the single water flow mode under 395 nm wavelength illumination, and increased to 47.8% after air entry, with a residence time of only 1.1 min. The film maintained stable activity during 150 min operation and belonged to a microchannel flow-bed reactor. Pellejero et al. 3D-printed ABS curved mold, treated by plasma, then loaded Au@POM/TiO_2 by dip coating, and then cast PDMS and dissolved the mold to make microchannel flow-bed reactors with 0.5×0.5 mm and 1×1 mm cross sections [287]. Under 365 nm LED irradiation, the conversion rate of 4-nitrophenol was 93% when the 1×1 mm design was treated at a flow rate of 2 mL h^{-1}. The 0.5×0.5 mm design had a larger specific surface area and better performance under a short residence time (6.3 min), achieving uniform fixation of the catalyst in the microchannel and efficient photocatalytic reaction (Fig. 16e).

4.1.2 Fixed bed reactor

Compared with the fluidized bed photoreactor, the catalyst in the fixed bed photoreactor is loaded on the surface of the carrier or structure inside the reactor in a fixed form, and will not be taken away by the reaction medium. The mass transfer and reaction of the reactants only occur on the surface of the catalyst. The

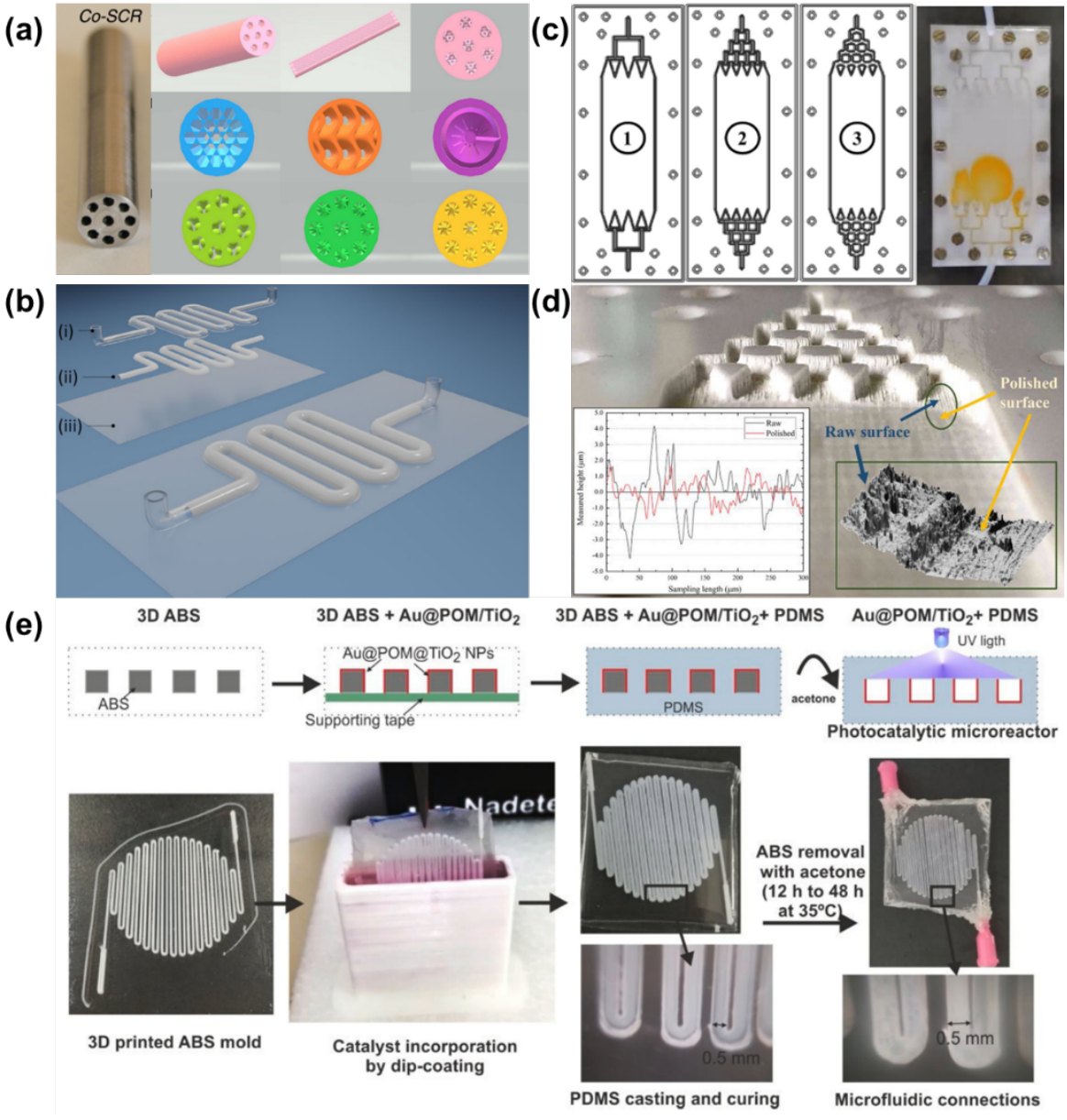

Fig. 16 (a) Real image and geometrical structures of Co-SCRs.[283] (Copyright 2020, Springer) (b) Schematic illustration of reactor A, which comprised (i)a 1 mm thick PLA gutter, mostly lined with (ii)a 0.5 mm thick coating of 5 wt.% TiO_2/PLA, sealed onto (iii)a 100 μm PLA film.[284] (Copyright 2022, Springer) (c) Plate design (1 to 3), the assembled reactor in its physical form and (d) microscopic images.[285] (Copyright 2021, Springer) (e) Scheme of the fabrication protocol of silicone microreactors with integrated photocatalysts by following the "scaffold-removal" method.[287] (Copyright 2020, Elsevier)

light supply mode is similar to that of the fluidized bed. The light source can be introduced from the outside through the transparent reactor wall, and the immersed light source can be placed inside the reactor to ensure the effective delivery of light to the active site of the catalyst. When using 3D printed integrated catalysts, the key factor affecting the reactor performance is more inclined to the regulation ability of the printing technology on the reactor structure. The geometric parameters of the 3D printed flow channel, such as curvature, section size, and branch Angle, directly determine the flow behavior of the reaction medium. Too narrow flow channel can easily lead to excessive pressure drop, while too wide flow channel may make the residence time of reactants insufficient. The optical properties of the printing material significantly affect

the transmission efficiency of optical radiation [62]. The high transparency resin helps to reduce light attenuation, and the specular reflection of the metal surface helps to optimize the light field distribution. The integration accuracy of the reactor with the light source is also controlled by the print size tolerance. For example, if the alignment deviation between the LED array and the catalytic region is too large, the photon utilization efficiency will be reduced. In addition, the interlayer bonding strength and pore sealing performance of the printed structure directly affect the thermal and corrosion resistance of the reactor. Inter layer defects may trigger leakage or structural damage, especially when dealing with acidic or alkaline reaction media.

The advantages of fixed-bed photoreactors are evident. Catalyst immobilization avoids the difficulty of catalyst separation and recovery in fluidized beds, reducing operational costs and the risk of secondary pollution. The design flexibility of the support structure allows optimization of light absorption and mass transfer processes. Fabian and colleagues prepared catalytic materials using a two-step mixing process, with TiO_2-polypropylene (PP) composite filaments as the core [62]. First, recycled PP and TiO_2 were melt-compounded into blocks, which were then crushed, pelletized, and extruded into filaments. Subsequently, 3D printing was used to fabricate a cyclone fixed-bed reactor with a cylinder-cone structure, along with six different TiO_2-PP catalytic inserts, including grid-type and double-grid-type. Among them, the grid-type insert, due to optimized flow field, achieved a 19% degradation rate of MB after 76 h. The double-grid insert showed the highest initial rate for nitrobenzene reduction, at 0.53 nmol s^{-1}. The study achieved layered integration of photocatalysis and acid catalysis by mechanically depositing and immobilizing solid acids on 3D-printed PP cylinders. The quinoline selectivity reached 8%, higher than the 3% in the suspension system. Moreover, no downstream separation was required, effectively addressing issues such as difficult catalyst separation and mass transfer-lighting imbalance in traditional reactors (Fig. 17a). Pan et al. prepared a biomimetic palisade cell structure $BiOBr/Sr_2Nb_2O_7/Al_6Si_2O_{13}$ photocatalytic reactor by combining 3D printing with solvothermal method [288]. The periodic porous structure regulated photon transfer and reactant adsorption, enabling sufficient light scattering inside and smooth reactant flow. The p-n heterojunction interface electric field formed by BiOBr and SNO ($Sr_2Nb_2O_7$) effectively separated photogenerated electron-hole pairs. Under simulated sunlight, the reactor achieved a CO production rate of 13.68 μmol g^{-1} h^{-1} and a CH_4 production rate of 6.37 μmol g^{-1} h^{-1}, which were 3.5 and 8 times higher than those with SNO alone, respectively, enhancing CO_2 reduction performance. After 4 cycles, its photocatalytic performance remained stable. Additionally, the structural ceramic matrix exhibited good mechanical properties, enabling it to withstand harsh reaction environments (Fig. 17b).

However, its drawbacks cannot be ignored: the exposure of active sites may be limited after catalyst loading, and the fixed structure may increase local mass transfer resistance. If the carrier pores become clogged, reaction efficiency will be further reduced. For example, although monolithic nickel-based nano-photocatalytic reactors simplify the recovery process, the loading of a single active source may limit the maximization of catalytic activity to some extent.

4.2 Design of photocatalytic reaction systems

Thanks to the excellent structural design flexibility, 3D printing technology can also realize the integrated design and functional integration from the catalyst to the system, providing customized solutions for core photocatalytic reaction process [292]. This method significantly surpasses the limitations of traditional manufacturing methods in complex structure forming and multi-function integration, and can realize the integrated and collaborative optimization of mass transfer, light transfer and catalysis in the photocatalytic reaction system [293]. Gok et al. prepared Pc-1@MCM-41 heterogeneous photocatalysts and used 3D printing technology to build a low-cost customized photoreactor [289]. The PETG reactor consisted of a base, a LED mounting side panel, and a top cover. The total cost of the reactor was about 115 euros. The catalyst achieved 89% conversion and greater than 99% selectivity in 15 min under atmospheric air conditions while maintaining high stability. The 3D printed reactor effectively improved the practicability and scalability of the photocatalytic reaction (Fig. 18a). In their other work, ZnPc was covalently bonded to functionalized MCM-41-Cl to prepare MCM-41-ZnPc catalyst, which was used to build a photoreactor by 3D printing [290]. The total cost of this study was 21 euros using PETG as material and the reactor was equipped with a 50 W red LED light source. The system was used for the degradation of MB, and the removal rate reached 86% within 90 min. The pollutants were removed by the synergistic effect of adsorption and photocatalysis, and the activity of the catalyst remained more than 67% after 4 cycles (Fig. 18b).

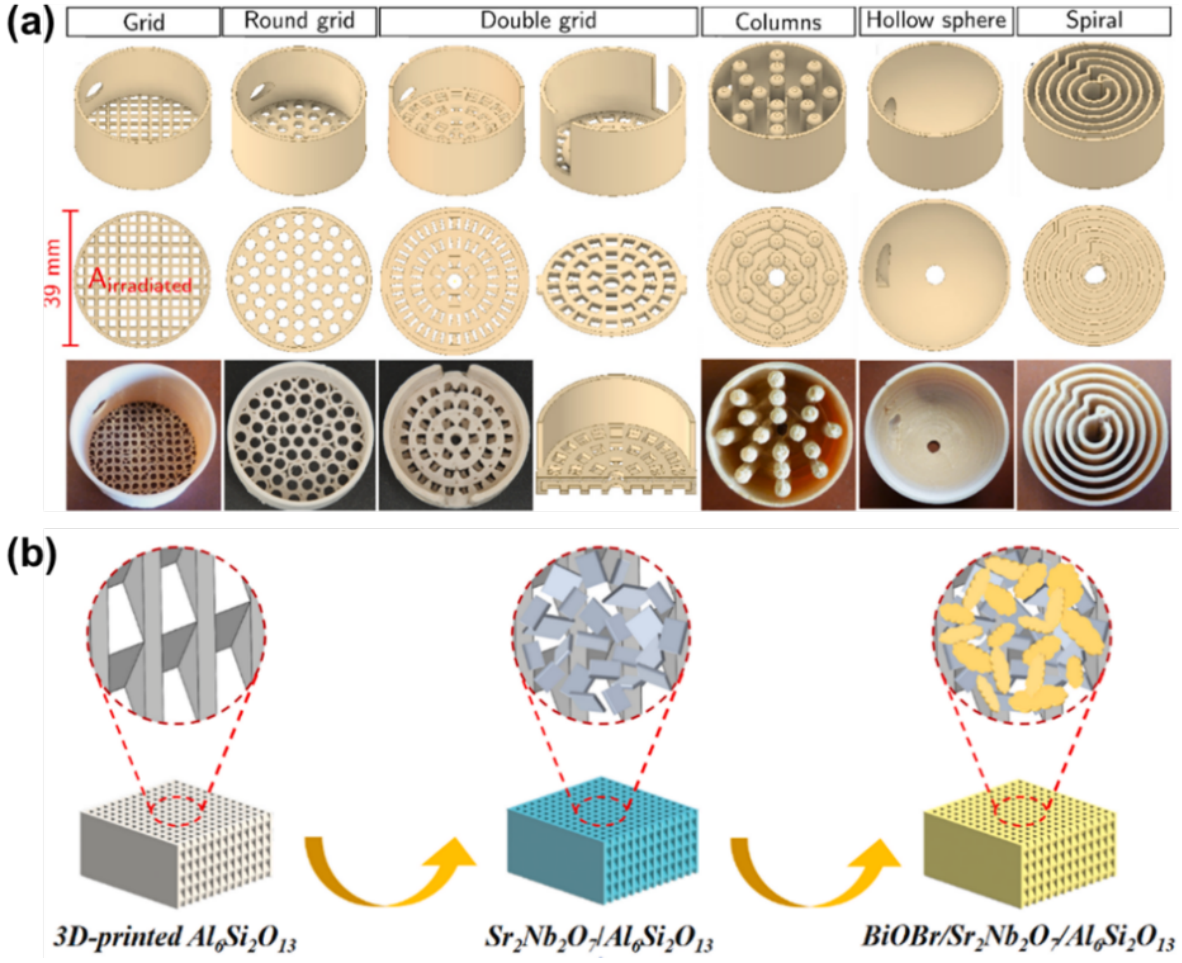

Fig. 17 (a) CAD drawings and 3D-printed TiO_2-PP inserts, the frontal view of the structures shows the irradiated area.[62] (Copyright 2025, Elsevier) (b) The fabrication process for synthesis of BOB/SNO/ASO bionic palisade cell.[288] (Copyright 2022, Elsevier)

In terms of light field control, the use of transparent materials to print built-in optical components such as microlens arrays or optical waveguide structures can realize the redistribution and accurate guidance of light sources, effectively eliminate the light dead zone in the reactor, and ensure uniform irradiation on the catalyst surface. Zheng et al. used 3D printing to fabricate a composite parabolic collector (CPC) photoreactor made of plastic with integrated reflective aluminum strips and quartz tubes, allowing precise control of the structure size [64]. The reactor was filled with g-C_3N_4/chitosan hydrogel beads (GCHBs) to construct a fluidized bed system for the treatment of phenol, sulfamethoxazole and other pollutants. Under simulated sunlight, the performance of the system was comparable to that of the suspension bed, and the activity was not significantly inhibited when processing water samples from real water plants. The outdoor 12-inch 3D printed CPC reactor could also operate stably, and the global single-day water yield was estimated, which proved the value of light regulation in the large-scale construction of photocatalytic system (Fig. 18c-e).

Different from a single process optimization, 3D printing can realize the multi-functional integration of photocatalytic system. By incorporating cavities and microfluidic channels into the printed structure, and integrating micro-sensors and micro-actuators, it is possible to construct an intelligent photocatalytic system. This system is capable of real-time monitoring of reaction conditions and dynamic adjustment of operational parameters, thereby achieving integrated perception, control, and catalysis at the system level. Although no such construction method has been applied to 3D printed photocatalytic integrated systems, it can be inspired by applications in other fields. Li et al. fabricated a circular concave support by 3D printing to

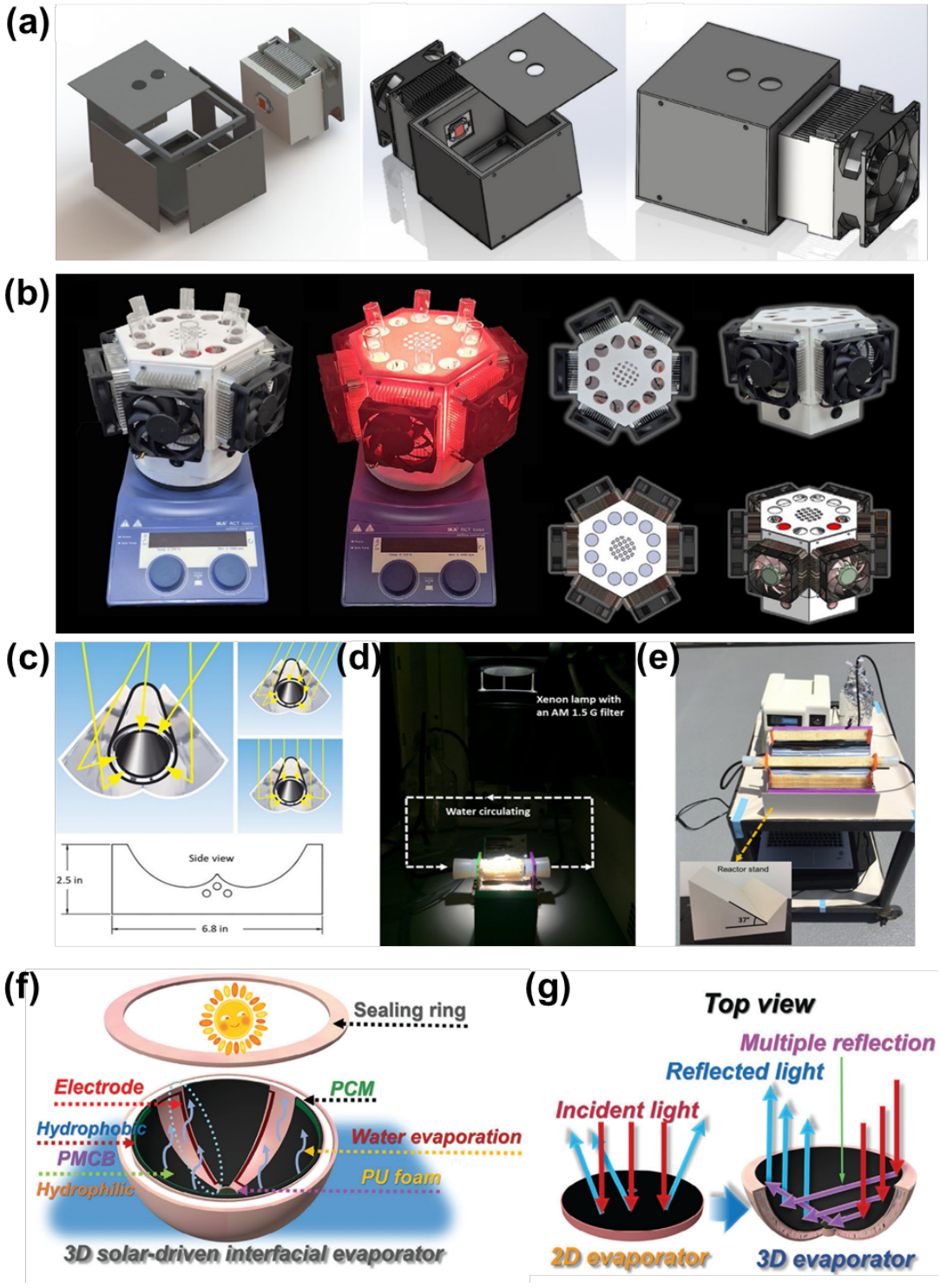

Fig. 18 (a) Decomposition diagram of 3D printed photo-reactor system.[289] (Copyright 2025, Wiley-VCH) (b) Image of the fully assembled photoreactor with its top and perspective views.[290] (Copyright 2025, Wiley-VCH) (c) Side view and dimension of the 3D printed compound parabolic collector reactor. Experimental setup for photocatalytic contaminant degradation under (d) simulated sunlight irradiation in the laboratory and (e) outdoor sunlight irradiation.[64] (Copyright 2020, Elsevier) (f) Schematic diagram of 3D solar evaporator, (g) Light incident and reflection of 2D plane and 3D solar evaporators.[291] (Copyright 2024, Wiley-VCH)

build a layered 3D solar energy reaction system integrated with phase change material (PCM), and the inner side of the support was covered with PMCB coating [291]. The system achieved a maximum output voltage of 3.51 V and an evaporation rate of 4.0 kg m^{-2} h^{-1} under natural sunlight. PCM shortened the capacitor charging time by 57.9% and increased fresh water production by 29.9%. 3D printing support optimizes the sunlight capture efficiency and establishes a photocatalytic reaction system that considers both power output and freshwater production. The ingenious structure of the reaction system realizes the integration of a variety of sensors and actuators (Fig. 18f, g).

5 Conclusions and perspectives

This review systematically describes the rapidly developing applications of 3D printing technology in photocatalysis, including the design of catalysts and catalytic carriers, as well as the manufacturing of advanced photocatalytic reactors and integrated systems. The core advantage of 3D printing lies in its high-precision geometric control and customized manufacturing ability, which can effectively deal with the problems of low light utilization efficiency, mass transfer limitation, difficulty in catalyst recovery and insufficient stability in traditional photocatalytic technology. In terms of photocatalyst design, a variety of 3D printing techniques such as FDM, DIW, SLS/SLM, and SLA are used to fabricate catalyst structures with high porosity, complex channel networks, and customized specific surface areas. These structures significantly increased the active site exposure and improved reactant diffusion, thereby enhancing the photocatalytic efficiency. In addition, in the development of catalyst support, 3D printing supports the flexible use of a variety of materials (polymers, carbon materials, metals, ceramics, etc.), and can prepare support structures with specific properties according to specific photocatalytic requirements, which provides the possibility to construct high-performance integrated catalytic systems. 3D printing has also promoted innovation in the design of photocatalytic reactors and systems. This technology can be used to construct novel reactor configurations to optimize fluid distribution and light field configuration, thereby improving the overall efficiency of energy and mass transfer. More importantly, it makes it possible to integrate functional components such as sensors, mixers, and light-guiding structures into the reaction system, creating conditions for the development of scalable, efficient, and intelligent photocatalytic processes.

3D printing has brought revolutionary design freedom to the field of photocatalysis, and its layered manufacturing characteristics have solved the complex structural customization that traditional processes cannot achieve. The ability to co-print multiple materials has realized the integrated integration of catalysts, carriers, and functional components, reflecting the unique value of this interdisciplinary field. However, there are still limitations that cannot be ignored. Firstly, the adaptability of the ink system is poor. Most existing printing inks rely on polymer or ceramic slurries, which make it difficult to balance printing smoothness and catalytic activity, and it is difficult to print photocatalysts with a high proportion of active components. Secondly, the contradiction between technical cost and scale is prominent. High-precision technology equipment such as SLA/SLM has a unit price exceeding one million, while the precision defects of low-cost FDM cannot meet high-end demands. Thirdly, the long-term stability lacks verification. Most research only focuses on short-term catalytic activity, and issues such as mechanical strength degradation and active component detachment of 3D printed structures in acid-base environments or continuous flow reactions have not been systematically solved.

Based on the analysis of technological progress and limitations mentioned above, we can further identify future challenges and development opportunities (Fig. 19). Perhaps we can carry out in-depth work from the following aspects:

Fig. 19 Challenges and prospects of 3D Printing Technology in Photocatalysis Applications.

1. Currently, the types of 3D printing inks suitable for photocatalysis are relatively limited, and it is often difficult to meet the requirements of printing process and catalytic function at the same time. The development of multifunctional ink with excellent printability, high catalytic efficiency and long-term stability is an important prerequisite for realizing high-performance customized catalytic structure.

2. The photocatalytic system needs to integrate catalytic materials, optical elements and support systems. However, the problems of interface bonding, thermal expansion matching and chemical compatibility between different parts have not been systematically solved. The key of building a complex functional system is to realize multi-material integrated printing and stable integration.

3. In the process of industrial application, the current 3D printing technology is still difficult to maintain high resolution, large size and low cost at the same time. It is an important direction for practical application to develop new printing technology suitable for large-scale production and optimize the balance between printing efficiency and structural performance.

4. Most studies have focused on the initial activity of the catalysts, but there is still a lack of sufficient verification of the mechanical stability and catalytic durability of the printed structures under continuous operation, high temperatures, strong light exposure, and chemical corrosion environments. It is crucial to establish a systematic life evaluation method and develop effective strengthening strategies.

5. By leveraging artificial intelligence, machine learning and computational fluid dynamics, it is possible to achieve collaborative design and optimization of the catalyst's microstructure, the macroscopic reactor flow channels and the optical path. This significantly shortens the research and development cycle and provides the possibility of constructing intelligent catalytic systems that are customizable on demand and have predictable performance. This significantly shortens the research and development cycle and provides the possibility of constructing intelligent catalytic systems that are customizable on demand and have predictable performance.

6. The development of environment-friendly printing materials and energy-saving printing processes, combined with CO_2 conversion, pollutant degradation and other environmental application scenarios, will significantly improve the sustainability of the technology in the whole life cycle.

In conclusion, 3D printing has brought unprecedented design freedom and functional integration capabilities to the field of photocatalysis. The future development urgently requires in-depth collaboration among multiple disciplines such as materials, engineering, chemistry and information, in order to achieve breakthrough progress environmental remediation and energy conversion areas.

Declaration of competing interest

The authors declare that they have no known competing financial interests or personal relationships that could have appeared to influence the work reported in this article. Jizhou Jiang is the Editor-in-Chief, and Hui Xu is an Associate Editor of this journal and they were not involved in the editorial review or the decision to publish this article.

Acknowledgements

This study was supported by the National Natural Science Foundation of China (No. 22378174, 22308128, 22178152, 62004143), the Key Project of Scientific Research Plan of Hubei Provincial Department of Education (No. D20241501), the Drug Efficacy and Health Risk Assessment Key Laboratory of Zhenjiang (SS2024006), and the National Training Program of Innovation and Entrepreneurship for Undergraduates (202510299025).

References

[1] Wang Xiaowen, Zheng Zhen, Jia Weidong, Tai Kaile, Xu Yujie, He Yuming. Response mechanism and evolution trend of carbon effect in the farmland ecosystem of the middle and lower reaches of the yangtze river. Agronomy, 2024, 14 (10), 2354. https://doi.org/10.3390/agronomy14102354.

[2] Muhammad Junaid Nazir, Li Guanlin. Muhammad Mudassir Nazir, Faisal Zulfiqar, Kadambot H. M. Siddique, Babar Iqbal, Daolin Du. Harnessing soil carbon sequestration to address climate change challenges in agriculture. Soil and Tillage Research, 2024, 237, 105959. https://doi.org/10.1016/j.still.2023.105959.

[3] Wang Li, Huang Xingyi, Wang Chengquan, Tian Xiaoyu, Chang Xianhui, Ren Yi, Yu Shanshan. Applications of surface functionalized Fe_3O_4 NPs-based detection methods in food safety. Food Chemistry, 2021, 342, 128343. https://doi.org/10.1016/j.foodchem.2020.128343.

[4] Sun Jing, Zhai Ningning, Miao Jichao, Sun Huaping. Can green finance effectively promote the carbon emission reduction in "local-neighborhood" areas? —empirical evidence from china. Agriculture, 2022, 12 (10), 1550. https://doi.org/10.3390/agriculture12101550.

[5] Waqas Muhammad, Yahya Farzan, Ahmed Ammar, Rasool Yasir, Hongbo Li. Unlocking employee's green behavior in

fertilizer industry: The role of green hrm practices and psychological ownership. International Food and Agribusiness Management Review, 2021, 24 (5), 827-844. https://doi.org/10.22434/ifamr2020.0109.

[6] Yasmin Khan Kiran, Tang Yi, Cheng Pengfei, Song Yunliang, Li Xinyu, Lou Jiabao, Iqbal Babar, Zhao Xin, Hameed Rashida, Li Guanlin, Du Daolin. Effects of degradable and non-degradable microplastics and oxytetracycline co-exposure on soil N_2O and CO_2 emissions. Applied Soil Ecology, 2024, 197, 105331. https://doi.org/10.1016/j.apsoil.2024.105331.

[7] Zhang Chuan, Akhlaq Muhammad, Yan Haofang, Ni Yuxin, Liang Shaowei, Zhou Junan, Xue Run, Li Min. Rana Muhammad Adnan, Jun Li. Chlorophyll fluorescence parameter as a predictor of tomato growth and yield under CO_2 enrichment in protective cultivation. Agricultural Water Management, 2023, 284, 108333. https://doi.org/10.1016/j.agwat.2023.108333.

[8] Fan Meihong, Liang Xiao, Li Qiuju, Cui Lili, He Xingquan, Zou Xiaoxin. Boron: A key functional component for designing high-performance heterogeneous catalysts. Chinese Chemical Letters, 2023, 34 (1), 107275. https://doi.org/10.1016/j.cclet.2022.02.080.

[9] Zhang Baolong, Liu Fangxuan, Sun Bin, Gao Tingting, Zhou Guowei. Hierarchical S-scheme heterojunctions of $ZnIn_2S_4$-decorated TiO_2 for enhancing photocatalytic H_2 evolution. Chinese Journal of Catalysis, 2024, 59, 334-345. https://doi.org/10.1016/S1872-2067(23)64633-9.

[10] Wang Keke, Yuan Xiuhong, Li Wenzhang. Assembly of Al-oxo porphyrin frameworks on Si nanowire for enhanced photoelectrocatalytic hydrogen evolution. Journal of Central South University, 2024, 31 (12), 4560-4571. https://doi.org/10.1007/s11771-024-5830-1.

[11] Siti Nor Qurratu Aini Abd Aziz, Chee Meng Koe, Pung Swee-Yong, Lockman Zainovia, Ul-Hamid Anwar, Tan Wai Kian. Rapid growth of zinc oxide nanorods on kanthal wires by direct heating method and its photocatalytic performance in pollutants removal. Journal of Industrial and Engineering Chemistry, 2023, 118, 226-238. https://doi.org/10.1016/j.jiec.2022.11.008.

[12] Hu Jie, Lao Hongxin, Xu Xiuwu, Wang Weikang, Wang Lele, Liu Qinqin. In situ meso-tetra (4-carboxyphenyl) porphyrin ligand substitution in Hf-MOF for enhanced catalytic activity and stability in photoredox reactions. Rare Metals, 2024, 43 (6), 2682-2694. https://doi.org/10.1007/s12598-023-02595-4.

[13] Li Li, Ma Haiyang, Xing Jiayi, Liu Fulai, Wang Yaosheng. Effects of water deficit and nitrogen application on leaf gas exchange, phytohormone signaling, biomass and water use efficiency of oat plants. Journal of Plant Nutrition and Soil Science, 2020, 183 (6), 695-704. https://doi.org/10.1002/jpln.202000183.

[14] Jiang Di, Yuan Haifeng, Liu Zhen, Chen Yuke, Li Yangyang, Zhang Xiaoli, Xue Guobin, Liu Hong, Liu Xiaoyan, Zhao Lili, Zhou Weijia. Defect-anchored single-atom-layer Pt clusters on TiO_{2-x}/Ti for efficient hydrogen evolution via photothermal reforming plastics. Applied Catalysis B: Environment and Energy, 2023, 339, 123081-123091. https://doi.org/10.1016/j.apcatb.2023.123081.

[15] Wu Zhaohui, Chong Meichi, Zhang Shiying, Li Junshan, Zhu Yongfa. Regulating the crystal phase of bismuth-based semiconductors for promoted photocatalytic performance. Science China Chemistry, 2024, 67 (6), 1839-1864. https://doi.org/10.1007/s11426-023-1943-5.

[16] Xu Jinghang, Shen Jun, Jiang Haopeng, Yu Xiaohui. Waqar Ahmad Qureshi, Chanez Maouche, Jingsong Gao, Juan Yang, Qinqin Liu. Progress and challenges in full spectrum photocatalysts: Mechanism and photocatalytic applications. Journal of Industrial and Engineering Chemistry, 2023, 119, 112-129. https://doi.org/10.1016/j.jiec.2022.11.057.

[17] Liu Jinyuan, Zhu Shumin, Wang Bin, Yang Ruizhe, Wang Rong, Zhu Xingwang, Song Yanhua, Yuan Junjie, Xu Hui, Li Huaming. A candy-like photocatalyst by wrapping Co, N-co-doped hollow carbon sphere with ultrathin mesoporous carbon nitride for boosted photocatalytic hydrogen evolution. Chinese Chemical Letters, 2023, 34 (2), 107749. https://doi.org/10.1016/j.cclet.2022.107749.

[18] Zhang Yong, Qiu Junyi, Zhu Bicheng, Sun Guotai, Cheng Bei, Wang Linxi. Hollow spherical covalent organic framework supported gold nanoparticles for photocatalytic H_2O_2production. Chinese Journal of Catalysis, 2024, 57, 143-153. https://doi.org/10.1016/S1872-2067(23)64580-2.

[19] Chang Fei, Wei Zhixun, Zhao Zhongyuan, Qi Yingfei, Liu Dengguo. 2D-2D heterostructured composites $Bi_4O_5Br_2$-SnS_2 with boosted photocatalytic NO_x abatement. Journal of Industrial and Engineering Chemistry, 2023, 117, 265-272. https://doi.org/10.1016/j.jiec.2022.10.015.

[20] Xue Junpeng, Yu Zhongkai, Mi, Noh Hyeon, Lee Bo Ram, Chun Choi Byung, Heum Park Sung, Hyun Jeong Jung, Du Peng, Song Mingjun. Designing multi-mode optical thermometers via the thermochromic $LaNbO_4$:Bi^{3+}/Ln^{3+} (Ln = Eu, Tb, Dy, Sm) phosphors. Chemical Engineering Journal, 2021, 415, 128977-128991. https://doi.org/10.1016/j.cej.2021.128977.

[21] Zhang Shuai, Li Haobo, Wang Lei, Liu Jiandang, Liang Guijie, Davey Kenneth, Ran Jingrun, Qiao Shizhang. Boosted photoreforming of plastic waste via defect-rich $NiPS_3$ nanosheets. Journal of the American Chemical Society, 2023, 145 (11), 6410-6419. https://doi.org/10.1021/jacs.2c13590.

[22] Miao Yingxuan, Zhao Yunxuan, I. N. Geoffrey, Waterhouse, Shi Run, Wu LiZhu, Zhang Tierui. Photothermal recycling of waste polyolefin plastics into liquid fuels with high selectivity under solvent-free conditions. Nature Communications, 2023, 14 (1), 4242. https://doi.org/10.1038/s41467-023-40005-6.

[23] Zhu Xianglin, Zhou Enlong, Tai Xishi, Zong Huibin, Yi Jianjian, Yuan Zhimin, Zhao Xingling, Huang Peng, Xu Hui, Jiang Zaiyong. g-C_3N_4 S-scheme homojunction through van der Waals interface regulation by intrinsic polymerization

tailoring for enhanced photocatalytic H_2 evolution and CO_2 reduction. Angewandte Chemie International Edition, 2025, 64 (13), e202425439. https://doi.org/10.1002/anie.202425439.

[24] Liang Jiakang, Li Haoxin, Chen Li, Ren Manni. Olugbenga Abiola Fakayode, Jingyi Han, Cunshan Zhou. Efficient hydrogen evolution reaction performance using lignin-assisted chestnut shell carbon-loaded molybdenum disulfide. Industrial Crops and Products, 2023, 193, 116214. https://doi.org/10.1016/j.indcrop.2022.116214.

[25] Ji Qinghua, Yu Xiaojie, Chen Li. Otu Phyllis Naa Yarley, Cunshan Zhou. Facile preparation of sugarcane bagasse-derived carbon supported MoS_2 nanosheets for hydrogen evolution reaction. Industrial Crops and Products, 2021, 172, 114064. https://doi.org/10.1016/j.indcrop.2021.114064.

[26] Wu Guanyu, Gao Xue, Sun Peipei, Mo Zhao, Wang Qiuheng, Chen Hanxiang, Liao Henghui, Yan Pengcheng, She Xiaojie, Xu Hui. High-intensity interfacial electric fields between co-catalysts and semiconductor: A determinant factor in enhancing photocatalytic hydrogen production. Applied Catalysis B: Environment and Energy, 2025, 371, 125265. https://doi.org/10.1016/j.apcatb.2025.125265.

[27] Sun Peipei, Zhong Kang, Huang Xunhuai, Wu Guanyu, Miao Zhihuan, Chen Zhigang, Mo Zhao, Yang Jinman, Xu Hui. Synergistic utilization of photogenerated electrons and holes in carbon nitride nanosheet assembly for enhanced photocatalytic H_2O_2 production. Applied Catalysis B: Environment and Energy, 2025, 366, 124998. https://doi.org/10.1016/j.apcatb.2024.124998.

[28] Miao Honghai, Wu Jiangbo, Luo Xi, Li Xin, Mo Zhao, Liu Jinyuan, Jiang Zaiyong, Yi Jianjian, Zhu Xianglin, Xu Hui. Mechanism decoding of an S-scheme $ZnIn_2S_4/H_2WO_4$ heterojunction with favorable surface electronic potential for enhanced and anti-corrosion photocatalytic hydrogen evolution. Inorganic Chemistry, 2025, 64 (20), 10290-10301. https://doi.org/10.1021/acs.inorgchem.5c01250.

[29] Tang Daojian, Dang Kun, Wang Jiaming, Chen Chuncheng, Zhao Jincai, Zhang Yuchao. Solar-driven green synthesis of epoxides. Science China Chemistry, 2023, 66 (12), 3415-3425. https://doi.org/10.1007/s11426-023-1757-4.

[30] Yang Jinman, Yang Kefen, Zhu Xingwang, Wang Zhaolong, Yang Zhengrui, Ding Xingdong, Zhong Kang, He Minqiang, Li Huaming, Xu Hui. Band engineering of non-metal modified polymeric carbon nitride with broad spectral response for enhancing photocatalytic CO_2 reduction. Chemical Engineering Journal, 2023, 461, 141841. https://doi.org/10.1016/j.cej.2023.141841.

[31] Cheng Kai, Du Jin, Xu Fengfeng, Wang Zengkai, Zhang Liwei, Bai Mengqi, Wang Xueqin, Liu Jun. Preparation and characterization of zein-based active packaging films integrated with TiO_2 nanotube arrays. Food Packaging and Shelf Life, 2024, 45, 101348. https://doi.org/10.1016/j.fpsl.2024.101348.

[32] Li Songmei, Wang Changhua, Li Dashuai, Xing Yanmei, Zhang Xintong, Liu Yichun. Bi_4TaO_8Cl/Bi heterojunction enables high-selectivity photothermal catalytic conversion of CO_2-H_2O flow to liquid alcohol. Chemical Engineering Journal, 2022, 435, 135133-135148. https://doi.org/10.1016/j.foodchem.2022.132657.

[33] Bai Saishuai, Yang Meiqing, Jiang Jizhou, He Xiaomiao, Zou Jing, Xiong Zhiguo, Liao Guodong, Liu Song. Recent advances of MXenes as electrocatalysts for hydrogen evolution reaction. npj 2D Materials and Applications, 2021, 5 (1), 78. https://doi.org/10.1038/s41699-021-00259-4.

[34] Wang Jiamei, Qin Qin, Li Fangyi, Anjarsari Yulianti, Sun Wei, Azzahiidah Rifda, Zou Jing, Xiang Kun, Ma Huijuan, Jiang Jizhou, Arramel. Recent advances of MXenes Mo_2C-based materials for efficient photocatalytic hydrogen evolution reaction. Carbon Letters, 2022, 33 (5), 1381-1394. https://doi.org/10.1007/s42823-022-00401-2.

[35] Dhawan Aastha, Sudhaik Anita, Raizada Pankaj, Thakur Sourbh, Ahamad Tansir, Thakur Pankaj, Singh Pardeep. Chaudhery Mustansar Hussain, $BiFeO_3$-based Z scheme photocatalytic systems: Advances, mechanism, and applications. Journal of Industrial and Engineering Chemistry, 2023, 117, 1-20. https://doi.org/10.1016/j.jiec.2022.10.001.

[36] Miao Honghai, Zeng Guixin. Wu. Jiangbo, Haotian Qi, Zhimin Yuan, Haibo Wang, Xianglin Zhu, Zhao Mo, Zhigang Chen, Hui Xu. *In situ* construction of metal phosphide-anchored $Zn_{0.5}Cd_{0.5}S$ schottky junction photocatalysts for efficient hydrogen evolution via photocatalytic reforming of plastics. International Journal of Hydrogen Energy, 2025, 102, 963-971. https://doi.org/10.1016/j.ijhydene.2025.01.145.

[37] Wang Weikang, Mei Shaobin, Jiang Haopeng, Wang Lele, Tang Hua, Liu Qinqin. Recent advances in TiO_2-based S-scheme heterojunction photocatalysts. Chinese Journal of Catalysis, 2023, 55, 137-158. https://doi.org/10.1016/S1872-2067(23)64551-6.

[38] Li Qi, Li Jiehao, Bai Huimin, Li Fatang. Progress on facet engineering of catalysts for application in photo/electro-catalysis. Chinese Journal of Catalysis, 2024, 58, 86-104. https://doi.org/10.1016/S1872-2067(23)64600-5.

[39] Yang Jinman, Jing Liquan, Zhu Xingwang, Zhang Wei, Deng Jiujun, She Yuanbin, Nie Kaiqi, Wei Yuechang, Li Huaming, Xu Hui. Modulating electronic structure of lattice o-modified orange polymeric carbon nitrogen to promote photocatalytic CO_2 conversion. Applied Catalysis B: Environmental, 2023, 320, 122005. https://doi.org/10.1016/j.apcatb.2022.122005.

[40] Zhu Xianglin, Zong Huibin, J Camilo, Pérez Viasus, Miao Honghai, Sun Wei, Yuan Zhimin, Wang Shenghua, Zeng Guixin, Xu Hui, Jiang Zaiyong, A. Ozin Geoffrey. Supercharged CO_2 photothermal catalytic methanation:High conversion, rate, and selectivity. Angewandte Chemie International Edition, 2023, 62 (22), e202218694. https://doi.org/10.1002/anie.202218694.

[41] Bachirou Guene Lougou, Geng Bo-Xi, Pan Ru-Ming, Wang Wei, Yan Tian-Tian, Li Fang-Hua, Zhang Hao. Oraléou

Sangué Djandja, Yong Shuai, Meisam Tabatabaei, Daniel Sabi Takou. Solar-driven photothermal catalytic CO_2 conversion: A review. Rare Metals, 2024, 43 (7), 2913-2939. https://doi.org/10.1007/s12598-024-02638-4.

[42] Zuo Gancheng, Wang Yuting, Teo Wei Liang, Xian Qiming, Zhao Yanli. Direct Z-scheme TiO_2-$ZnIn_2S_4$ nanoflowers for cocatalyst-free photocatalytic water splitting. Applied Catalysis B: Environment and Energy, 2021, 291, 120126-120134. https://doi.org/10.1016/j.apcatb.2021.120126.

[43] Friedmann Donia, F. Lee Adam, Wilson Karen, Jalili Rouhollah, A Rachel, Caruso. Printing approaches to inorganic semiconductor photocatalyst fabrication. Journal of Materials Chemistry A, 2019, 7 (18), 10858-10878. https://doi.org/10.1039/c9ta00888h.

[44] Xue Yongtao, Kamali Mohammadreza, Zhang Xi, Askari Najmeh, De Preter Clem, Appels Lise, Dewil Raf. Immobilization of photocatalytic materials for (waste)water treatment using 3D printing technology - advances and challenges. Environmental Pollution, 2023, 316, 120549. https://doi.org/10.1016/j.envpol.2022.120549.

[45] S Ana Paula Kitos Vasconcelos. Cem Millik, Antonio Vazquez, Naroa Sadaba, Sahana Sateesh, Shannon Daily, Siwei Yu, Meijing Zhang, Natwara Manitsirisuk, Alshakim Nelson. Light-based 3D printing of polymeric materials. Annual Review of Materials Research, 2025, 55 (1), 491-521. https://doi.org/10.1146/annurev-matsci-080423-123810.

[46] Yao Pinjing, Li Wangyang, Ke Bingyuan, Chen Lihui, Jian Yijia, Qiao Huawei, Zhang Huagui, Ying Yang Hui, Wang Xinghui. 3D printing of serrated $NiCo_2S_4$-based electrodes for wearable micro-supercapacitors. Science China Materials, 2024, 67 (6), 1956-1964. https://doi.org/10.1007/s40843-024-2920-x.

[47] Liu Guo, Lu Xinya, Zhang Xiaofeng, Zhao Yan, Yi Shenghui, Xu Jingjun, Zhan Yuqi, Yin Jianan, Feng Chengcheng, Zhou Zhifeng, Wang Peiyu, Chen Zhou, He Yunhu, Chen Siyao, Liu Pengchao, Zuo Jun, Dai Yu, Wu Jian, Liu Sida, Lu Jian. 3D/4D additive-subtractive manufacturing of heterogeneous ceramics. Journal of Materials Science & Technology, 2024, 201, 210-221. https://doi.org/10.1016/j.jmst.2024.02.069.

[48] Li Yishan, Huang Lijie, Wang Xiyue, Wang Yanan, Lu Xuyang, Wei Zhehao, Mo Qi, Sheng Yao, Zhang Shuya, Huang Chongxing, Duan Qingshan. Blending and functionalisation modification of 3D printed polylactic acid for fused deposition modeling. Reviews on Advanced Materials Science, 2023, 62 (1), 20230140. https://doi.org/doi:10.1515/rams-2023-0140.

[49] Zhang Xueqin, Su Ruyue, Xionggao, Chen Jingyi, Liu Guo, He Rujie, Li Ying. Circumventing brittleness of 3D-printed Al_2O_3 cellular ceramic structures via compositing with polyurea. Rare Metals, 2024, 43 (11), 5994-6005. https://doi.org/10.1007/s12598-024-02850-2.

[50] Li Ning, Wang Yitong, Chang Xianglin, Gao Wenjie, Kong Lingchao, Yan Beibei, Chen Guanyi. Revolutionizing catalytic water treatment: A critical review on the role of 3D printed catalysts. Separation and Purification Technology, 2025, 363, 132194. https://doi.org/10.1016/j.seppur.2025.132194.

[51] Bai Shenwei, Mei Hui, Zhang Minggang, Zhou Shixiang, Yan Yuekai, Cheng Laifei, Zhang Litong, Lu Jian. 3D printing assemble technology toward advanced photocatalysis. Materials Today Nano, 2023, 24, 100385. https://doi.org/10.1016/j.mtnano.2023.100385.

[52] Li Nannan, Tong Kai, Yang Lijun, Du Xiaoze. Review of 3D printing in photocatalytic substrates and catalysts. Materials Today Energy, 2022, 29, 101100. https://doi.org/10.1016/j.mtener.2022.101100.

[53] Jhon Mauricio Aguirre-Cortés. Adriana Isabel Moral-Rodríguez, Esther Bailón-García, Arantxa Davó-Quiñonero, Agustín Francisco Pérez-Cadenas, Francisco Carrasco-Marín. 3D printing in photocatalysis: Methods and capabilities for the improved performance. Applied Materials Today, 2023, 32, 101831. https://doi.org/10.1016/j.apmt.2023.101831.

[54] Liu Xuehui, Zhao Shengjian, Li Quanhong, He Peigang, Duan Xiaoming, Jia Dechang, Zhou Yu. 3D printed Go-g-C_3N_4-geopolymer components with acid treatment for the removal of methylene blue from wastewater. Journal of the American Ceramic Society, 2025, 108 (5), e20377. https://doi.org/10.1111/jace.20377.

[55] Liu Xuehui, Zhao Shengjian, Li Quanhong, He Peigang, Duan Xiaoming, Jia Dechang, Colombo Paolo, Zhou Yu. Enhancing methylene blue removal performance through interfacial charge transfer effect in 3D printing g-C_3N_4/geopolymer/Fe(iii) composite. Journal of Environmental Chemical Engineering, 2025, 13 (5), 117846. https://doi.org/10.1016/j.jece.2025.117846.

[56] Jiun Phang Sue, Wong Voon-Loong, How Cheah Kean, Tan Lling-Lling. 3D-printed photoreactor with robust g-C_3N_4 homojunction based thermoset coating as a new and sustainable approach for photocatalytic wastewater treatment. Journal of Environmental Chemical Engineering, 2021, 9 (6), 106437. https://doi.org/10.1016/j.jece.2021.106437.

[57] Fu Runfang, Shi Qianqian, Yong Zijun, C James, Griffith, Yap Lim Wei, Cheng Wenlong. Self-assembled janus plasmene nanosheets as flexible 2D photocatalysts. Materials Horizons, 2021, 8 (1), 259-266. https://doi.org/10.1039/d0mh01275k.

[58] C. Lopes Joana, Peñas-Garzón Manuel, J. Sampaio Maria, G. Silva Cláudia, L. Faria Joaquim. Photocatalytic oxidative coupling of benzyl alcohol and benzylamine for imine synthesis using immobilized $Cs_3Bi_2Br_9$ perovskite. Small, 2024, 21 (5), 2409037. https://doi.org/10.1002/smll.202409037.

[59] Lin He, Ma Ming, Qi Huan, Wang Xin, Xing Zheng, Alowasheeir Azhar, Tang Huiping, Jun Seong Chan, Yamauchi Yusuke, Liu Shude. 3D-printed photocatalysts for revolutionizing catalytic conversion of solar to chemical

energy. Progress in Materials Science, 2025, 151. https://doi.org/10.1016/j.pmatsci.2025.101427.

[60] Zhong Kang, Sun Peipei, Xu Hui. Advances in defect engineering of metal oxides for photocatalytic CO_2 reduction. Small, 2024, 21 (28), 2310677. https://doi.org/10.1002/smll.202310677.

[61] Amir Hossein Ghasemi, Javad Zoqi Mohamad. Payam Zanganeh Ranjbar. Enhanced photocatalytic degradation of methylene blue using a novel counter-rotating disc reactor. Frontiers in Chemistry, 2024, 12, 1335180. https://doi.org/10.3389/fchem.2024.1335180.

[62] Guba Fabian, Timm Jana, Thu Duong Hong, Pashkova Aneta, Z. Bloh Jonathan, Marschall Roland, Ziegenbalg Dirk. Photoreactors manufactured from 3D-printed (photo-) catalytic materials. Chemical Engineering Journal, 2025, 520, 164902. https://doi.org/10.1016/j.cej.2025.164902.

[63] Roibu Anca, Udroiu Razvan, Abreu-Jaureguí Coset, Silvestre-Albero Joaquin, Andronic Luminita. Wavelength-dependent activity screening of reduced titania for photocatalytic degradation of imidacloprid in batch and flow-mode. Journal of Environmental Chemical Engineering, 2024, 12 (3), 112752. https://doi.org/10.1016/j.jece.2024.112752.

[64] Zheng Qinmin, Aiello Ashlee, Sil Choi Yoon, Tarr Kayla, Shen Hongchen, P David, Durkin, Shuai Danmeng. 3D printed photoreactor with immobilized graphitic carbon nitride: A sustainable platform for solar water purification. Journal of Hazardous materials, 2020, 399, 123097. https://doi.org/10.1016/j.jhazmat.2020.123097.

[65] Majooni Yalda, Philip Sava Simon, Fayazbakhsh Kazem, Yousefi Nariman. Sustainable 3D-printed platforms with durable photocatalytic coatings for efficient water treatment. Advanced Sustainable Systems, 2025, e00135. https://doi.org/10.1002/adsu.202500135.

[66] Jin Haize, Zhu Mengyao, Nie Chang, Liu Junyi, Hong Kaiqiang, Li Cuixia, Wang Qikun. *In-situ* interspersed geopolymer nanoclusters on nitrogen defective g-C_3N_4 to promote the matching of adsorption and photocatalytic kinetics. Surfaces and Interfaces, 2025, 60, 106050. https://doi.org/10.1016/j.surfin.2025.106050.

[67] Verma Gulshan, Islam Monsur, Gupta Ankur. ZnO nanowire-decorated 3D printed pyrolytic carbon for solar light-driven photocatalytic degradation of wastewater contaminants. Advanced Composites and Hybrid Materials, 2025, 8 (1), 109. https://doi.org/10.1007/s42114-024-01125-9.

[68] Hegde Chidanand, Rosental Tamar, Tan Joel Ming Rui, Magdassi Shlomo, Helena Wong Lydia. Angle-independent solar radiation capture by 3D printed lattice structures for efficient photoelectrochemical water splitting. Materials Horizons, 2023, 10 (5), 1806-1815. https://doi.org/10.1039/d2mh01475k.

[69] Zheng Ziye, Tian Shuang, Feng Yuxiao, Zhao Shan, Li Xin, Wang Shuguang, He Zuoli. Recent advances of photocatalytic coupling technologies for wastewater treatment. Chinese Journal of Catalysis, 2023, 54, 88-136. https://doi.org/10.1016/s1872-2067(23)64536-x.

[70] Fujishima Akira, Honda Kenichi. Electrochemical photolysis of water at a semiconductor electrode. Nature, 1972, 238 (5358), 37-38. https://doi.org/10.1038/238037a0.

[71] Qi Yaozhong, Shen Yanbai, Zhao Sikai, Jiang Xiaoyu, Gao Shuling, Han Cong, Liu Wenbao, San Xiaoguang, Meng Dan. Dual-loading strategy to construct Au-BiOBr-TiO_2 photocatalysts for fast and efficient degradation of xanthates under visible light. Journal of Central South University, 2023, 30 (10), 3289-3302. https://doi.org/10.1007/s11771-023-5453-y.

[72] Javed Qaiser, Wu Yanyou, Xing Deke, Azeem Ahmad, Ullah Ikram, Zaman Muhammad. Re-watering: An effective measure to recover growth and photosynthetic characteristics in salt-stressed Brassica napus L. Chilean journal of agricultural research, 2017, 77 (1), 78-86. https://doi.org/10.4067/s0718-58392017000100010.

[73] Zhong Kang, Wu Guanyu, Sun Peipei, Chen Si, Dai Xiaomei, Yang Jinman, Li Huaming, Mo Zhao, Xu Hui. Synergistic Cl and O co-doping in self-assembled red carbon nitride nanorods for enhanced photocatalytic H_2O_2 production. Applied Catalysis B: Environment and Energy, 2026, 380, 125804. https://doi.org/10.1016/j.apcatb.2025.125804.

[74] Zhou Dongxue, Xue Xiangdong, Luan Qingjie, Zhang Liguo, Li Baozhen, Wang Xing, Dong Wenjun, Wang Ge, Hou Changmin. A unique janus PdZn-Co catalyst for enhanced photocatalytic syngas production from CO_2 and H_2O. Chinese Chemical Letters, 2023, 34 (7), 107798. https://doi.org/10.1016/j.cclet.2022.107798.

[75] Zhang Shengya, Du Peiyao, Lu Xiaoquan. Advancements in semiconductor-based interface engineering strategies and characterization techniques for carrier dynamics in photoelectrochemical water splitting. Science China Materials, 2024, 67 (5), 1379-1392. https://doi.org/10.1007/s40843-023-2819-8.

[76] Wu Guanyu, Zhang Wei, Mo Zhao, Zhao Xinyu, Sun Peipei, Wang Qiuheng, Yan Pengcheng, She Xiaojie, Xu Hui. S-scheme homojunction carbon nitride for photocatalytic overall water splitting. ACS Catalysis, 2025, 15 (11), 8822-8832. https://doi.org/10.1021/acscatal.5c01086.

[77] Liang Huimin, Ye Caichao, Wu Yao, Li Yezi, Long Ran, Xiong Jun, Jiang Wei, Di Jun. Fe single atom trigger asymmetric In-In polarized site pairs boosting near-infrared N_2 photoreduction. Materials Today, 2025, 86, 96-103. https://doi.org/10.1016/j.mattod.2025.03.014.

[78] Huang Yue, Zhang Jinfeng, Ruzimuradov Olim, Mamatkulov Shavkat, Dai Kai, Low Jingxiang. Selective oxygen vacancy engineering for shrinking the potential barrier of S-scheme heterojunction toward highly efficient photocatalytic CO_2 conversion. Composite Functional Materials, 2025, 1 (1), 20250103. https://doi.org/10.63823/20250103.

[79] Fu Hui, Tian Jin, Zhang Qianqian, Zheng Zhaoke, Cheng

Hefeng, Liu Yuanyuan, Huang Baibiao, Wang Peng. Single-atom modified graphene cocatalyst for enhanced photocatalytic CO_2 reduction on halide perovskite. Chinese Journal of Catalysis, 2024, 64, 143-151. https://doi.org/10.1016/s1872-2067(24)60081-1.

[80] Wu Junyan, Zhao Lina, Gao Xu, Li Yuxin. Multiscale structural regulation of two-dimensional materials for photocatalytic reduction of CO_2. Progress in Materials Science, 2025, 148, 101386. https://doi.org/10.1016/j.pmatsci.2024.101386.

[81] Li Zhiyang, Chen Yaogang, Zhang Yinghe, Ai Wei, Lei Qian, Yao Tingjun, Zhong Dan, Liu Wenjie, Jin Wenbiao, Yang Lei. Tuning interfacial charge transfer for efficient visible-light-driven photodegradation and simultaneous H_2 evolution. Journal of Materials Science & Technology, 2024, 168, 35-49. https://doi.org/10.1016/j.jmst.2023.05.033.

[82] Feng Yu, Fang Xiao, Zang Jinnuo, Song Bin, Hu Chunlian, Dong Xiaoyu, Ding Yong. Improvement of charge-transfer kinetics via MXene and cobalt containing polyoxometalate loading on CdS for photocatalytic hydrogen production. Science China Chemistry, 2025, 68 (2), 772-780. https://doi.org/10.1007/s11426-024-2358-3.

[83] Li Bei, Zhang Xiangxiang, Lv Min, Huang Baibiao, Zheng Zhaoke. Imaging charge carrier transfer in facet-dependent semiconductor photocatalysts by single-particle fluorescence spectroscopy. Science China Chemistry, 2025, 68 (5), 1794-1809. https://doi.org/10.1007/s11426-024-2199-7.

[84] Jia Guangri, Zhang Yingchuan, C. Yu Jimmy, Guo Zhengxiao. Asymmetric atomic dual-sites for photocatalytic CO_2 reduction. Advanced Materials, 2024, 36 (38), 2403153. https://doi.org/10.1002/adma.202403153.

[85] Wu Wenli, Zhang Nan, Wang Yuhua. Construction of Au/$ZnWO_4$/CdS ternary photocatalysts with oxygen vacancy modification for efficient photocatalytic hydrogen production. Advanced Functional Materials, 2024, 34 (32), 2316604. https://doi.org/10.1002/adfm.202316604.

[86] Cui Entian, Lu Yulian, Jiang Jizhou, Arramel, Wang Dingsheng, Zhai Tianyou. Tailoring cuni heteronuclear diatomic catalysts: Precision in structural design for exceptionally selective CO_2 photoreduction to ethanol. Chinese Journal of Catalysis, 2024, 59, 126-136. https://doi.org/10.1016/S1872-2067(23)64630-3.

[87] Yuan Lin, Zhang Lei, Li Xiaoxin, Liu Jiang, Liu Jingjing, Dong Longzhang, Li Dongsheng, Li Shunli, Lan Yaqian. Uncovering the synergistic photocatalytic behavior of bimetallic molecular catalysts. Chinese Chemical Letters, 2023, 34 (1), 107146. https://doi.org/10.1016/j.cclet.2022.01.039.

[88] He Shanyue, Zhang Xin, Chen Mei, Jiang Hongquan, Qu Yang, Liu Yanduo, Jiang Jizhou. Photocatalytic H_2O_2 production over $Ti(HPO_4)_2$ S-scheme heterojunction through push-pull electronic effects enhance the oxygen reduction. Composite Functional Materials, 2025, 1 (2), 20250203. https://doi.org/10.63823/20250203.

[89] Zhang Tao, Li Bo, Wang Chaofeng, Wu Shuilin, Zhu Shengli, Jiang Hui, Zheng Yufeng, Li Zhaoyang, Cui Zhenduo, Zhang Yu, K. Chu Paul, Liu Xiangmei. Tunning the bandgap of MnO_2 homojunction by building active high-index facet to achieve rapid electron transfer for enhanced photocatalytic sterilization. Journal of Materials Science & Technology, 2024, 168, 265-275. https://doi.org/10.1016/j.jmst.2023.05.059.

[90] Guo Fan, He Zongzheng, Wang Peng, Zhang Xiaoyu, Yu Hongjian, Wang Qinchao, Sun Weiyin. Construction of N-doped copper metal-organic frameworks for promoting photocatalytic carbon dioxide reduction to ethylene. Science China Chemistry, 2025, 68 (2), 601-609. https://doi.org/10.1007/s11426-024-2229-2.

[91] Zhou Baowen, Li Jinglin, Dong Xinyue, Yao Lin. Gan nanowires/Si photocathodes for CO_2 reduction towards solar fuels and chemicals: Advances, challenges, and prospects. Science China Chemistry, 2023, 66 (3), 739-754. https://doi.org/10.1007/s11426-022-1508-y.

[92] Zhan Haiyin, Zhou Ruiren, Liu Kewang, Ma Zhihui, Wang Pengfei, Zhan Sihui, Zhou Qixing. Progress and challenges of photocatalytic reduction of CO_2 with g-C_3N_4-based photocatalysts in the context of carbon neutrality. Science China Materials, 2024, 67 (6), 1740-1764. https://doi.org/10.1007/s40843-024-2900-5.

[93] Yang Qiang, Li Xiang, Tian Qingwen, Pan Aixiang, Liu Xingjian, Yin Hang, Shi Yingqiao, Fang Guigan. Synergistic effect of adsorption and photocatalysis of BiOBr/lignin-biochar composites with oxygen vacancies under visible light irradiation. Journal of Industrial and Engineering Chemistry, 2023, 117, 117-129. https://doi.org/10.1016/j.jiec.2022.09.044.

[94] Singla Shelly, Basu Soumen, Devi Pooja. Solar light responsive 2D/2D $BiVO_4$/SnS_2 nanocomposite for photocatalytic elimination of recalcitrant antibiotics and photoelectrocatalytic water splitting with high performance. Journal of Industrial and Engineering Chemistry, 2023, 118, 119-131. https://doi.org/10.1016/j.jiec.2022.10.051.

[95] Wu Xinhe, Tan Lihong, Chen Guoqiang, Kang Jiayue, Wang Guohong. g-C_3N_4-based S-scheme heterojunction photocatalysts. Science China Materials, 2024, 67 (2), 444-472. https://doi.org/10.1007/s40843-023-2755-2.

[96] Zhou Min, Wu Honghui, Wu Yuan, Wang Hui, Liu Xiongjun, Jiang Suihe, Zhang Xiaobin, Lu Zhaoping. Phase field modeling of grain stability of nanocrystalline alloys by explicitly incorporating mismatch strain. Rare Metals, 2024, 43 (7), 3370-3382. https://doi.org/10.1007/s12598-024-02678-w.

[97] Wang Jilei, Cao Jiapeng, Du Zeyu, Liu Xiaomei, Li Jianian, Ping Qingdong, Zang Tingting, Xu Yan. Four novel Z-shaped hexanuclear vanadium oxide clusters as efficient heterogeneous catalysts for cycloaddition of CO_2 and oxidative desulfurization reactions. Chinese Chemical Letters,

2023, 34 (1), 106917. https://doi.org/10.1016/j.cclet.2021.11.005.

[98] Wang Zhonghao, Zou Guojun, Hyeok Park Jong, Zhang Kan. Progress in design and preparation of multi-atom catalysts for photocatalytic CO_2 reduction. Science China Materials, 2024, 67 (2), 397-423. https://doi.org/10.1007/s40843-023-2698-5.

[99] Yang Jinman, Zhu Xingwang, Yu Qing, He Minqiang, Zhang Wei, Mo Zhao, Yuan Junjie, She Yuanbin, Xu Hui, Li Huaming. Multidimensional In_2O_3/In_2S_3 heterojunction with lattice distortion for CO_2 photoconversion. Chinese Journal of Catalysis, 2022, 43 (5), 1286-1294. https://doi.org/10.1016/s1872-2067(21)63954-2.

[100] Huang Qianqian, Wang Rui, Li Xiya, Liu Tianfu. A R Mahammed Shaheer, Rong Cao. The effects of local environment towards yield and selectivity on photocatalytic CO_2 reduction catalyzed by metal-organic framework. Chinese Chemical Letters, 2023, 34 (12), 108517. https://doi.org/10.1016/j.cclet.2023.108517.

[101] Li Shijie, Wang Chunchun, Dong Kexin, Zhang Peng, Chen Xiaobo, Li Xin. MIL-101(Fe)/BiOBr S-scheme photocatalyst for promoting photocatalytic abatement of Cr(VI) and enrofloxacin antibiotic: Performance and mechanism. Chinese Journal of Catalysis, 2023, 51, 101-112. https://doi.org/10.1016/S1872-2067(23)64479-1.

[102] Wen Dongxiao, Wang Nan, Peng Jiahe, Majima Tetsuro, Jiang Jizhou. Unique Cu_x^+/Cu_0 active-site switches in Cu-loaded g-C_3N_4 nanosheets for efficient photocatalytic CO_2 reduction. Journal of Materials Science & Technology, 2025, 226, 93-108. https://doi.org/10.1016/j.jmst.2024.12.010.

[103] Liang Ying, Huang Guohe, Xin Xiaying, Yao Yao, Li Yongping, Yin Jianan, Li Xiang, Wu Yuwei, Gao Sichen. Black titanium dioxide nanomaterials for photocatalytic removal of pollutants: A review. Journal of Materials Science & Technology, 2022, 112, 239-262. https://doi.org/10.1016/j.jmst.2021.09.057.

[104] Yang Lanhao, Zhang Jingyu, Tong Haojie, Li Xiaoyu, Zhao Dongyuan, Lan Kun. Synthesis of mesoporous titania nanomaterials for evolving photocatalytic applications. Advanced Energy Materials, 2025, e02405. https://doi.org/10.1002/aenm.202502405.

[105] K. Mourya Adarsh, P. Singh Rudra, Amin Mohd, R. Barad Sakshi, Abedi Mohammadmahdi, V. Wankhade Atul. Tuning photocatalytic performance via oxygen vacancies and in situ ZnS formation on ZnO for hydrogen evolution. Renewable Energy, 2025, 249, 123166. https://doi.org/10.1016/j.renene.2025.123166.

[106] Chen Yanan, Xiang Wenzhuo, Zhang Zizhong, Ji Tao, Su Wenyue. Enhanced CO_2 conversion to co using an S-scheme 2D/2D $WO_3/InVO_4$ photocatalysts. Chemical Engineering Journal, 2025, 508, 160993. https://doi.org/10.1016/j.cej.2025.160993.

[107] Huang Shiyu, Fan Deqi, Zhao Chengxiao, Li Xin, Yang Xiaofei. Efficient photoreduction of CO_2 to complete Co catalyzed by electrospun Cu-doped In_2O_3 nanofibers. Sustainable Materials and Technologies, 2025, 45, e01611. https://doi.org/10.1016/j.susmat.2025.e01611.

[108] Jie Longfei, Gao Xue, Cao Xiaoqing, Wu Shan, Long Xiaoxing, Ma Qiongyan, Su Jixin. A review of cds photocatalytic nanomaterials: Morphology, synthesis methods, and applications. Materials Science in Semiconductor Processing, 2024, 176, 108288. https://doi.org/10.1016/j.mssp.2024.108288.

[109] Wu Panpan, Liu Haizhen, Xie Ziyu, Xie Linjun, Liu Guozhong, Xu Yingchao, Chen Jing, Lu Can-Zhong. Excellent charge separation of NCQDs/ZnS nanocomposites for the promotion of photocatalytic H_2 evolution. ACS Applied Materials & Interfaces, 2024, 16 (13), 16601-16611. https://doi.org/10.1021/acsami.3c15957.

[110] Chen Kaihong, Xiao Jiadong, Hisatomi Takashi, Domen Kazunari. Transition-metal (oxy)nitride photocatalysts for water splitting. Chemical Science, 2023, 14 (35), 9248-9257. https://doi.org/10.1039/d3sc03198e.

[111] Feng Xuezhen, Zheng Renji, Gao Caiyan, Wei Wenfei, Peng Jiangguli, Wang Ranhao, Yang Songhe, Zou Wensong, Wu Xiaoyong, Ji Yongfei, Chen Hong. Unlocking bimetallic active sites via a desalination strategy for photocatalytic reduction of atmospheric carbon dioxide. Nature Communications, 2022, 13 (1), 2146. https://doi.org/10.1038/s41467-022-29671-0.

[112] Qiao Qianyu, Chen Yao, Wang Yue, Ren Yuqing, Cao Jiazhen, Huang Fengjiao, Bian Zhenfeng. Surface modification of phosphate ion to promote photocatalytic recovery of precious metals. Chinese Chemical Letters, 2023, 34 (2), 107394. https://doi.org/10.1016/j.cclet.2022.03.117.

[113] Li Min, Yu Shixin, Huang Hongwei. Emerging polynary bismuth-based photocatalysts: Structural classification, preparation, modification and applications. Chinese Journal of Catalysis, 2024, 57, 18-50. https://doi.org/10.1016/S1872-2067(23)64593-0.

[114] Wen Dongxiao, Wang Nan, Peng Jiahe, Majima Tetsuro, Jiang Jizhou. Collaborative photocatalytic C-C coupling with Cu and P dual sites to produce C_2H_4 over Cu_xP/g-C_3N_4heterojunction. Chinese Journal of Catalysis, 2025, 69, 58-74. https://doi.org/10.1016/S1872-2067(24)60183-X.

[115] Yu Tingting, Yang Bing, Zhang Rong, Yang Chenyu, Arramel, Jiang Jizhou. Fabrication of a novel Z-S-scheme photocatalytic fuel cell with the Z-scheme TiO_2/GO/g-C_3N_4 photoanode and S-scheme $BiOAc_{1-x}Br_x$/BiOBr photocathode for TC degradation. Journal of Materials Science & Technology, 2024, 188, 11-26. https://doi.org/10.1016/j.jmst.2023.12.004.

[116] Wang Haitao, Jiang Jizhou, Yu Lianglang, Peng Jiahe, Song Zhou, Xiong Zhiguo, Li Neng, Xiang Kun, Zou Jing, Hsu Jyh-Ping, Zhai Tianyou. Tailoring advanced n-defective and S-doped g-C_3N_4 for photocatalytic H_2 evolution. Small, 2023, 19 (28), 2301116. https://doi.org/10.1002/smll.202301116.

[117] Guan Yuchen, Ren Zhixin, Lang Yan, Liu Tianze, Gong Zhao, Lv Yuguang. Preparation and photocatalytic degradation of sulfamethoxazole by g-C_3N_4 nano composite samples. Reviews on Advanced Materials Science, 2023, 62 (1), 20220280. https://doi.org/doi:10.1515/rams-2022-0280.

[118] Minale Mengist, Gu Zaoli, Guadie Awoke. Daniel Manaye Kabtamu, Yuan Li, Xuejiang Wang. Application of graphene-based materials for removal of tetracyclines using adsorption and photocatalytic-degradation: A review. Journal of Environmental Management, 2020, 276, 111310. https://doi.org/10.1016/j.jenvman.2020.111310.

[119] Ahmadi Abbas, Hajilou Mersad, Zavari Saman, Yaghmaei Soheila. A comparative review on adsorption and photocatalytic degradation of classified dyes with metal/non-metal-based modification of graphitic carbon nitride nanocomposites: Synthesis, mechanism, and affecting parameters. Journal of Cleaner Production, 2023, 382, 134967. https://doi.org/10.1016/j.jclepro.2022.134967.

[120] Zhao Guoqing, Hu Jun, Long Xuan, Zou Jiao, Yu Jingang, Jiao Feipeng. A critical review on black phosphorus-based photocatalytic CO_2 reduction application. Small, 2021, 17 (49), 2102155. https://doi.org/10.1002/smll.202102155.

[121] Wang Wang, Chen Zhongyue, Li Chengming, Cheng Bei, Yang Kai, Zhang Song, Luo Guoqiang, Yu Jiaguo, Cao Shaowen. Graphene quantum dot-modified $Mn_{0.2}Cd_{0.8}S$ for efficient overall photosynthesis of H_2O_2. Advanced Functional Materials, 2025, 35 (28), 2422307. https://doi.org/10.1002/adfm.202422307.

[122] Jang Dawoon, Lee Suyeon, Hee Kwon Nam, Kim Taehoon, Park Sangjoon, Yeon Jang Kyung, Yoon Eojin, Choi Seungjoo, Han Juheon, Lee Tae-Woo, Kim Jeongho, Hwang Seong-Ju, Park Sungjin. Preparation of carbon nitride nanotubes with P-doping and their photocatalytic properties for hydrogen evolution. Carbon, 2023, 208, 290-302. https://doi.org/10.1016/j.carbon.2023.03.038.

[123] Shen Zhikai, Cheng Miao, Yuan Yongjun, Pei Lang, Zhong Jiasong, Guan Jie, Li Xinyue, Li Zijian, Bao Liang, Zhang Xuefeng, Yu Zhentao, Zou Zhigang. Identifying the role of interface chemical bonds in activating charge transfer for enhanced photocatalytic nitrogen fixation of Ni_2P-black phosphorus photocatalysts. Applied Catalysis B: Environmental, 2021, 295, 120274. https://doi.org/10.1016/j.apcatb.2021.120274.

[124] L. Nguyen Ha. Reticular materials for artificial photoreduction of CO_2. Advanced Energy Materials, 2020, 10 (46), 2002091. https://doi.org/10.1002/aenm.202002091.

[125] Chen ChengXia, Xiong Yangyang, Zhong Xin, Lan Pui Ching, Wei Zhangwen, Pan Hongjun, Su Peiyang, Song Yujie, Chen Yifan, Nafady Ayman, Sirajuddin, Ma Shengqian. Enhancing photocatalytic hydrogen production via the construction of robust multivariate Ti-MOF/COF composites. Angewandte Chemie International Edition, 2022, 61 (3), e202114071. https://doi.org/10.1002/anie.202114071.

[126] Wang Xuewei, Zhu LingFeng, Lv Zhouwei, Qi Zhulin, Xu Yun, Miao Tifang, Fu Xianliang, Li Longfeng. Coupled visible-light driven photocatalytic reactions over porphyrin-based mof materials. Chemical Engineering Journal, 2022, 442, 136186. https://doi.org/10.1016/j.cej.2022.136186.

[127] Deng Man, Guo Jiayun, Ma Xin, Fu Yangjie, Du Hao, Hao Derek, Wang Qi. Enhanced photocatalytic Cr(VI) reduction performance by novel PDI/COFs composite. Separation and Purification Technology, 2023, 326, 124786. https://doi.org/10.1016/j.seppur.2023.124786.

[128] Fang Yongjin, Yu Xinyao, Lou Xiongwen. Bullet-like Cu_9S_5 hollow particles coated with nitrogen-doped carbon for sodium-ion batteries. Angewandte Chemie International Edition, 2019, 58 (23), 7744-7748. https://doi.org/10.1002/anie.201902988.

[129] Ma Jie, Cheng Yujuan, Wang Lei, Dai Xiaohu, Yu Fei. Free-standing $Ti_3C_2T_x$ MXene film as binder-free electrode in capacitive deionization with an ultrahigh desalination capacity. Chemical Engineering Journal, 2020, 384, 123329. https://doi.org/10.1016/j.cej.2019.123329.

[130] Zhang Xiao, Zhang Xiaoran, Yang Ping, Ping Jiang San. Layered graphitic carbon nitride: Nano-heterostructures, photo/electro-chemical performance and trends. Journal of Nanostructure in Chemistry, 2021, 12 (5), 669-691. https://doi.org/10.1007/s40097-021-00442-5.

[131] Jiang Haopeng, Xu Mengyang, Zhao Xiaoxue, Wang Huiqin, Huo Pengwei. Fabricated local surface plasmon resonance Cu_2O/Ni-MOF hierarchical heterostructure photocatalysts for enhanced photoreduction of CO_2. Journal of Environmental Chemical Engineering, 2023, 11 (2), 109504. https://doi.org/10.1016/j.jece.2023.109504.

[132] Ali Hamid, Orooji Yasin, Al Alwan Basem, E. L. Jery Atef, M Ahmed, Abu-Dief, Al-Faze Rawan, Guo Shengrong, Wu Bo, Hayat Asif. Morphology-driven innovations in quantum dots: Unlocking enhanced photocatalytic potential. Journal of Energy Chemistry, 2025, 111, 790-846. https://doi.org/10.1016/j.jechem.2025.07.080.

[133] Chen Yongzhi, Jiang Donglin. Photocatalysis with covalent organic frameworks. Accounts of Chemical Research, 2024, 57 (21), 3182-3193. https://doi.org/10.1021/acs.accounts.4c00517.

[134] Wang Bin, He Ru, Xie Linhua, Lin Zujin, Zhang Xin, Wang Jing, Huang Hongliang, Zhang Zhangjing, S Kirk, Schanze, Zhang Jian, Xiang Shengchang, Chen Banglin. Microporous hydrogen-bonded organic framework for highly efficient turn-up fluorescent sensing of aniline. Journal of the American Chemical Society, 2020, 142 (28), 12478-12485. https://doi.org/10.1021/jacs.0c05277.

[135] Yu Baoqiu, Li Lianjie, Liu Shanshan, Wang Hailong, Liu Heyuan, Lin Chenxiang, Liu Chao, Wu Hui, Zhou Wei, Li Xiyou, Wang Tianyu, Chen Banglin, Jiang Jianzhuang. Robust biological hydrogen-bonded organic framework with post-functionalized rhenium(I) sites for efficient

heterogeneous visible-light-driven CO_2 reduction. Angewandte Chemie International Edition, 2021, 60 (16), 8983-8989. https://doi.org/10.1002/anie.202016710.

[136] Kant Paul, L Laura, Trinkies, Gensior Nils, Fischer Domenik, Rubin Michael, Alan Ozin Geoffrey, Dittmeyer Roland. Isophotonic reactor for the precise determination of quantum yields in gas, liquid, and multi-phase photoreactions. Chemical Engineering Journal, 2023, 452, 139204. https://doi.org/10.1016/j.cej.2022.139204.

[137] A Anira Latif. Manan Memon, Tanveer A. Gadhi, Imtiaz Ali Bhurt, Najeebullah Channa, Rasool Bux Mahar, Imran Ali, Alessandro Chiadò, Barbara Bonelli. Bi_2O_3 immobilized 3D structured clay filters for solar photocatalytic treatment of wastewater from batch to scaleup reactors. Materials Chemistry and Physics, 2022, 276, 125297. https://doi.org/10.1016/j.matchemphys.2021.125297.

[138] Yesica Téllez Garcia, Rajput Darshana, Landa Munoz Rodrigo. Raúl Olivera Flores, Claramaria Rodríguez González, Susana Citlaly Gaucin Gutiérrez, Raúl Pérez-Hernández, Srinivas Godavarthi, José de Jesús Pérez Bueno, J. A. Diaz-Real, Goldie Oza. Designing a microfluidic platform using g-C_3N_4/$NiTiO_3$ for photocatalytic CO_2 reduction: An artificial photosynthesis approach. International Journal of Hydrogen Energy, 2025, 144, 1257-1266. https://doi.org/10.1016/j.ijhydene.2025.05.007.

[139] Tsai Yi-Hsuan, Cattoen Martin, Masson Guillaume, Christen Gabrielle, Traber Lisa, Donnard Morgan, R Frédéric, Leroux, Bentzinger Guillaume, Guizzetti Sylvain, M Jean-Christophe, Monbaliu. On a seamlessly replicable circular photoreactor for lab-scale continuous flow applications. Reaction Chemistry & Engineering, 2024, 9 (7), 1646-1655. https://doi.org/10.1039/d4re00109e.

[140] Xu Xiaohan, Wang Yi, Deng Zhuo, Wang Jin, Wei Xile, Wang Peng, Zhang Dun. Shining a light on sewage treatment: Building a high-activity and long-lasting photocatalytic reactor with the elegance of a “kongming lantern”. Catalysts, 2024, 14 (9), 645. https://doi.org/10.3390/catal14090645.

[141] Tommasi Matteo, Conte Francesco. Mohammad Imteyaz Alam, Gianguido Ramis, Ilenia Rossetti. Highly efficient and effective process design for high-pressure CO_2 photoreduction over supported catalysts. Energies, 2023, 16 (13), 4990. https://doi.org/10.3390/en16134990.

[142] A. Borges Rita, F. Pedrosa Marta, A. Manrique Yaidelin, G. Silva Cláudia, M. T. Adrián, Silva, L. Faria Joaquim, J. Sampaio Maria. 3D structured photocatalysts for sustainable H_2O_2 generation from saccharides derivatives. Chemical Engineering Journal, 2023, 470, 144066. https://doi.org/10.1016/j.cej.2023.144066.

[143] A Jose, Cordero Santamaria, Lopez Hannia, Ledezma Marisol. Leslie W. Pineda, J. Esteban Duran. Carbon dioxide reduction utilizing a bismuth halide perovskite as immobilized photocatalyst in a 3D printed microreactor. Journal of Micromechanics and Microengineering, 2024, 34 (2), 025002. https://doi.org/10.1088/1361-6439/ad1b1c.

[144] I. Stefanov Bozhidar, Lebrun Delphine, Mattsson Andreas. Claes G. Granqvist, Lars Österlund. Demonstrating online monitoring of air pollutant photodegradation in a 3D printed gas-phase photocatalysis reactor. Journal of Chemical, 2014, 92 (4), 678-682. https://doi.org/10.1021/ed500604e.

[145] Li Fangyi, Zhu Guihua, Jiang Jizhou, Yang Lang, Deng Fengxia, Arramel, Li Xin. A review of updated S-scheme heterojunction photocatalysts. Journal of Materials Science & Technology, 2024, 177, 142-180. https://doi.org/10.1016/j.jmst.2023.08.038.

[146] Wang Jiamei, Jiang Jizhou, Li Fangyi, Zou Jing, Xiang Kun, Wang Haitao, Li Youji, Li Xin. Emerging carbon-based quantum dots for sustainable photocatalysis. Green Chemistry, 2023, 25 (1), 32-58. https://doi.org/10.1039/d2gc03160d.

[147] Song Ning, Jiang Jizhou, Hong Shihuan, Wang Yun, Li Chunmei, Dong Hongjun. State-of-the-art advancements in single atom electrocatalysts originating from MOFs for electrochemical energy conversion. Chinese Journal of Catalysis, 2024, 59, 38-81. https://doi.org/10.1016/s1872-2067(23)64622-4.

[148] Fu Cong, Li Fei, Zhang Jiachen, Li Dan, Qian Kun, Liu Yong, Tang Junwang, Fan Fengtao, Zhang Qun, Gong Xueqing, Huang Weixin. Site sensitivity of interfacial charge transfer and photocatalytic efficiency in photocatalysis:Methanol oxidation on anatase TiO_2nanocrystals. Angewandte Chemie International Edition, 2021, 60 (11), 6160-6169. https://doi.org/10.1002/anie.202014037.

[149] Ana Rita Almeida, A. Moulijn Jacob, Mul Guido. Photocatalytic oxidation of cyclohexane over TiO_2: Evidence for a mars-van krevelen mechanism. The Journal of Physical Chemistry C, 2011, 115, 1330-1338. https://doi.org/10.1021/jp107290r.

[150] Cai Zhenfeng. Juan Pedro Merino, Wei Fang, Naresh Kumar, Jeremy O. Richardson, Steven De Feyter, Renato Zenobi. Molecular-level insights on reactive arrangement in on-surface photocatalytic coupling reactions using tip-enhanced raman spectroscopy. Journal of the American Chemical Society, 2021, 144 (1), 538-546. https://doi.org/10.1021/jacs.1c11263.

[151] Zhang Yumin, Zhao Jianhong, Wang Hui, Xiao Bin, Zhang Wen, Zhao Xinbo, Lv Tianping, Thangamuthu Madasamy, Zhang Jin, Guo Yan, Ma Jiani, Lin Lina, Tang Junwang, Huang Rong, Liu Qingju. Single-atom Cu anchored catalysts for photocatalytic renewable H_2 production with a quantum efficiency of 56%. Nature Communications, 2022, 13, 58. https://doi.org/10.1038/s41467-021-27698-3.

[152] Liu Lianjun, Zhao Cunyu, T Jeffrey, Miller, Li Ying. Mechanistic study of CO_2 photoreduction with H_2O on Cu/TiO_2 nanocomposites by in situ X-ray absorption and infrared spectroscopies. The Journal of Physical Chemistry C, 2016, 121 (1), 490-499. https://doi.org/10.1021/acs.jpcc.6b10835.

[153] Xu Can, Hu Xianwei, Yu Jiangyu, Li Pengwei, Liu Aimin, Luo Shaohua, Shi Zhongning, Wang Zhaowen. Raman spectroscopy and quantum chemical calculation on YCL_3-KCL molten salt system. Rare Metals, 2023, 42 (11), 3886-3896. https://doi.org/10.1007/s12598-023-02458-y.

[154] Jin Huilong, Li Qiannan, Tian Yunyan, Wang Shuoao, Chen Xing, Liu Jieyu, Wang Changhong. Machine-learning-aided Au-based single-atom alloy catalysts discovery for electrochemical no reduction reaction to NH_3. Rare Metals, 2024, 43 (11), 5813-5822. https://doi.org/10.1007/s12598-024-02833-3.

[155] Li Neng, Yang Yufei, Shi Zuhao, Lan Zhigao, Arramel Arramel, Zhang Peng, Ong Wee-Jun, Jiang Jizhou, Lu Jianfeng. Shedding light on the energy applications of emerging 2D hybrid organic-inorganic halide perovskites. iScience, 2022, 25 (2), 103753. https://doi.org/10.1016/j.isci.2022.103753.

[156] Wang Lijing, Yang Tianyi, Feng Bo, Xu Xiangyu, Shen Yuying, Li Zihan, Arramel, Jiang Jizhou. Constructing dual electron transfer channels to accelerate CO_2 photoreduction guided by machine learning and first-principles calculation. Chinese Journal of Catalysis, 2023, 54, 265-277. https://doi.org/10.1016/S1872-2067(23)64546-2.

[157] Liao Lingrong, Zheng Dongchun, Ou Pinxi, Zhao Qixin, Xuan Weimin, Zheng Qi. π-conjugated chromophore functionalized high-nuclearity titanium-oxo clusters containing structural unit of anatase for photocatalytic selective oxidation of sulfides. Rare Metals, 2024, 43 (4), 1736-1746. https://doi.org/10.1007/s12598-023-02545-0.

[158] Zou Jing, Wu Jing, Wang Yizhou, Deng Fengxia, Jiang Jizhou, Zhang Yizhou, Liu Song, Li Neng, Zhang Han, Yu Jiaguo, Zhai Tianyou, N Husam, Alshareef. Additive-mediated intercalation and surface modification of MXenes. Chemical Society Reviews, 2022, 51 (8), 2972-2990. https://doi.org/10.1039/d0cs01487g.

[159] Jiang Jizhou, Li Fangyi, Ding Lei, Zhang Chengxun, Arramel, Li Xin. MXenes/CNTs-based hybrids: Fabrications, mechanisms, and modification strategies for energy and environmental applications. Nano Research, 2023, 17 (5), 3429-3454. https://doi.org/10.1007/s12274-023-6302-x.

[160] Subagyo Riki, Yudhowijoyo Azis. Novia Amalia Sholeha, Sutrisno Salomo Hutagalung, Didik Prasetyoko, Muhammad Danang Birowosuto, Arramel Arramel, Jizhou Jiang, Yuly Kusumawati. Recent advances of modification effect in Co_3O_4-based catalyst towards highly efficient photocatalysis. Journal of Colloid and Interface Science, 2023, 650, 1550-1590. https://doi.org/10.1016/j.jcis.2023.07.117.

[161] Wu Junhao, Lu Xinhui, Yan Qianqian, Qiu Jixia, Zhou Wei, Zhu Yuanyuan, Wang Xiao, Zhang Sheng, Li Kui, Lu Xing. Staggered abc-stacking cobalt-triptycene framework for accelerating CO_2 photoreduction. Angewandte Chemie International Edition, 2025, 64 (29), e202504155. https://doi.org/10.1002/anie.202504155.

[162] Kaur Balvinder, Singh Pardeep, Thakur Sourbh, Singh Archana, Chaudhary Vishal, Kumar Naveen. Aftab Aslam Parwaz Khan, Malik Abdul Rub, Naved Azum, Pankaj Raizada. Harnessing 3D printing for tailored TiO_2 structures redefining organic pollutant degradation. Journal of Environmental Chemical Engineering, 2025, 13 (2), 116042. https://doi.org/10.1016/j.jece.2025.116042.

[163] Mutawara Mahmood Baig, Ayoub Khan Suhail, Ahmad Hamza, Liang Jin, Zhu Guoyin, Pang Huan, Zhang Yizhou. 3D printing of hydrogels for flexible micro-supercapacitors. FlexMat, 2024, 1 (1), 79-99. https://doi.org/10.1002/flm2.14.

[164] Li Pimao, Jiang Lishuai, Wen Zhijie, Wu Chaolei, Yang Yiming, Peng Xiaohan, Wu Quansen, Wu Quanlin. Effect of fractures on mechanical behavior of sand powder 3D printing rock analogue under triaxial compression. Journal of Central South University, 2024, 31 (8), 2703-2716. https://doi.org/10.1007/s11771-024-5721-5.

[165] Liu Xuehui, Ma Siqi, He Peigang, Wang Meirong, Duan Xiaoming, Jia Dechang, Colombo Paolo, Zhou Yu. 3D printing of green and environment-friendly rGO@ZnO/GP for removal of methylene blue from wastewater. Journal of Physics and Chemistry of Solids, 2023, 174, 111158. https://doi.org/10.1016/j.jpcs.2022.111158.

[166] Cao Leiqing, Bu Fan, Wang Yuxuan, Gao Yong, Zhao Wenbo, Yang Jiayu, Chen Jipeng, Xu Xi, Guan Cao. Multifunctional anchoring effect enables ultra-stable 3D-printed zinc powder-based anode. Science China Materials, 2025, 68 (3), 897-905. https://doi.org/10.1007/s40843-024-3174-9.

[167] Liu Xin, Lu Sihan, Wang Tianlin, Wang Xiaohong, Yang Ke, Yang Huazhe. Advances and prospects of 3D printed antibacterial bone implants: A systematic review. Journal of Materials Science & Technology, 2024, 200, 227-242. https://doi.org/10.1016/j.jmst.2024.02.040.

[168] Lee Seung Yeon, Kim Joo Hyun, Yi Sun Shin, Yeo Hyeon-Gu, Lee Youngjeon, Hwang Yongsung, Lee Jin Woo. Systematic evaluation of antibiotic activity of a cefazolin-loaded scaffold with varying 3D printing temperatures and its application in treating osteomyelitis. Journal of Industrial and Engineering Chemistry, 2023, 124, 539-549. https://doi.org/10.1016/j.jiec.2023.05.009.

[169] Li Yufan, Chen Li, Stehle Yijing, Lin Mingyue, Wang Chenxin, Zhang Rui, Huang Min, Li Yubao, Zou Qin. Extrusion-based 3D-printed “rolled-up” composite scaffolds with hierarchical pore structure for bone growth and repair. Journal of Materials Science & Technology, 2024, 171, 222-234. https://doi.org/10.1016/j.jmst.2023.07.018.

[170] Zhu Junbing, Hu Wenxi, Ni Jiangfeng, Li Liang. High areal energy zinc-ion micro-batteries enabled by 3D printing. Journal of Materials Science & Technology, 2024, 196, 183-189. https://doi.org/10.1016/j.jmst.2024.01.053.

[171] Gao Zhiqiang, Liu Xin, Zhao Hao, Xia Shengpeng, Liu Wenli, Bai Haotian, Lv Fengting, Zheng Xiongfei, Huang Yiming, Gu Qi, Wang Shu. Synthesis of easily-processable collagen

bio-inks using ionic liquid for 3D bioprinted liver tissue models with branched vascular networks. Science China Chemistry, 2023, 66 (5), 1489-1499. https://doi.org/10.1007/s11426-022-1472-6.

[172] Khoo Valerine, Ng Sue-Faye, Haw Choon-Yian, Ong Wee-Jun. Additive manufacturing: A paradigm shift in revolutionizing catalysis with 3D printed photocatalysts and electrocatalysts toward environmental sustainability. Small, 2024, 20 (31), 202401278. https://doi.org/10.1002/smll.202401278.

[173] Ana Paula Fagundes. Eduardo Guilherme Cividini Neiva, Lizandra Maria Zimmermann, Natan Padoin, Cíntia Soares, Humberto Gracher Riella. Melting and solution mixing in the production of photocatalytic filaments for 3D printing. Chemical Engineering Science, 2025, 302, 120862. https://doi.org/10.1016/j.ces.2024.120862.

[174] Prediger Richard, Sriyotha Nitipoom, G Karl, Schell, Kluck Sebastian, Hambitzer Leonhard, Kotz-Helmer Frederik. Two-photon polymerization of nanocomposites for additive manufacturing of transparent magnesium aluminate spinel ceramics. Advanced Science, 2024, 11 (20), 2307175. https://doi.org/10.1002/advs.202307175.

[175] G. Gordeev Evgeniy, S. Erokhin Kirill, D. Kobelev Andrey, V. Burykina Julia, V. Novikov Pavel, P. Ananikov Valentine. Exploring metallic and plastic 3D printed photochemical reactors for customizing chemical synthesis. Scientific Reports, 2022, 12 (1), 3780. https://doi.org/10.1038/s41598-022-07583-9.

[176] Chen Guanchen, Huang Weitse. Poching Lee, C. B. Lin. *In situ* precipitation 3D printing of highly ordered silver cluster-silver chloride photocatalysts. The International Journal of Advanced Manufacturing Technology, 2023, 126 (1-2), 797-811. https://doi.org/10.1007/s00170-023-11177-8.

[177] Rebber Matthias, Sannemüller Hendrik, Jaruszewski Michael, Pfannkuche Daniela, Urakawa Atsushi, Koziej Dorota. Light and mass transport computations guide the fabrication of 3D-structured TiO_2 and Au/TiO_2 aerogel photocatalysts for efficient hydrogen production in the gas phase. Chemistry of Materials, 2023, 35 (10), 3849-3858. https://doi.org/10.1021/acs.chemmater.2c03503.

[178] Manuel Alejandro Ávila-López, E Tania, Lara-Ceniceros. Francisco Enrique Longoria, Alfredo Aguilar Elguezabal, Azael Martínez de la Cruz, M. A. Garza-Navarro, José Bonilla-Cruz. Photodegradation of air and water contaminants using 3D-printed TiO_2 nanoparticle scaffolds. ACS Applied Nano Materials, 2022, 5 (8), 11437-11446. https://doi.org/10.1021/acsanm.2c02498.

[179] Wang Y., Zhang Y., Wang S., Guan Y., Zhang Y.. A 3D printed synergistic aerogel microreactor toward stable and high-efficiency photocatalytic degradation. Materials Today Chemistry, 2021, 22, 100566. https://doi.org/10.1016/j.mtchem.2021.100566.

[180] Dhillon Manshu, Moitra Tushar, Dhingra Shivali, Kailasam Kamalakannan, Chakraborty Basab, Kumar Basu Aviru. Resilient 3D printed porous biodegradable polylactic acid coated with bismuth ferrite for piezo enhanced photocatalysis degradation assisted by machine learning. Nano Energy, 2025, 140, 111010. https://doi.org/10.1016/j.nanoen.2025.111010.

[181] Grebille Bénédicte, Khrouz Lhoussain, Mulatier Jean-Christophe, Bucher Christophe, Lacôte Emmanuel, Schoumacker Magalie, Bourgeat-Lami Elodie, Lansalot Muriel, Fioux Philippe, Kalout Hanine, Lalevée Jacques, Banyasz Akos, Monnereau Cyrille, Andraud Chantal. Mechanistic and physicochemical insights into the photoactivation pathways of a charge transfer atrp photoinitiator. ChemPhotoChem, 2025, 00, e202500074. https://doi.org/10.1002/cptc.202500074.

[182] Grandcolas Mathieu, Lind Anna. 3D-printed polyamide structures coated with tio_2 nanoparticles, towards a 360-degree rotating photocatalytic reactor. Materials Letters, 2022, 307, 131044. https://doi.org/10.1016/j.matlet.2021.131044.

[183] Yoann de Rancourt de Mimérand, Kun Li, Cong Zhou, Xiaoyun Jin, Xiaoxian Hu, Yufei Chen, Jia Guo. Functional supported ZnO/Bi_2MoO_6 heterojunction photocatalysts with 3D-printed fractal polymer substrates and produced by innovative plasma-based immobilization methods. ACS Applied Materials & Interfaces, 2020, 12 (38), 43138-43151. https://doi.org/10.1021/acsami.0c12286.

[184] Zahabizadeh Behzad. Iran Rocha Segundo, João Pereira, Elisabete Freitas, Aires Camões, Carlos J. Tavares, Vasco Teixeira, Vítor M. C. F. Cunha, Manuel F. M. Costa, Joaquim O. Carneiro. Development of photocatalytic 3D-printed cementitious mortars: Influence of the curing, spraying time gaps and tio_2 coating rates. Buildings, 2021, 11 (9), 381. https://doi.org/10.3390/buildings11090381.

[185] Robson Dias Wouters. Pâmela Cristine Ladwig Muraro, Daniel Moro Druzian, Altevir Rossato Viana, Eduarda de Oliveira Pinto, Jamile Kisner Lacerda da Silva, Bruno Stefanello Vizzotto, Yolice Patricia Moreno Ruiz, André Galembeck, Giovani Pavoski, Denise Crocce Romano Espinosa, William Leonardo da Silva. Zinc oxide nanoparticles: Biosynthesis, characterization, biological activity and photocatalytic degradation for tartrazine yellow dye. Journal of Molecular Liquids, 2023, 371, 121090-121101. https://doi.org/10.1016/j.molliq.2022.121090.

[186] J María, de Vidales Martín, Nieto-Márquez Antonio, Morcuende David, Atanes Evangelina, Blaya Fernando, Soriano Enrique, Fernández-Martínez Francisco. 3D printed floating photocatalysts for wastewater treatment. Catalysis Today, 2019, 328, 157-163. https://doi.org/10.1016/j.cattod.2019.01.074.

[187] J. Kennedy Alan, D. McQueen Andrew. Mark L. Ballentine, Lauren R. May, Brianna M. Fernando, Arit Das, Kyle L. Klaus, Christopher B. Williams, Michael J. Bortner. Degradation of microcystin algal toxin by 3D printable polymer immobilized photocatalytic TiO_2. Chemical

Engineering Journal, 2023, 455, 140866. https://doi.org/10.1016/j.cej.2022.140866.

[188] Ng Siowwoon, Iffelsberger Christian, Sofer Zdenek, Pumera Martin. Tunable room-temperature synthesis of ReS_2 bicatalyst on 3D- and 2D-printed electrodes for photo- and electrochemical energy applications. Advanced Functional Materials, 2020, 30 (19), 1910193. https://doi.org/10.1002/adfm.201910193.

[189] Nouseen Shaista, Ghosh Kalyan, Pumera Martin. Hydrofluoric acid-free etched max on 3D-printed nanocarbon electrode for photoelectrochemical hydrogen production. Applied Materials Today, 2024, 36, 101995. https://doi.org/10.1016/j.apmt.2023.101995.

[190] Ma Zewen, Jiang Liyong, Cao Yanqiang. 3D printing technology for the design of eco-friendly palisade solar evaporators for enhanced desalination and wastewater treatment. Desalination, 2024, 586, 117880. https://doi.org/10.1016/j.desal.2024.117880.

[191] Sangiorgi A., Gonzalez Z., Ferrandez-Montero A., Yus J., Sanchez-Herencia A. J., Galassi C., Sanson A., Ferrari B.. 3D printing of photocatalytic filters using a biopolymer to immobilize TiO_2nanoparticles. Journal of The Electrochemical Society, 2019, 166 (5), H3239-H3248. https://doi.org/10.1149/2.0341905jes.

[192] Yuan Xiaojiao, Sunyer-Pons Neus, Terrado Aleix, Luis León José, Hadziioannou Georges, Cloutet Eric, Villa Katherine. 3D-printed organic conjugated trimer for visible-light-driven photocatalytic applications. ChemSusChem, 2023, 16 (10), e202202228. https://doi.org/10.1002/cssc.202202228.

[193] Sarah C. Galarza-Perez, J. M. Maximiliano, Zapata, Zanata Cinthia, Cena Cicero, Wender Heberton, A. Martins Cauê. 3D-printed plastic windows for photoelectrochemical applications. ACS Applied Polymer Materials, 2025, 7 (6), 3925-3934. https://doi.org/10.1021/acsapm.5c00207.

[194] Kotani Takashi, Hananouchi Takehito, Sakai Shinji. Enhancing visible light-induced 3D bioprinting: Alternating extruded support materials for bioink gelation. Biomedical Materials, 2025, 20 (3), 035005. https://doi.org/10.1088/1748-605X/adc0d6.

[195] Ortega-Columbrans Pablo, Ferrandez-Montero Ana, Yus Joaquin. Antonio Javier Sanchez-Herencia, Begoña Ferrari. Processing of membranes and 3D scaffolds based on n-TiO_2 colloidally dispersed on a thermoplastic matrix for photocatalytic pollutant removal. Catalysis Today, 2024, 426, 114371. https://doi.org/10.1016/j.cattod.2023.114371.

[196] Khezri Bahareh, Villa Katherine, Novotný Filip, Sofer Zdeněk, Pumera Martin. Smartdust 3D-printed graphene-based Al/Ga robots for photocatalytic degradation of explosives. Small, 2020, 16 (33), 2002111. https://doi.org/10.1002/smll.202002111.

[197] Muñoz Jose, Rojas Daniel, Pumera Martin. Faceted crystal nanoarchitectonics of organic-inorganic 3D-printed visible-light photocatalysts. ACS Applied Energy Materials, 2022, 5 (3), 3252-3258. https://doi.org/10.1021/acsaem.1c03863.

[198] Yoann de Rancourt de Mimérand, Kun Li, Jia Guo. Photoactive hybrid materials with fractal designs produced via 3D printing and plasma grafting technologies. ACS Applied Materials & Interfaces, 2019, 11 (27), 24771-24781. https://doi.org/10.1021/acsami.9b06982.

[199] Yang Zhengrong, Lee Poching, Kuo Chunyu, Shin Chunghao, Lin Chingbin. Application of high specific surface area Ag/AgCl/TiO_2 coupled photocatalyst fabricated by fused filament fabrication. The International Journal of Advanced Manufacturing Technology, 2022, 120 (7-8), 4539-4550. https://doi.org/10.1007/s00170-022-09038-x.

[200] López-Camacho Anyul, José Grande María. Daniel Carazo-Álvarez, M. Dolores La Rubia. Study of the bactericidal properties of polylactic acid-based 3D filament. Journal of Vinyl and Additive Technology, 2025, 31 (5), 1151-1171. https://doi.org/10.1002/vnl.22216.

[201] Li Kun. Yoann de Rancourt de Mimérand, Xiaoyun Jin, Jungang Yi, Jia Guo. Metal oxide (ZnO and TiO_2) and Fe-based metal-organic-framework nanoparticles on 3D-printed fractal polymer surfaces for photocatalytic degradation of organic pollutants. ACS Applied Nano Materials, 2020, 3 (3), 2830-2845. https://doi.org/10.1021/acsanm.0c00096.

[202] Chen Shunyu, Qiu Zhoucheng, Zhao Lihua, Huang Xiaojing, Xiao Xiufeng. Functionalized BP@(Zn+Ag)/EPLA nanofibrous scaffolds fabricated by cryogenic 3D printing for bone tissue engineering. Advanced Healthcare Materials, 2024, 2401038. https://doi.org/10.1002/adhm.202401038.

[203] Ma Jiami, Hu Zhixin, Guo Weihong, Ni Cheng, Li Pan, Chen Bosheng, Chen Songhua, Wang Jinlong, Guo Yanbing. Mechanism for airborne ozone decomposition on X-MIL-53(Fe) (X = H, NH_2, NO_2). Journal of Hazardous materials, 2024, 480, 135849. https://doi.org/10.1016/j.jhazmat.2024.135849.

[204] Jin Haize, Liu Junyi, Guo Yaru, Hong Kaiqiang, Zhu Mengyao, Li Cuixia, Wang Qikun. Nanoscale intergrowth of adsorption-photocatalysis active sites of geopolymer/ $Ag_9(SiO_4)_2NO_3$ for efficient synergistic capture and photocatalytic degradation of tetracycline. Journal of Environmental Chemical Engineering, 2025, 13 (3), 116319. https://doi.org/10.1016/j.jece.2025.116319.

[205] Elkoro Ander, Soler Lluís, Llorca Jordi, Casanova Ignasi. 3D printed microstructured Au/TiO_2 catalyst for hydrogen photoproduction. Applied Materials Today, 2019, 16, 265-272. https://doi.org/10.1016/j.apmt.2019.06.007.

[206] Jacob E. Kupferberg, Syrgiannis Zois, Đorđević Luka, P. Bruckner Eric, J. Jaynes Tyler, H. Ha Hakim, Qi Evan, S. Wek Kristen. Adam J. Dannenhoffer, Nicholas A. Sather, H. Christopher Fry, Liam C. Palmer, Samuel I. Stupp. Biopolymer-supramolecular polymer hybrids for photocatalytic hydrogen production. Soft Matter, 2024, 20 (31), 6275-6288. https://doi.org/10.1039/d4sm00373j.

[207] Xu Xi, Xiao Shuning, Jean Willy Habimana, Xiong Ting,

Borayek Ramadan, Chen Wei, Zhang Dieqing, Ding Jun. 3D-printed grids with polymeric photocatalytic system as flexible air filter. Applied Catalysis B: Environment and Energy, 2020, 262, 118307. https://doi.org/10.1016/j.apcatb.2019.118307.

[208] Yu Yajie, Tan Kok Bing, Xu Kaiji, Sun Kang, Bian Juanjuan, Zhou Shufeng, Zhan Guowu. *In situ* assembly of Cu-BTC nanoparticles onto pollen template with enhanced hydrolytic stability and mechanical performance. Chemical Engineering Science, 2024, 293, 120073. https://doi.org/10.1016/j.ces.2024.120073.

[209] Lu Mingjie, Lin Shiyuan, Ma Xiaolin, Xu Zhenzhan, Yang Hao, Wang Mengfei, Piao Junxiu, Zhang Jinqiang, Dong Pei, Zhao Chaocheng. Enhanced mass transfer by 3D printing to promote the degradation of organic pollutants in electro-fenton system. Chemical Engineering Journal, 2024, 495, 153720. https://doi.org/10.1016/j.cej.2024.153720.

[210] Alves, V Francisco, Santos dos, S Daniel, Correa. 3D-printed mof/mos_2 aerogel for dye adsorption and photocatalytic degradation. Materials Today Chemistry, 2024, 40, 102248. https://doi.org/10.1016/j.mtchem.2024.102248.

[211] Shao Yan, Wang Jingshan, Wu Han, Yan Yifan, Jin Qijie, Zhang Xueying. Shape stability control of a 3D-printed clay/biochar-based monolith to support fe catalyst for continuous levofloxacin degradation with low metal leaching. Colloids and Surfaces A: Physicochemical and Engineering Aspects, 2024, 680, 132664. https://doi.org/10.1016/j.colsurfa.2023.132664.

[212] Alysson Stefan Martins. Garyfalia A. Zoumpouli, Shan Yi, Antonio Jose Exposito, Jannis Wenk, Davide Mattia. 3D-printed indium oxide monoliths for PFAS removal. Chemical Engineering Journal, 2024, 497, 154366. https://doi.org/10.1016/j.cej.2024.154366.

[213] Barisic Ivan, Brucculeri Riccardo, Airoldi Lorenzo, Warren Zachary, S Alysson, Martins, Coduri Mauro, Auricchio Ferdinando. Umberto Tamburini Anselmi, Davide Mattia. Fast sintering of titania monoliths for photocatalytic degradation of organic micropollutants. Applied Materials Today, 2024, 38, 102172. https://doi.org/10.1016/j.apmt.2024.102172.

[214] Liu Xuehui, Ma Siqi, Yang Hualong, He Peigang, Duan Xiaoming, Jia Dechang, Colombo Paolo, Zhou Yu. 3D-printed green and low-cost porous g-C_3N_4/geopolymer components for the removal of methylene blue from wastewater. Journal of the American Ceramic Society, 2024, 107 (5), 3068-3082. https://doi.org/10.1111/jace.19654.

[215] Nouseen Shaista, Deshmukh Sujit, Pumera Martin. Nanoarchitectonics of laser induced MAX 3D-printed electrode for photo-electrocatalysis and energy storage application with long cyclic durability of 100000 cycles. Advanced Functional Materials, 2024, 34 (45), 2407071. https://doi.org/10.1002/adfm.202407071.

[216] Sopha Hanna, Kashimbetova Adelia, Baudys Michal. Pavan Kumar Chennam, Marcela Sepúlveda, Jakub Rusek, Eva Kolibalova, Ladislav Celko, Edgar B. Montufar, Josef Krysa, Jan M. Macak. Flow-through gas phase photocatalysis using TiO_2 nanotubes on wirelessly anodized 3D-printed tinb meshes. Nano Letters, 2023, 23 (14), 6406-6413. https://doi.org/10.1021/acs.nanolett.3c01149.

[217] Guo Wei, Liu Yuanlan, Sun Yinghui, Wang Yawen, Qin Wei, Zhao Bo, Liang Zhiqiang, Jiang Lin. Vertical 3D printed forest-inspired hierarchical plasmonic superstructure for photocatalysis. Advanced Functional Materials, 2021, 31 (23), 2100768. https://doi.org/10.1002/adfm.202100768.

[218] Luo Xiaobo, Hu Songhan, Duan Qiudong, Zhou Dacheng, Chen Jialin, Wen Yugeng, Qiu Jianbei. Direct laser printing of 3D optical imaging based on full-spectrum solar-absorption-enhanced perovskite-type oxides. Materials Research Bulletin, 2024, 171, 112634. https://doi.org/10.1016/j.materresbull.2023.112634.

[219] Zhang Xiaoxiang, Liu Zheng, Zhu Di, Peng Xiaotong, Gigmes Didier, Schmitt Michael, Xiao Pu, Dumur Frédéric, Lalevée Jacques. Photoinitiating ability of pyrene-chalcone-based oxime esters with different substituents. Macromolecular Chemistry and Physics, 2023, 224 (20), 2300293. https://doi.org/10.1002/macp.202300293.

[220] Zhang Lei, Liu Hanwen, Song Bo, Gu Jialun, Li Lanxi, Shi Wenhui, Li Gan, Zhong Shiyu, Liu Hui, Wang Xiaobo, Fan Junxiang, Zhang Zhi, Wang Pengfei, Yao Yonggang, Shi Yusheng, Lu Jian. Wood-inspired metamaterial catalyst for robust and high-throughput water purification. Nature Communications, 2024, 15 (1), 2046. https://doi.org/10.1038/s41467-024-46337-1.

[221] Sreedhar Nurshaun, Kumar Mahendra, Al Jitan Samar, Thomas Navya, Palmisano Giovanni, A Hassan, Arafat. 3D printed photocatalytic feed spacers functionalized with β-FeOOH nanorods inducing pollutant degradation and membrane cleaning capabilities in water treatment. Applied Catalysis B: Environmental and Energy, 2022, 300, 120318. https://doi.org/10.1016/j.apcatb.2021.120318.

[222] Liu Yufeng, Xu Jianhui, Fu Xin, Wang Pengxu, Li Dan, Zhang Yunfei, Chen Shenggui, Zhang Chunhui, Liu Peng. Development of MoS_2-stainless steel catalyst by 3D printing for efficient destruction of organics via peroxymonosulfate activation. Journal of Environmental Sciences, 2024, 135, 108-117. https://doi.org/10.1016/j.jes.2023.01.016.

[223] Chen Yin, Yang Huanhua, Li Mingliang, Zhu Shilu, Chen Shuo, Dong Liuyi, Niu Fuzhou, Yang Runhuai. 3D-printed light-driven microswimmer with built-in micromotors. Advanced Materials Technologies, 2021, 7 (1), 2100687. https://doi.org/10.1002/admt.202100687.

[224] Bernasconi Roberto, Bellè Umberto, Brigatti Stefano. Maria Vittoria Diamanti. 3D printing of photocatalytic nanocomposites containing titania nanoparticles. Additive Manufacturing, 2024, 79, 103916. https://doi.org/10.1016/j.addma.2023.103916.

[225] Liu Tao, Zhou Guangming, Yu Bingyan, Fu Lihu, Yu Simiao,

Xu Zhenjie, Lu Gang. Preparation of nickel oxide-loaded hierarchical porous alumina ceramic for photocatalytic degradation of methylene blue. Catalysis Letters, 2025, 155 (5), 179. https://doi.org/10.1007/s10562-025-05012-w.

[226] Sun Ke, Zhang Yijun, Zhu Di, Peng Xiaotong, Zhang Jing, Gong Tao, Ma Ming, Xiao Pu. Visible-light photopolymerization activated by nanocarbon materials as photocatalysts. Journal of Photochemistry and Photobiology C: Photochemistry Reviews, 2023, 57, 100637. https://doi.org/10.1016/j.jphotochemrev.2023.100637.

[227] Wu Yang, Zhang Qian, Yang Xuxuan, Zhang Xiaoping, Nie Xiongfeng, Xiao Meng, Yao Yuan, Xu Ziyang, Liu Wenguang. 3D-printed tough zwitterionic polycarbonate polyurethane meniscus substitute ameliorates cartilage abrasion. Science China Materials, 2023, 66 (9), 3744-3756. https://doi.org/10.1007/s40843-023-2489-5.

[228] Güler Saadet, Özler Berk. Fabrication and analysis of Fe_3O_4/ZnO/epoxy composites via stereolithography: Structural and photocatalytic properties. Polymer Composites, 2025, 46 (5), 4829-4840. https://doi.org/10.1002/pc.29621.

[229] Jędrzej P. Winczewski. Joel Arriaga Dávila, Manuel Herrera-Zaldívar, Francisco Ruiz-Zepeda, R. Margoth Córdova-Castro, Camilo R. Pérez de la Vega, Clément Cabriel, Ignacio Izeddin, Han Gardeniers, Arturo Susarrey-Arce. 3D-architected alkaline-earth perovskites. Advanced Materials, 2024, 36 (11), 2307077. https://doi.org/10.1002/adma.202307077.

[230] Zanini Alice. Pedro Amador Celdran, Olaf Walter, Sara Maria Carturan, Jacobus Boshoven, Antonio Bulgheroni, Lisa Biasetto, Mattia Manzolaro, Rachel Eloirdi, Stefano Corradetti, Giorgia Franchin. First structured uranium-based monoliths produced via vat photopolymerization for nuclear applications. Advanced Functional Materials, 2024, 34 (46), 2406916. https://doi.org/10.1002/adfm.202406916.

[231] K. Finch Alicia, Gillhuber Sebastian, Frisch Hendrik, W. Roesky Peter, Barner-Kowollik Christopher. Catalytically active light printed microstructures. Advanced Materials, 2025, 37 (34), 2506663. https://doi.org/10.1002/adma.202506663.

[232] Warren Zachary. Thais Tasso Guaraldo, Ivan Barisic, Garyfalia A. Zoumpouli, Jannis Wenk, Davide Mattia. Mixed-phase titania foams via 3D-printing for pharmaceutical degradation. Journal of Materials Chemistry A, 2024, 12 (18), 10913-10922. https://doi.org/10.1039/d4ta00869c.

[233] Luo Jiachengjun, Ruta Vincenzo, Seon Kwon Ik, Albertazzi Jody, Allasia Nicolò, Nevskyi Oleksii, Busini Valentina, Moscatelli Davide, Vilé Gianvito. Fabricating a structured single-atom catalyst via high-resolution photopolymerization 3D printing. Advanced Functional Materials, 2024, 34 (42), 2404794. https://doi.org/10.1002/adfm.202404794.

[234] Thi Huong Vu, Duc Bui Van, An Nguyen Thuy, Anh Tran Thi Phuong. Tejraj M. Aminabhavi, Yasser Vasseghian, Sang-Woo Joo. 3D-Printed WO_3-UiO-66@reduced graphene oxide nanocomposites for photocatalytic degradation of sulfamethoxazole. Chemical Engineering Journal, 2024, 483, 149277. https://doi.org/10.1016/j.cej.2024.149277.

[235] Hu Meiyang, Wu Ciwei, Xie Qihui, Yu Jiyuan, Guo Yanming, Shuai Yong, Wang Xiaowei, Wang Zhaolong. 3D printed degradable hydrogel evaporator for high-efficiency, environmental-friendly solar alkaline-water evaporation. Chemical Engineering Journal, 2024, 499, 156132. https://doi.org/10.1016/j.cej.2024.156132.

[236] Miguel Ángel Gracia-Pinilla. Norma Alicia Ramos-Delgado, Cristian Rosero-Arias, Remco Sanders, Stephan Bartling, Jędrzej Winczewski, Han Gardeniers, Arturo Susarrey-Arce. Additive manufacturing of hollow connected networks for solar photo-fenton-like catalysis. RSC Sustainability, 2024, 2 (12), 3897-3908. https://doi.org/10.1039/d4su00312h.

[237] Singh Nishikanta, Sinha Priyank, Sahu Bhanendra, Mandal Srayee, Bhattacharyya Santanu, Banerjee Sanjib. Ultrasmall sulfur-dots-mediated facile photopolymerization for the production of smart injectable ink for 3D printing applications. Advanced Functional Materials, 2024, 35 (6), 2415125. https://doi.org/10.1002/adfm.202415125.

[238] Ashok Pawar Amol, Halivni Shira, Waiskopf Nir, Ben-Shahar Yuval, Soreni-Harari Michal, Bergbreiter Sarah, Banin Uri, Magdassi Shlomo. Rapid three-dimensional printing in water using semiconductor-metal hybrid nanoparticles as photoinitiators. Nano Letters, 2017, 17 (7), 4497-4501. https://doi.org/10.1021/acs.nanolett.7b01870.

[239] Fernand E. Torres-Davila, L. Chagoya Katerina, E. Blanco Emma, Shahzad Saqib. Lorianne R. Shultz-Johnson, Mirra Mogensen, Andre Gesquiere, Titel Jurca, Nabil Rochdi, Richard G. Blair, Laurene Tetard. Room temperature 3D carbon microprinting. Nature Communications, 2024, 15 (1), 2745. https://doi.org/10.1038/s41467-024-47076-z.

[240] Li Kai, Sun Long, Du Fan, Wang Chao, Fang Junyang, Li Mingzhen, Wang Yexin, Wang Xiaoying, Li Jinbang. Laser-induced in-situ electrohydrodynamic jet printing of micro/nanoscale hierarchical structure. Optics & Laser Technology, 2025, 181, 111812. https://doi.org/10.1016/j.optlastec.2024.111812.

[241] Zahabizadeh Behzad. Iran Rocha Segundo, João Pereira, Elisabete Freitas, Aires Camões, Vasco Teixeira, Manuel F. M. Costa, Vítor M. C. F. Cunha, Joaquim O. Carneiro. Photocatalysis of functionalised 3D printed cementitious materials. Journal of Building Engineering, 2023, 70, 106373. https://doi.org/10.1016/j.jobe.2023.106373.

[242] Feng Jingyi, Wei Yingzhen, Li Xiao, Wang Qifei, Wang Bolun, Guo Yunyu, Feng Binyao, Jin Enquan, Yu Jihong. 3D-printed COF/zeolite composites for augmented photocatalytic hydrogen peroxide production. Angewandte Chemie International Edition, 2025, 64 (32), e202508226. https://doi.org/10.1002/anie.202508226.

[243] Kuo Chunyu, Shih Chunghao, Lee Chenkai, Shen Boheng, Lin Weihsiang, Lee Poching. C. B. Lin. Enhancing

photocatalytic performance of regular porous silver bromide structures through 3D printing. Additive Manufacturing, 2023, 78, 103866. https://doi.org/10.1016/j.addma.2023.103866.

[244] A. Gadhi Tanveer, Ali Bhurt Imtiaz, A. Qureshi Tayyab, Ali Imran, Latif Anira, Bux Mahar Rasool, Channa Najeebullah, Bonelli Barbara. Photocatalytic denitrification of nitrate using Fe-TiO_2-coated clay filters. Catalysts, 2023, 13 (4), 729. https://doi.org/10.3390/catal13040729.

[245] Khositanon Chetsada, Saothayanun Taya, Sirimongkhol Waichaya, Sukpancharoen Somboon, Ogawa Makoto, Bureekaew Sareeya, Weeranoppanant Nopphon. Continuous flow hydroxylation of benzene to phenol in a photocatalytic millistructured flat-plate reactor. ACS Sustainable Chemistry & Engineering, 2024, 12 (37), 13998-14008. https://doi.org/10.1021/acssuschemeng.4c04834.

[246] Liu Yanlei, Shan Mengbo, Du Lange, Sun Weihao, Wu Dapeng, Bi Qing, Wang Hongju, Liu Yufang. Robust TiO_2/CuS@TiO_2 composites loaded on Ti mesh with outstanding stability and photothermal effects for the enhanced photo-degradation of organic pollutions in a flowing device. Applied Surface Science, 2023, 623, 157006. https://doi.org/10.1016/j.apsusc.2023.157006.

[247] Liu Beitao, Zhang Cijian, Li Jiahui, Zhang Guangsheng, Jian Xigao, Weng Zhihuan. Upcyclable thermosetting photopolymer containing degradable sulfite bonds for sustainable 3D printing. Science China Materials, 2024, 67 (12), 4049-4058. https://doi.org/10.1007/s40843-024-3113-2.

[248] Zhang Haibo, Wang Zhongliao, Zhang Jinfeng, Dai Kai. Metal-sulfide-based heterojunction photocatalysts: Principles, impact, applications, and in-situ characterization. Chinese Journal of Catalysis, 2023, 49, 42-67. https://doi.org/10.1016/S1872-2067(23)64444-4.

[249] Yuan Haibo, Ouyang Yuxin, Wang Liangbing. Sol-gel synthesis of metal ions doped TiO_2 catalyst with efficient photodegradation of dye pollutant. Journal of Central South University, 2023, 30 (4), 1086-1094. https://doi.org/10.1007/s11771-023-5241-8.

[250] Liu Dingyong, Cai Hongjie, Zhou Weiming, Lei Dandan, Cao Changlin, Xia Xinshu, Xiao Liren, Qian Qingrong, Chen Qinghua. Application of 3D printing technology for green synthesis of Fe_2O_3 using ABS/TPU/chlorella skeletons for methyl orange removal. RSC Advances, 2024, 14 (2), 1501-1512. https://doi.org/10.1039/d3ra07143j.

[251] Peñas-Garzón Manuel, J Maria, Sampaio, Manrique Yaidelin, G Claudia, Silva, L Joaquim, Faria. Enhanced removal of emerging pollutants through visible light-activated carbon nitride materials immobilized over 3D printed structures. Journal of Environmental Chemical Engineering, 2023, 11 (6), 111343. https://doi.org/10.1016/j.jece.2023.111343.

[252] Meléndez-González P. C., Pech-Rodríguez W. J., Luévano-Hipólito E., Hernández-Ramírez A., Hernández-López J. M.. Innovative syntheses of immobilized Cu_xO semiconductors grown on 3D prints and their photoelectrochemical activity for sulfamethoxazole degradation. Journal of Environmental Chemical Engineering, 2024, 12 (3), 112551. https://doi.org/10.1016/j.jece.2024.112551.

[253] Son Soomin, Jung Pil-Hoon, Park Jaemin, Chae Dongwoo, Huh Daihong, Byun Minseop, Ju Sucheol, Lee Heon. Customizable 3D-printed architecture with ZnO-based hierarchical structures for enhanced photocatalytic performance. Nanoscale, 2018, 10 (46), 21696-21702. https://doi.org/10.1039/c8nr06788k.

[254] Kang Yongfu, Cai Junwen, Zhang Linfeng, Wang Hong-Wei, Jin Rui-Bo. Yoann de Rancourt de Mimérand, Xiaoyun Jin, Jia Guo. Controlled architectures in supported photocatalysis: Exploring the potential of cold plasma discharge, additive manufacturing, and fractal geometry to form hierarchically immobilized Ni-MOF/BiOI/$AgVO_3$. ACS Applied Materials & Interfaces, 2023, 15 (26), 31849-31866. https://doi.org/10.1021/acsami.3c05596.

[255] Li Nannan, Kong Weijun, Gao Jian, Wu Yunzhao, Kong Yanqiang, Chen Lei, Wang Weijia, Yang Lijun, Du Xiaoze. 3D printed textured substrate with $ZnIn_2S_4$-Pt-Co thermoset coating for photocatalytic hydrogen evolution. International Journal of Hydrogen Energy, 2024, 71, 1351-1362. https://doi.org/10.1016/j.ijhydene.2024.05.279.

[256] D. Perera Sachini, M. Johnson Rebecca, Pawle Robert, Elliott John, M. Tran Tien, Gonzalez Jasmine, Huffstetler Jesse, C. Ayers Lyndsay, Ganesh Vijayalakshmi. Milinda C. Senarathna, Karen P. Cortés-Guzmán, Soumik Dube, Samantha Springfield, Lawrence F. Hancock, Benjamin R. Lund, Ronald A. Smaldone. Hierarchically structured metal-organic framework polymer composites for chemical warfare agent degradation. ACS Applied Materials & Interfaces, 2024, 16 (8), 10795-10804. https://doi.org/10.1021/acsami.3c19446.

[257] Arumugam Selva Sharma, Ali Shujat, Sabarinathan Devaraj, Murugavelu Marimuthu, Li Huanhuan, Chen Quansheng. Recent progress on graphene quantum dots-based fluorescence sensors for food safety and quality assessment applications. Comprehensive Reviews in Food Science and Food Safety, 2021, 20 (6), 5765-5801. https://doi.org/10.1111/1541-4337.12834.

[258] Ma Shuai, Wang Meng, You Tianyan, Wang Kun. Using magnetic multiwalled carbon nanotubes as modified QuEChERS adsorbent for simultaneous determination of multiple mycotoxins in grains by UPLC-MS/MS. Journal of Agricultural and Food Chemistry, 2019, 67 (28), 8035-8044. https://doi.org/10.1021/acs.jafc.9b00090.

[259] Zeng Kun, Wei Wei, Jiang Ling, Zhu Fang, Du Daolin. Use of carbon nanotubes as a solid support to establish quantitative (centrifugation) and qualitative (filtration) immunoassays to detect gentamicin contamination in commercial milk. Journal of Agricultural and Food Chemistry, 2016, 64 (41), 7874-7881. https://doi.org/10.1021/acs.jafc.6b03332.

[260] Dai Ying, Peng Wangui, Ji Yi, Wei Jia, Che Junhao, Huang Yongqiang, Huang Weihong, Yang Wenming, Xu Wanzhen.

A self-powered photoelectrochemical aptasensor using 3D-carbon nitride and carbon-based metal-organic frameworks for high-sensitivity detection of tetracycline in milk and water. Journal of Food Science, 2024, 89 (11), 8022-8035. https://doi.org/10.1111/1750-3841.17398.

[261] Zou Yucheng, Shi Yongqiang, Wang Tianxing, Ji Shengyang, Zhang Xinai, Shen Tingting, Huang Xiaowei, Xiao Jianbo, A Mohamed, Farag, Shi Jiyong, Zou Xiaobo. Quantum dots as advanced nanomaterials for food quality and safety applications: A comprehensive review and future perspectives. Comprehensive Reviews in Food Science and Food Safety, 2024, 23 (3), e13339. https://doi.org/10.1111/1541-4337.13339.

[262] Hu Xuetao, Shi Jiyong, Shi Yongqiang, Zou Xiaobo, Arslan Muhammad, Zhang Wen, Huang Xiaowei, Li Zhihua, Xu Yiwei. Use of a smartphone for visual detection of melamine in milk based on Au@carbon quantum dots nanocomposites. Food Chemistry, 2019, 272, 58-65. https://doi.org/10.1016/j.foodchem.2018.08.021.

[263] Wang Xiaokun, Pan Yun, Wang Xiaohong, Guo Yaning, Ni Chenghao, Wu Jingbo, Hao Chen. High performance hybrid supercapacitors assembled with multi-cavity nickel cobalt sulfide hollow microspheres as cathode and porous typha-derived carbon as anode. Industrial Crops and Products, 2022, 189, 115863. https://doi.org/10.1016/j.indcrop.2022.115863.

[264] Ma Shuai, Pan Li gang, You Tianyan, Wang Kun. g-C_3N_4/Fe_3O_4 nanocomposites as adsorbents analyzed by UPLC-MS/MS for highly sensitive simultaneous determination of 27 mycotoxins in maize: Aiming at increasing purification efficiency and reducing time. Journal of Agricultural and Food Chemistry, 2021, 69 (16), 4874-4882. https://doi.org/10.1021/acs.jafc.1c00141.

[265] Liu Zhijun, Wang Li, Liu Pengfei, Zhao Kairen, Ye Shuying, Liang Guoxi. Rapid, ultrasensitive and non-enzyme electrochemiluminescence detection of hydrogen peroxide in food based on the ssDNA/g-C_3N_4 nanosheets hybrid. Food Chemistry, 2021, 357, 129753. https://doi.org/10.1016/j.foodchem.2021.129753.

[266] Guo Xinyu, Chen Chuchu, Jiao Huan, Wu Wenjuan, Jin Yongcan, Liang Zhiqiang, Jiang Bo. Direct ink writing of high-content lignin to construct hierarchical photocatalysts for efficient reduction of 4-nitrophenol. Industrial Crops and Products, 2025, 225, 120513. https://doi.org/10.1016/j.indcrop.2025.120513.

[267] Kandasamy Bhuvaneswari, Al Mahmud Abdullah, Lee Jintae, Hasan Imran, Palanisamy Govindasamy. Advancing the eradication of harmful dyes through stereolithography-produced 3D floating photocatalysis: Exploiting the synergistic potential of graphene/ MnO_2/Fe_3O_4 hybrid nanomaterials. Surfaces and Interfaces, 2024, 48, 104302. https://doi.org/10.1016/j.surfin.2024.104302.

[268] Qiu Yuxiang, Li Qiaolei, Yang Kun, Jin Funan, Fan Jun, Liang Jingjing, Zhou Yizhou, Sun Xiaofeng, Li Jinguo. Thermal shock resistant 3D printed ceramics reinforced with $MgAl_2O_4$ shell structure. Journal of Materials Science & Technology, 2024, 178, 100-111. https://doi.org/10.1016/j.jmst.2023.09.004.

[269] Mei Hui, Huang Weizhao, Liu Hongxia, Pan Longkai, Cheng Laifei. 3D printed carbon-ceramic structures for enhancing photocatalytic properties. Ceramics International, 2019, 45 (12), 15223-15229. https://doi.org/10.1016/j.ceramint.2019.05.008.

[270] Huang Weizhao, Mei Hui, Chang Peng, Jin Zhipeng, Bai Shenwei, Pan Longkai, Cheng Laifei. Bioinspired hierarchical-pore anchoring strategy advancing synergistic photocatalytic-mechanical properties. Journal of Environmental Chemical Engineering, 2023, 11 (2), 109337. https://doi.org/10.1016/j.jece.2023.109337.

[271] Hu Chechia, Chang Lee-Lee, Chen Wei, Hsu Wan-Yuan, Chien Szu-Chia, Chen Chien-Hua, Lin Yu-Ting, Hsu Tzu-Jung, Tung Kuo-Lun. 3D-printed Al_2O_3 framework supported carbon-bridged tri-s-triazine of g-C_3N_4 for photocatalytic tetracycline oxidation. Chemical Engineering Journal, 2024, 487, 150504. https://doi.org/10.1016/j.cej.2024.150504.

[272] Liu Hongxia, Zhang Minggang, Jin Zhipeng, Mei Hui, Zhu Gangqiang, Pan Longkai, Cheng Laifei, Zhang Litong. S-scheme $Bi_{12}TiO_{20}$/$Bi_4Ti_3O_{12}$ heterojunction immobilized on 3D-printed support as a monolithic photocatalyst for NO removal. Applied Surface Science, 2024, 654, 159477. https://doi.org/10.1016/j.apsusc.2024.159477.

[273] Pan Longkai, Yao Li, Mei Hui, Liu Hongxia, Jin Zhipeng, Zhou Shixiang, Zhang Minggang, Zhu Gangqiang, Cheng Laifei, Zhang Litong. Structurally designable Bi_2S_3/P-doped ZnO S-scheme photothermal metamaterial enhanced CO_2 reduction. Separation and Purification Technology, 2023, 312, 123365. https://doi.org/10.1016/j.seppur.2023.123365.

[274] Grandcolas Mathieu, Lind Anna, Grande Carlos. Rotating photocatalytic activity of TiO_2 nanotubes grown on 3D-printed titanium alloy structures. Materials Research Bulletin, 2025, 188, 113407. https://doi.org/10.1016/j.materresbull.2025.113407.

[275] Malik Uzma, Mazur Maciej, D. Gudi Ravindra, D Dharmendra, P. R. Mandaliya, Selvakannan, K Suresh, Bhargava. Colloidal carbon soot templated TiO_2/Ag surface functionalized 3D printed metal brushes as new generation surface enhanced raman scattering substrates. Journal of Colloid and Interface Science, 2024, 671, 325-335. https://doi.org/10.1016/j.jcis.2024.05.181.

[276] Kotz Frederik, Arnold Karl, Bauer Werner, Schild Dieter, Keller Nico, Sachsenheimer Kai, M Tobias, Nargang, Richter Christiane, Helmer Dorothea, E. Rapp Bastian. Three-dimensional printing of transparent fused silica glass. Nature, 2017, 544 (7650), 337-339. https://doi.org/10.1038/nature22061.

[277] Wang Gang, Zhang Jie, Zhong Liangshu, Tang Zhiyong. Extending the light transmission in the continuous flow

photocatalytic process by 3D printed silica packing. Ceramics International, 2024, 50 (20), 38532-38541. https://doi.org/10.1016/j.ceramint.2024.07.221.

[278] Sun Peipei, Chen Zhigang, Zhang Jinyuan, Wu Guanyu, Song Yanhua, Miao Zhihuan, Zhong Kang, Huang Lin, Mo Zhao, Xu Hui. Simultaneously tuning electronic reaction pathway and photoactivity of P, O modified cyano-rich carbon nitride enhances the photosynthesis of H_2O_2. Applied Catalysis B: Environment and Energy, 2023, 342, 123337-123346. https://doi.org/10.1016/j.apcatb.2023.123337.

[279] L José, Neto Bott, S. Martins Thiago, A. S. Sergio, Machado, N. Oliveira Osvaldo. Enhanced photocatalysis on graphitic carbon nitride sensitized with gold nanoparticles for photoelectrochemical immunosensors. Applied Surface Science, 2022, 606, 154952. https://doi.org/10.1016/j.apsusc.2022.154952.

[280] Zhakeyev Adilet, C Mary, Jones, G Christopher, Thomson, M John, Tobin, Wang Huizhi, Vilela Filipe, Xuan Jin. Additive manufacturing of intricate and inherently photocatalytic flow reactor components. Additive Manufacturing, 2021, 38, 101828. https://doi.org/10.1016/j.addma.2020.101828.

[281] Lei Lei, Wang Deyu, Kang Yongfu. Yoann de Rancourt de Mimérand, Xiaoyun Jin, Jia Guo. Phosphor-enhanced, visible-light-storing g-C_3N_4/Ag_3PO_4/$SrAl_2O_4$:Eu^{2+}, Dy^{3+} photocatalyst immobilized on fractal 3D-printed supports. ACS Applied Materials & Interfaces, 2022, 14 (9), 11820-11833. https://doi.org/10.1021/acsami.1c23650.

[282] Guima Katia-Emiko. Luiz Eduardo Gomes, Jesum Alves Fernandes, Heberton Wender, Cauê A. Martins. Harvesting energy from an organic pollutant model using a new 3D-printed microfluidic photo fuel cell. ACS Applied Materials & Interfaces, 2020, 12 (49), 54563-54572. https://doi.org/10.1021/acsami.0c14464.

[283] Wei Qinhong, Li Hangjie, Liu Guoguo, He Yingluo, Wang Yang, Tan Yen Ee, Wang Ding, Peng Xiaobo, Yang Guohui, Tsubaki Noritatsu. Metal 3D printing technology for functional integration of catalytic system. Nature Communications, 2020, 11 (1), 4098. https://doi.org/10.1038/s41467-020-17941-8.

[284] Zhou Ruicheng, Han Ri, Bingham Michael, O'Rourke Christopher, Mills Andrew. 3D printed, plastic photocatalytic flow reactors for water purification. Photochemical & Photobiological Sciences, 2022, 21 (9), 1585-1600. https://doi.org/10.1007/s43630-022-00242-y.

[285] Ramos Bruno, M João Gabriel, Carneiro. Leandro Issamu Nagamati, Antonio Carlos S. C. Teixeira. Development of intensified flat-plate packed-bed solar reactors for heterogeneous photocatalysis. Environmental Science and Pollution Research, 2021, 28 (19), 24023-24033. https://doi.org/10.1007/s11356-020-11806-9.

[286] Jiun Phang Sue, Wong Voon-Loong, How Cheah Kean, Tan Lling-Lling. Robust graphitic carbon nitrite-based thermoset coating for synergistic adsorption-photocatalysis process in 3D-printed photoreactors. Energy Reports, 2023, 9, 30-37. https://doi.org/10.1016/j.egyr.2022.11.159.

[287] Pellejero Ismael, Clemente Alberto, Reinoso Santiago, Cornejo Alfonso, Navajas Alberto, J José, Vesperinas, A Miguel, Urbiztondo, M Luis, Gandía. Innovative catalyst integration on transparent silicone microreactors for photocatalytic applications. Catalysis Today, 2022, 383, 164-172. https://doi.org/10.1016/j.cattod.2020.05.058.

[288] Pan Longkai, Zhang Minggang, Mei Hui, Yao Li, Jin Zhipeng, Liu Hongxia, Zhou Shixiang, Yao Ziyi, Zhu Gangqiang, Cheng Laifei, Zhang Litong. 3D bionic reactor optimizes photon and mass transfer by expanding reaction space to enhance photocatalytic CO_2 reduction. Separation and Purification Technology, 2022, 301, 121974. https://doi.org/10.1016/j.seppur.2022.121974.

[289] Zeki Gök Halil, Dönmez Soner, Gök Yaşar. Photodegradation of methylene blue using zinc phthalocyanine supported on mcm-41 under visible light in low-cost 3D printed photoreactor. ChemistrySelect, 2025, 10 (19), e00411 https://doi.org/10.1002/slct.202500411.

[290] Gök Yaşar, Donmez Soner, Erdem Recep, Zeki Gök Halil. Green photooxidation of 1-naphthol using a zinc phthalocyanine-loaded MCM-41 heterogeneous catalyst. ChemPlusChem, 2025, 00, e202500207. https://doi.org/10.1002/cplu.202500207.

[291] Li Wencheng, Zheng Zhiheng, Qian Zhiqiang, Liu Huan, Wang Xiaodong. Phase change material boosting electricity output and freshwater production through hierarchical-structured 3D solar evaporator. Advanced Functional Materials, 2024, 34 (26), 2316504. https://doi.org/10.1002/adfm.202316504.

[292] M. Desipio Matthew, E Scott, Bramer Van, Thorpe Ryan, Saha Dipendu. Photocatalytic and photo-fenton activity of iron oxide-doped carbon nitride in 3D printed and LED driven photon concentrator. Journal of Hazardous materials, 2019, 376, 178-187. https://doi.org/10.1016/j.jhazmat.2019.05.037.

[293] Alejandra Xochitl Maldonado Pérez. José de Jesús Pérez Bueno. Solar lighting systems applied in photocatalysis to treat pollutants - a review. Reviews on Advanced Materials Science, 2023, 62 (1), 20220293. https://doi.org/doi:10.1515/rams-2022-0293.